Supporting Information for

Ascaroside Profiling of *Caenorhabditis elegans* using GC-EIMS

Stephan H. von Reuss,[†,*] Franziska Dolke,[†] Chuanfu Dong[†]

†Department of Bioorganic Chemistry, Max Planck Institute for Chemical Ecology, Hans-Knoell Strasse 8, D-07745 Jena, Germany

*** *stephan.vonreuss@unine.ch***

Table of contents **Page**

Figure S1A: GC-EIMS spectra of TMS-derivatized ascaroside standards.

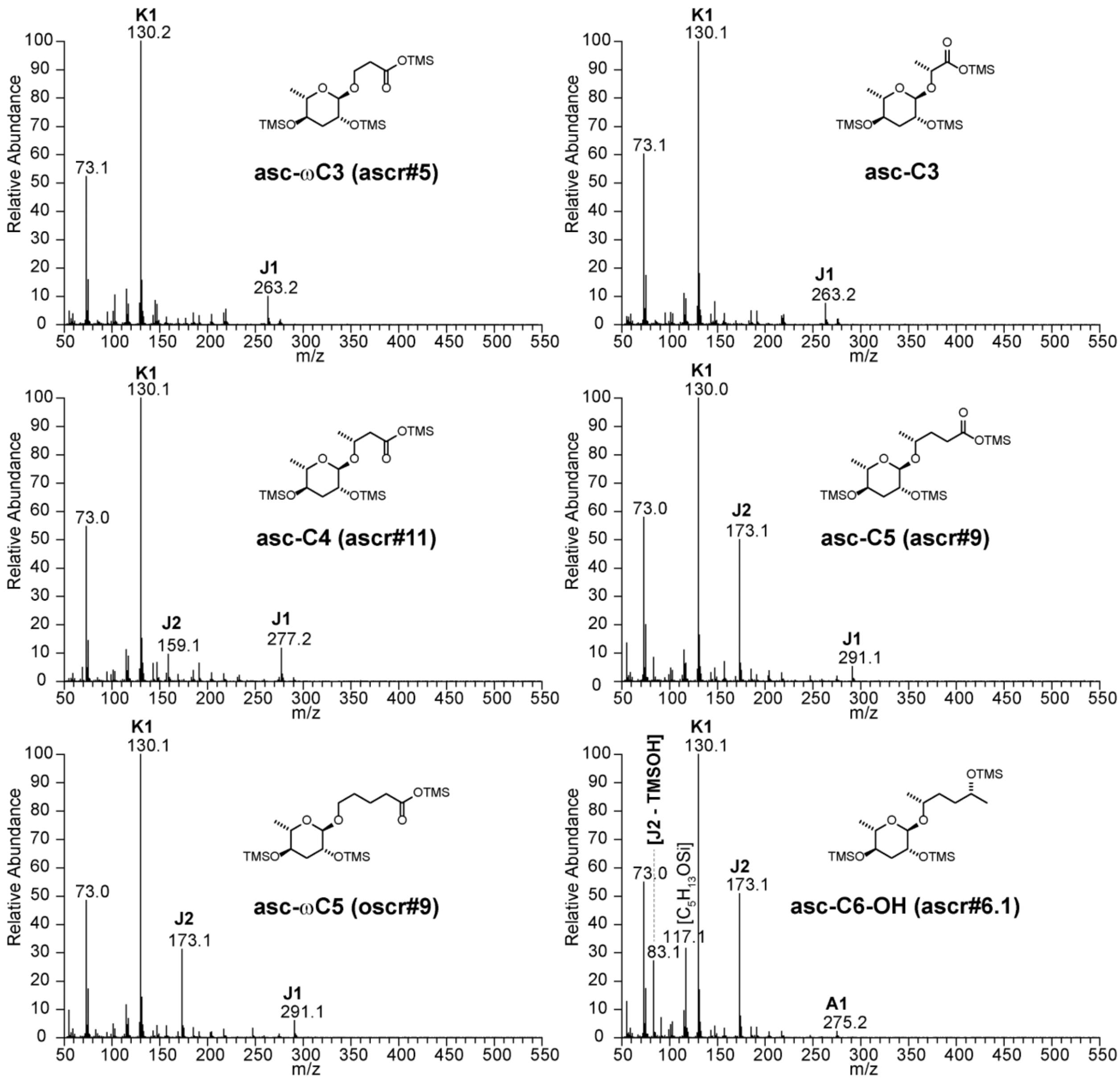

Figure S1B: GC-EIMS spectra of TMS-derivatized ascaroside standards.

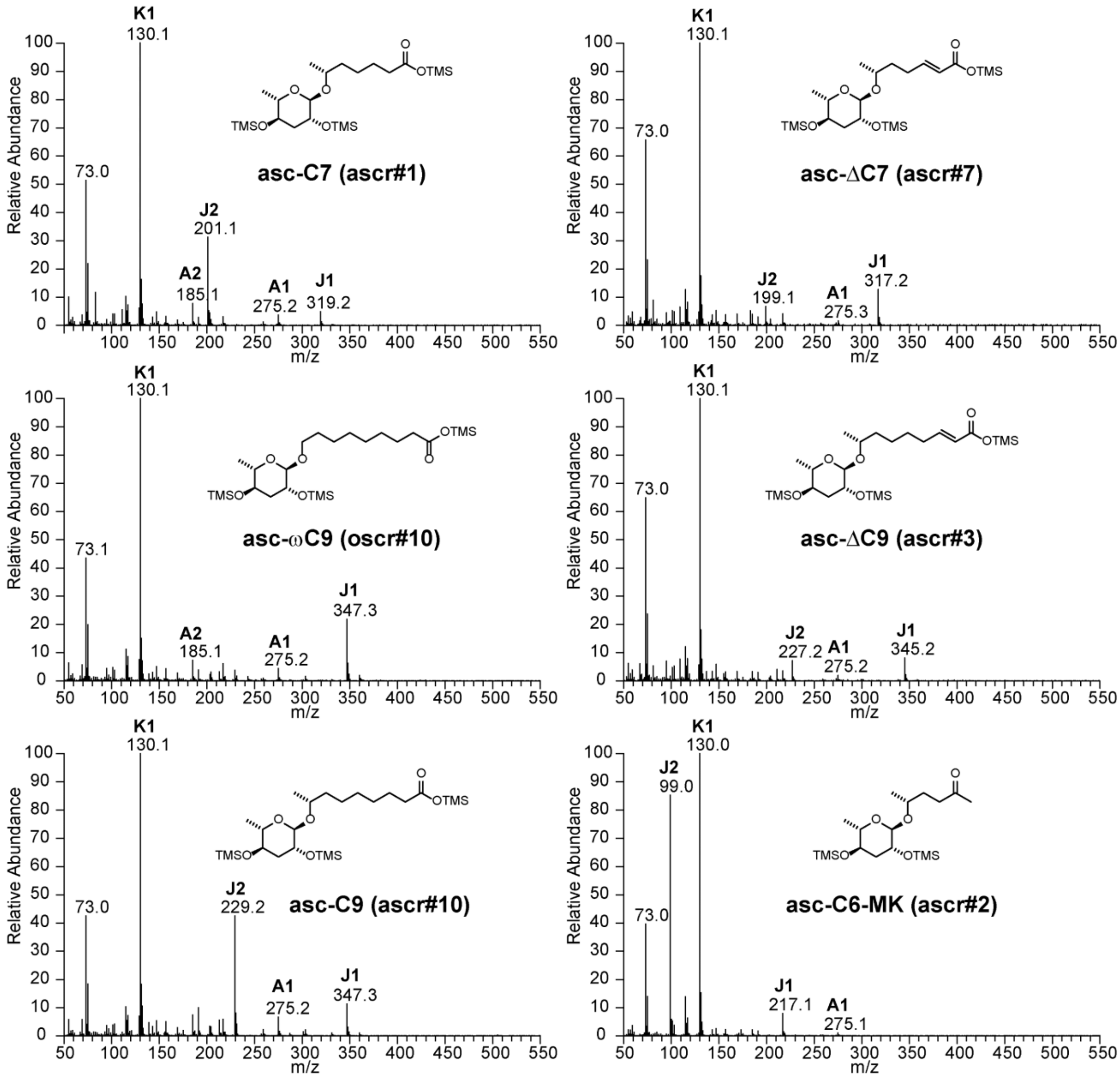

Figure S1C: GC-EIMS spectra of TMS-derivatized ascaroside standards.

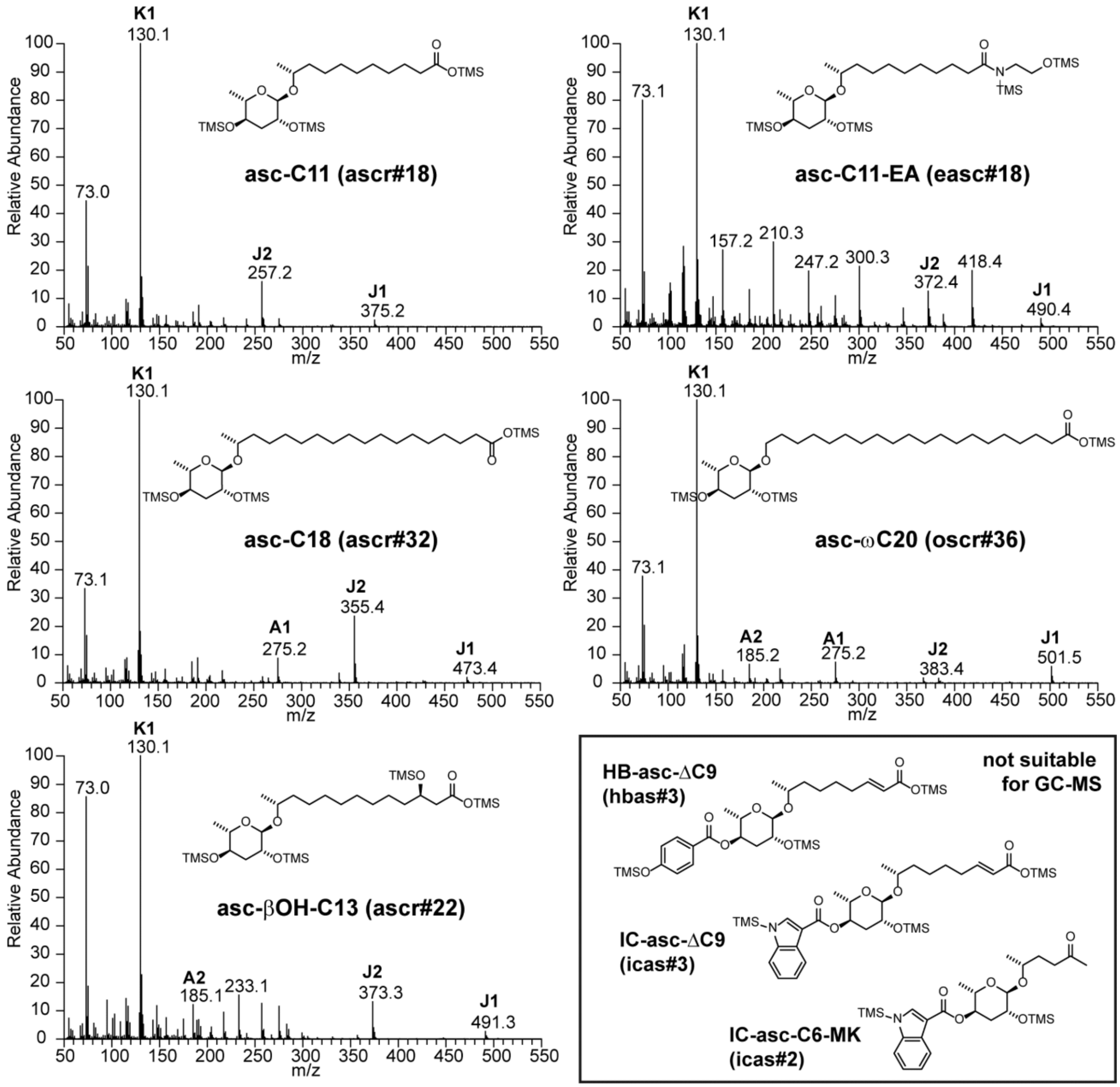

Figure S2: Ascaroside profiling of the *Panagrellus redivivus exo*-metabolome. (A): EIC for the K1-fragment at *m/z* 130.1 $[C_6H_{14}OSi]^{+\bullet}$ shows diversity of ascarosides; (B): EIC for fragment at *m/z* 233.2 $[C_9H_{21}O_3Si_2]^+$ from α-cleavage highlights β-hydroxyacyl ascarosides; (C): Structure assignment of the highly species-specific male-produced female attractant dhas#18 based on EI-induced fragmentation.[1]

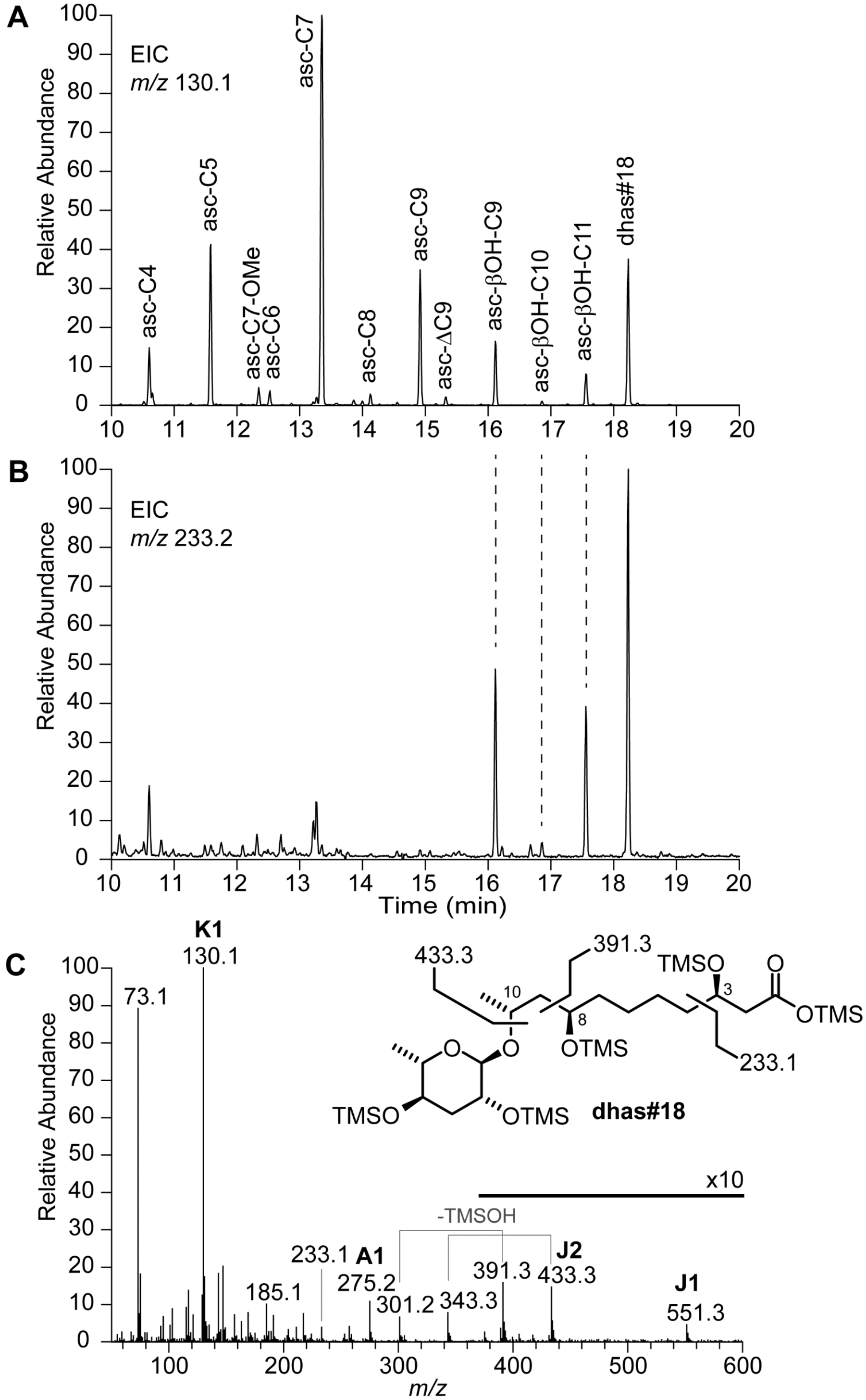

Figure S3: GC-EIMS analysis of asc-C11-EA (easc#18), the infective juvenile inducing signal in entomopathogenic *Heterorhabditis bacteriophora*.[2] (A): EIC for the K1-fragment at *m/z* 130.1 $[C_6H_{14}OSi]^{+\bullet}$ shows signals for tri- and tetra-silylated derivatives (after 30 min with MSTFA only tetra-silylated material is observed); (B & C): EIMS spectra for tri- and tetra-silylated asc-C11-EA.

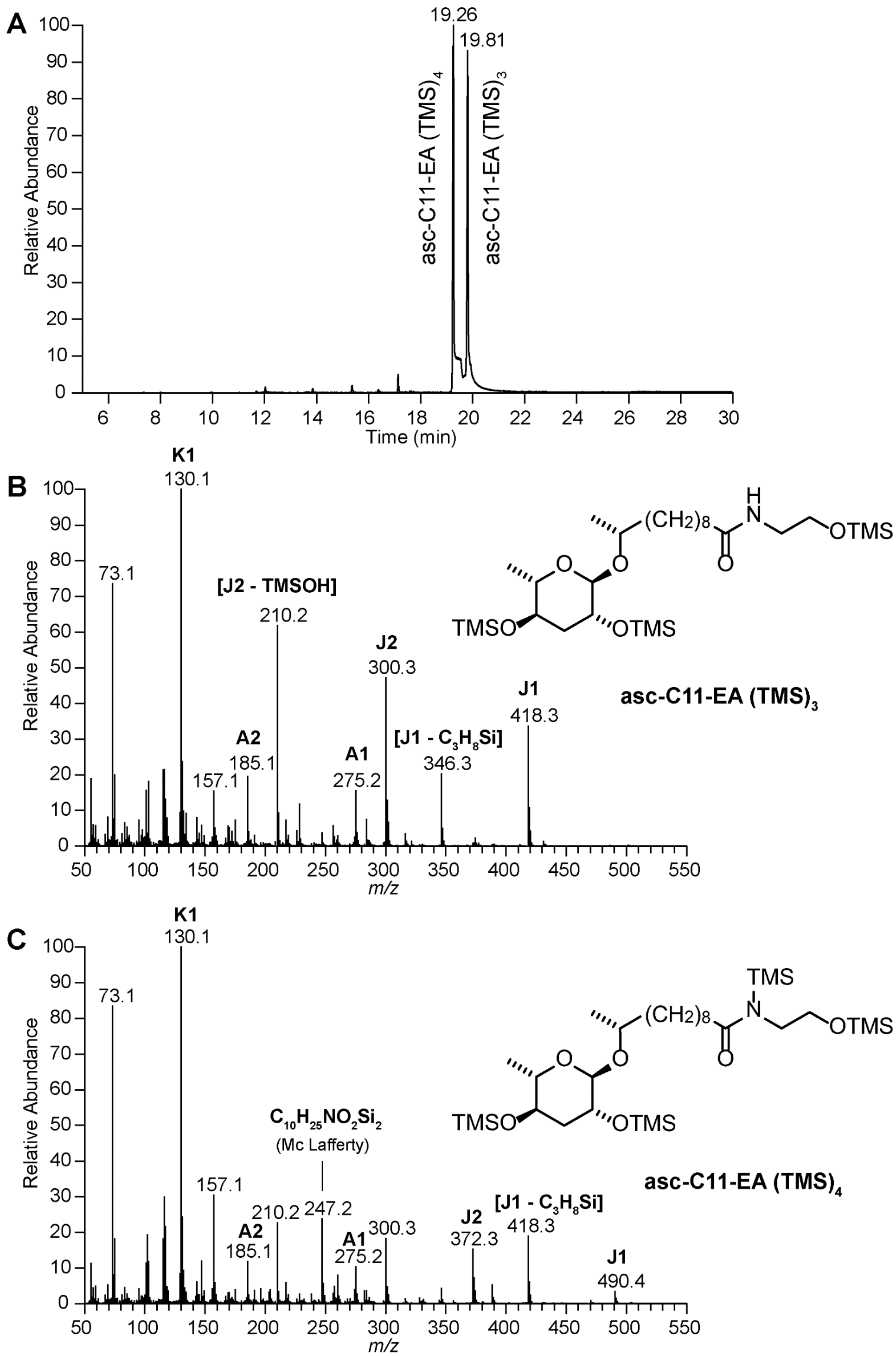

Figure S4: EIMS spectra of the TMS-derivatized decanoate-based rhamnoside rha-C10 and the corresponding ascaroside asc-C10 (ascr#16) demonstrate that the K1-fragment at *m/z* 130.1 $[C_6H_{14}OSi]^{+\bullet}$ is characteristic for 3,6-dideoxy-*arabino*-hexopyranosides, whereas 6-deoxy-*manno*-pyranosides produce a dominating H1a-fragment at *m/z* 204.1 $[C_8H_{20}O_2Si_2]^{+\bullet}$.

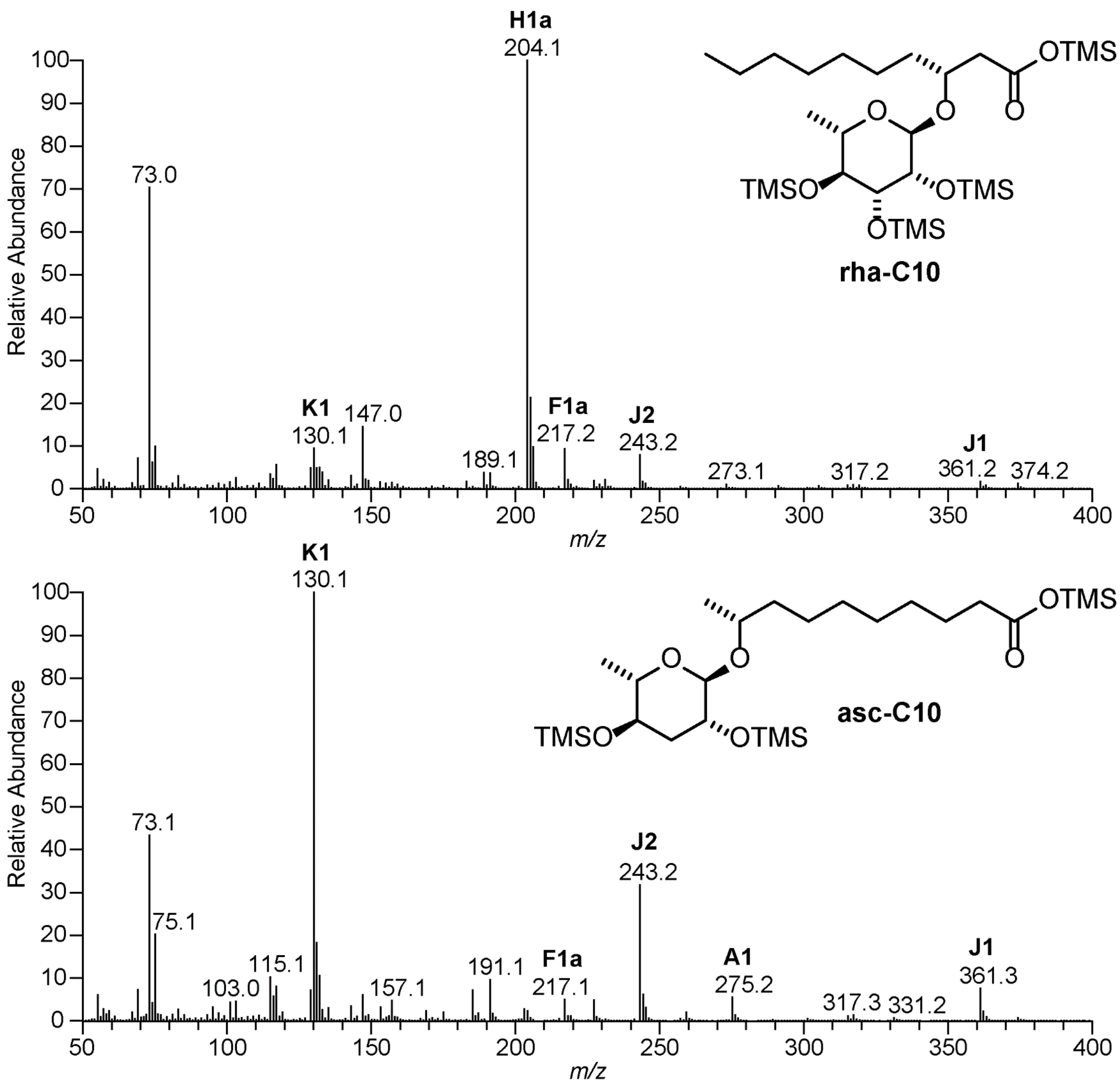

Figure S5: GC-EIMS analysis of TMS-derivatized ascaroside standards and their methyl esters.

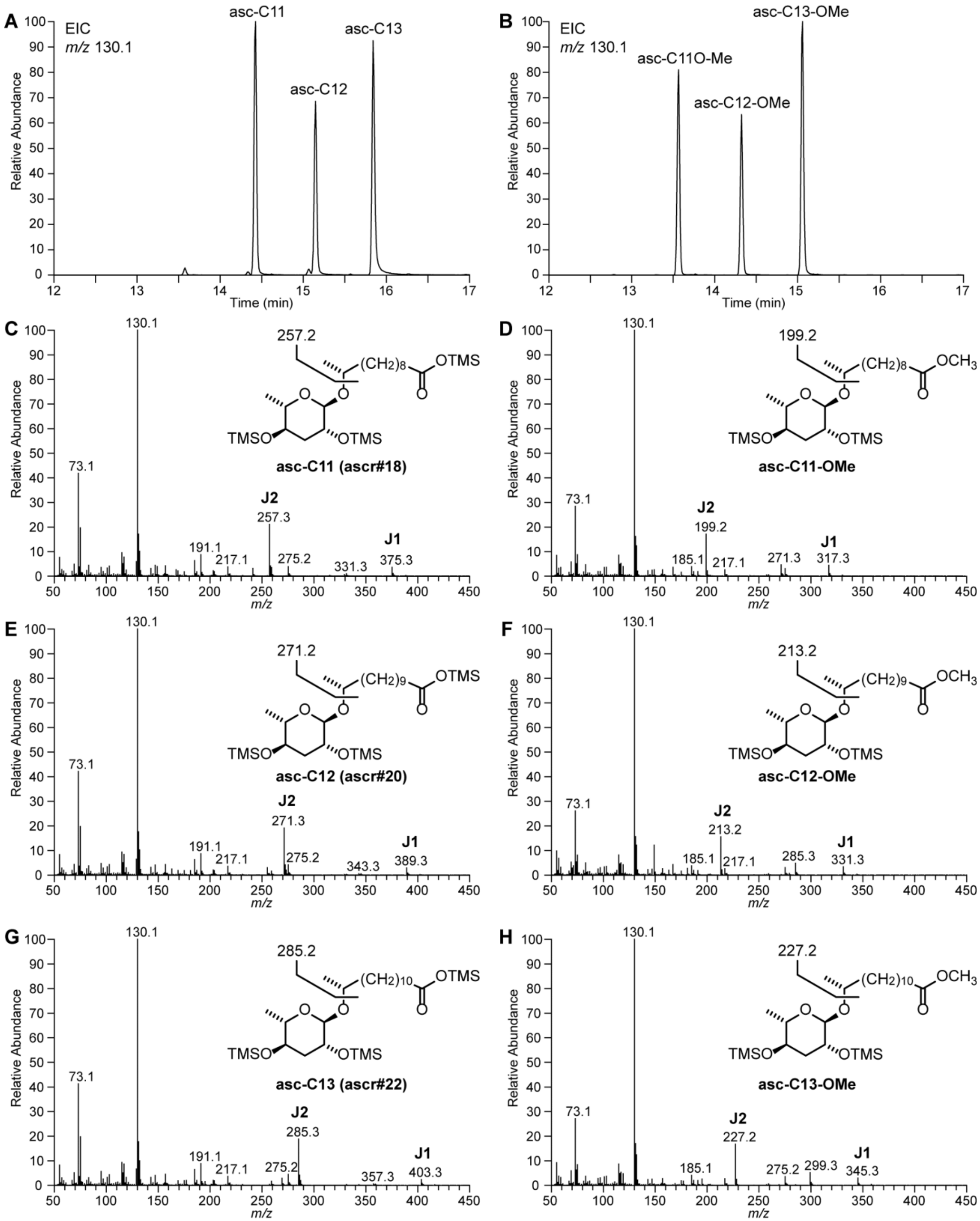

Figure S6: Ascaroside profiling of *exo*-metabolome fractions from the *C. elegans acox-1* mutant using EICs for the K1-fragment at *m/z* 130.1 $[C_6H_{14}OSi]^{+\bullet}$.

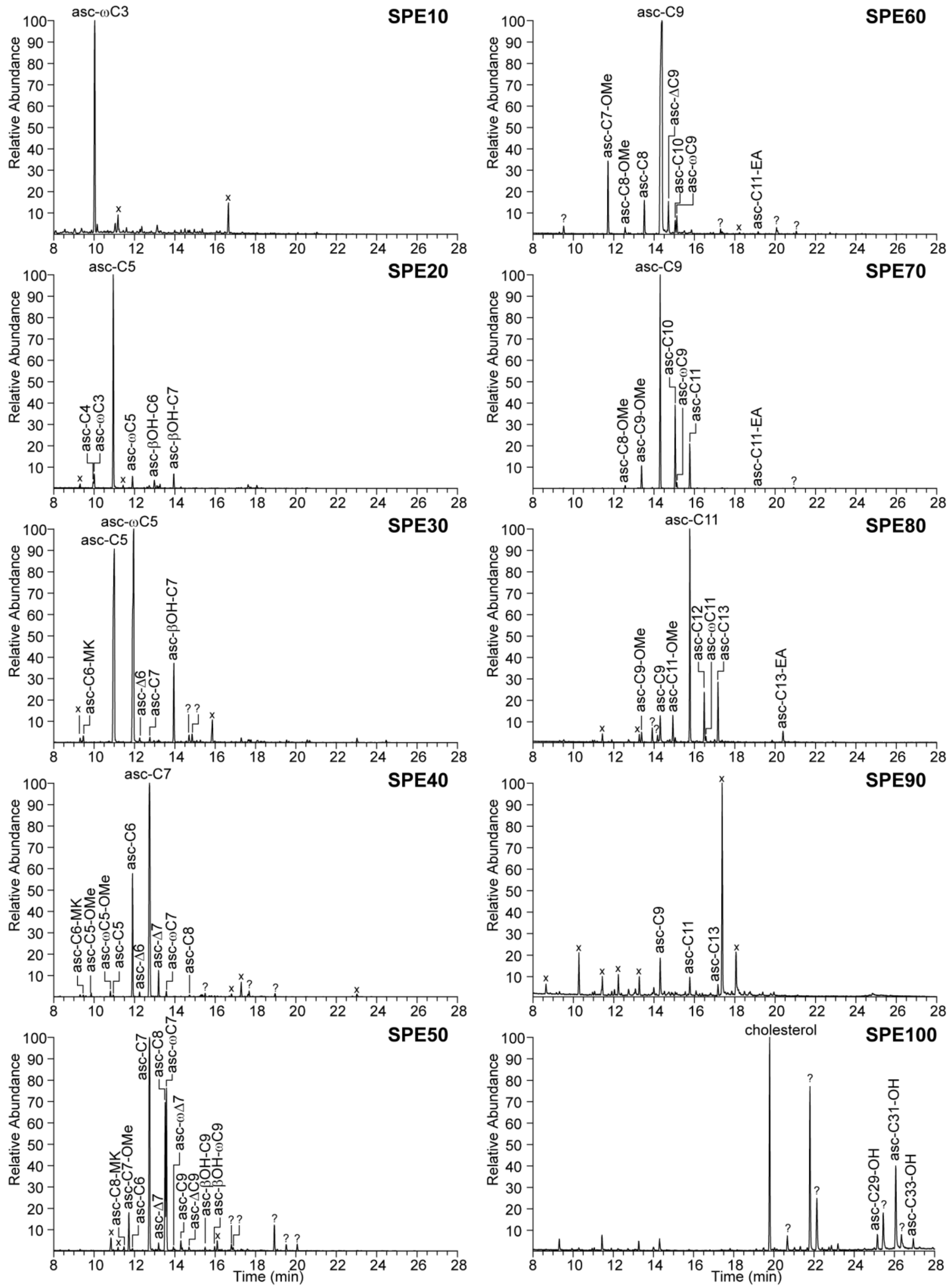

Figure S7a: Plots of GC Kovats retention indices versus length of the side chain.

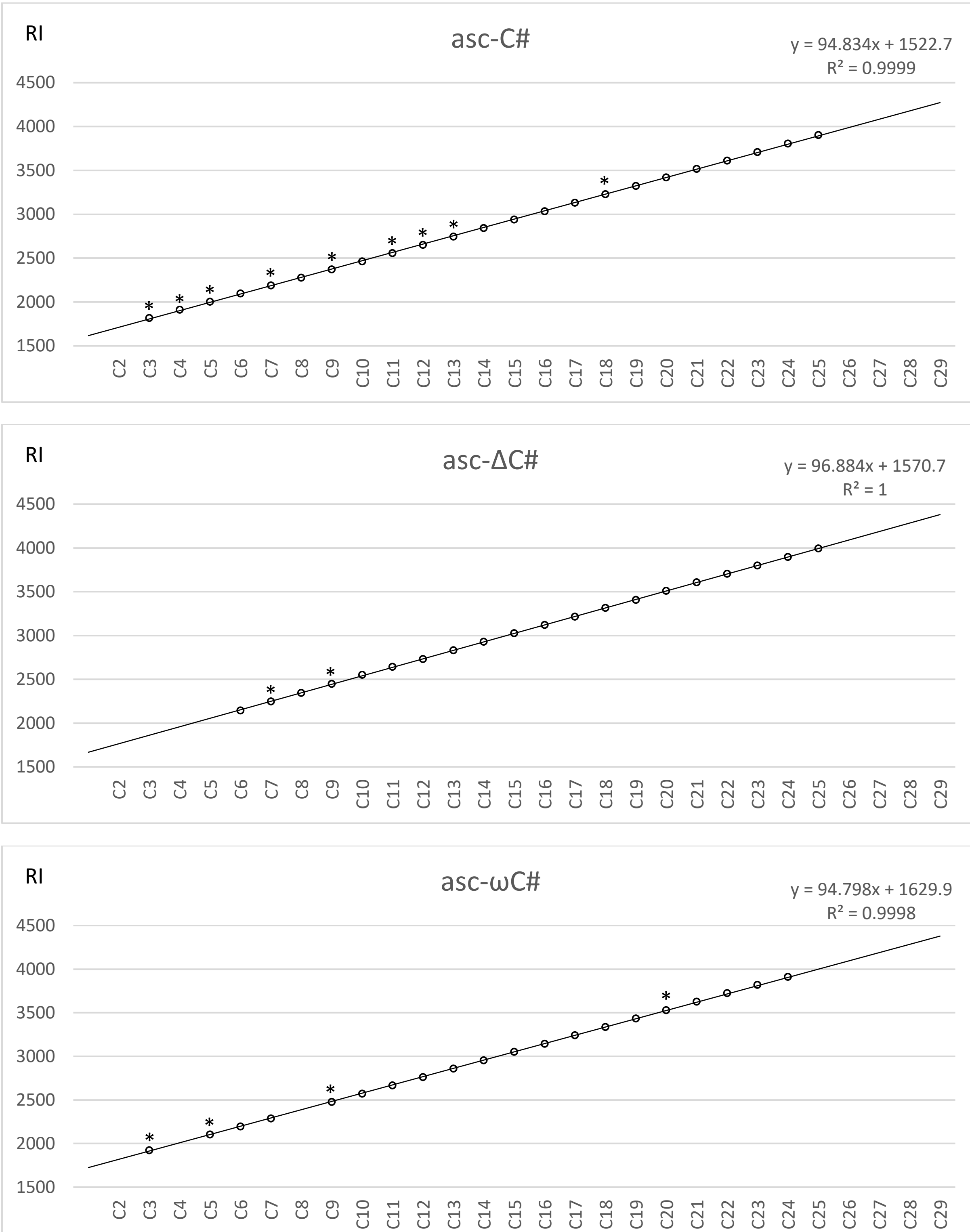

***: confirmed using an authentic standard**

Figure S7b: Plots of GC Kovats retention indices versus length of the side chain.

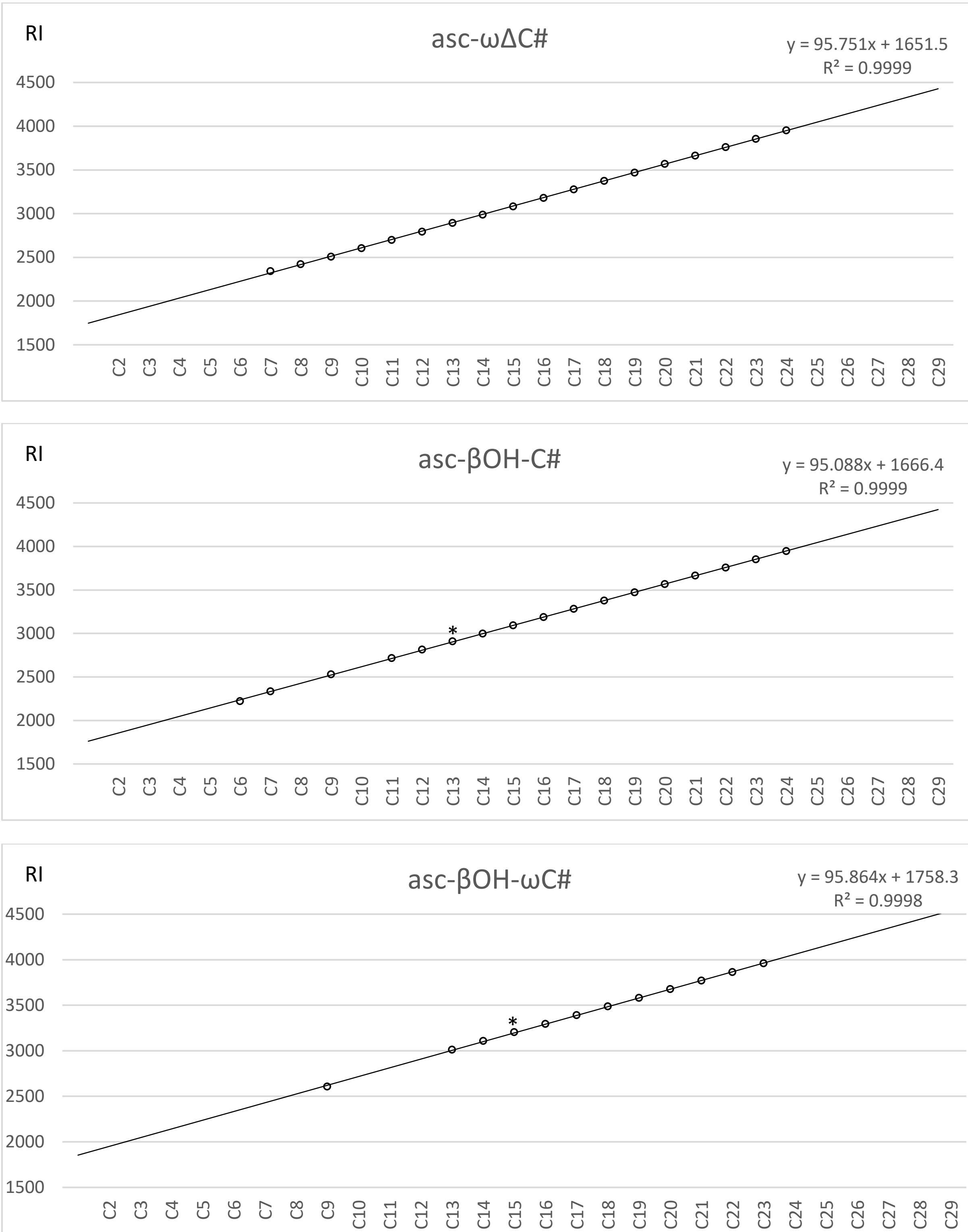

***: confirmed using an authentic standard**

Figure S7c: Plots of GC Kovats retention indices versus length of the side chain.

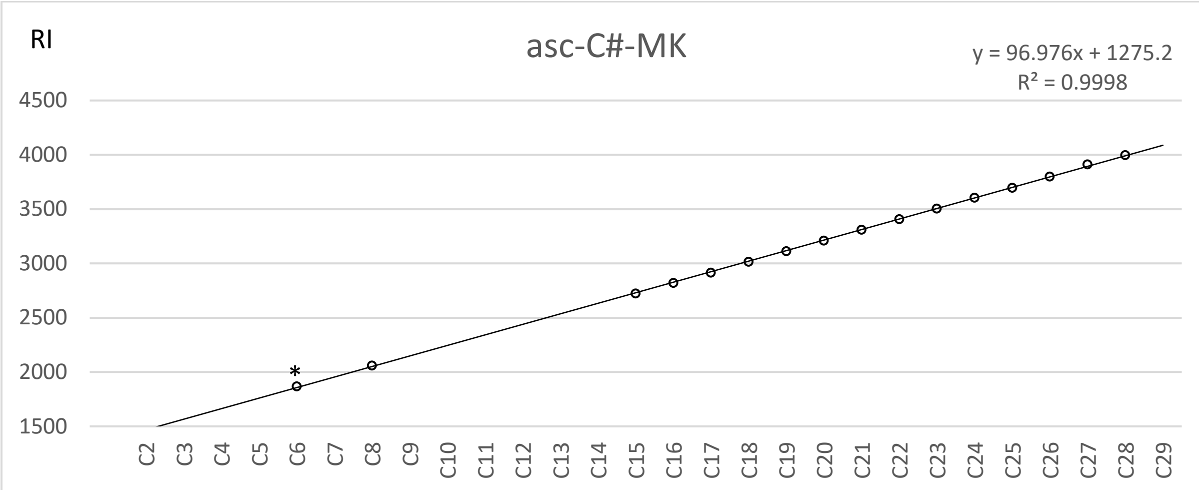

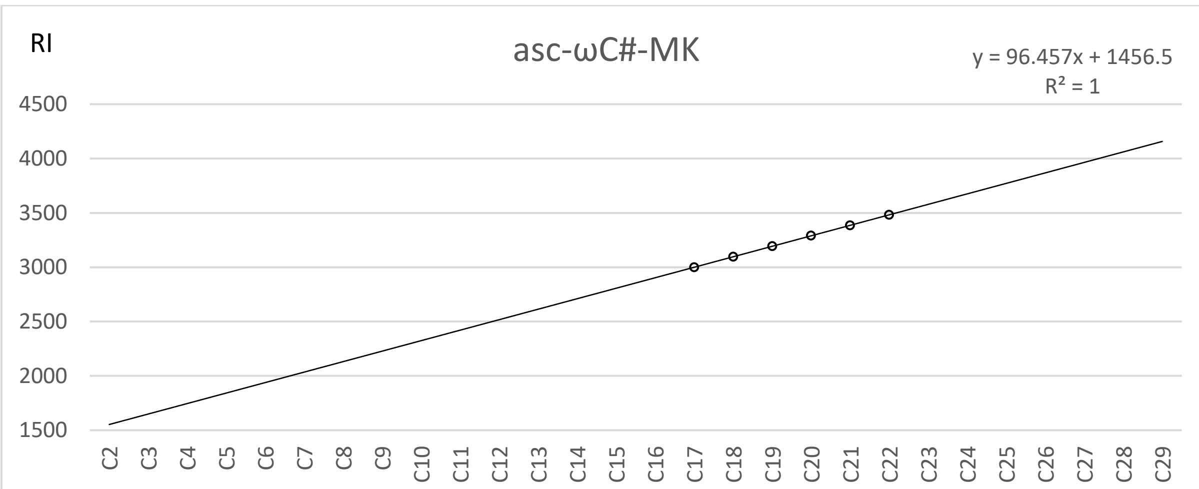

***: confirmed using an authentic standard**

Figure S8a: Assignment of β-hydroxyacyl ascarosides (asc-βOH-C#) and their α-methyl isomers (asc-βOH-*i*C24 and asc-βOH-*i*C26) based on combined screening for (A): the ascaroside-specific K1-fragment at *m/z* 130.1 $[C_6H_{14}OSi]^{+\bullet}$, along with (B): characteristic fragments at *m/z* 233.1 $[C_9H_{21}O_3Si_2]^+$ or (C): *m/z* 247.1 $[C_{10}H_{23}O_3Si_2]^+$ from α-cleavage.

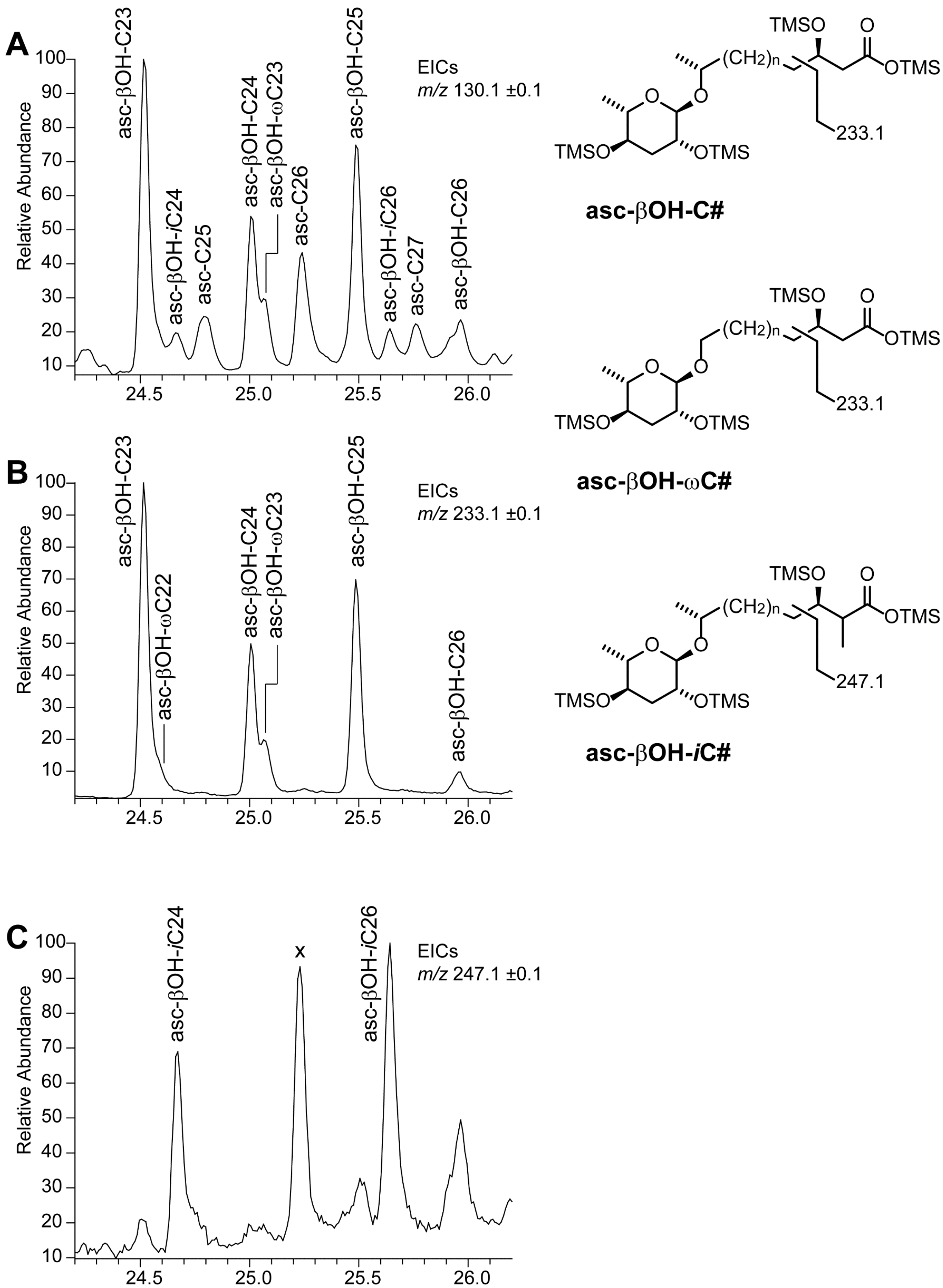

Figure S8b: EIMS spectra of TMS-derivatized β-hydroxyacyl ascarosides (asc-βOH-C#) characterized by a fragment ion at *m/z* 233.1 $[C_9H_{21}O_3Si_2]^+$ from α-cleavage (A-D) and their α-methyl derivatives, asc-βOH-*i*C24 and asc-βOH-*i*C26 (E & F) characterized by the homologous fragment ion at *m/z* 247.1 $[C_{10}H_{23}O_3Si_2]^+$ as well as a fragment ion at *m/z* 218.1 $[C_9H_{22}O_2Si_2]^{+\bullet}$ from McLafferty-type TMS transfer.

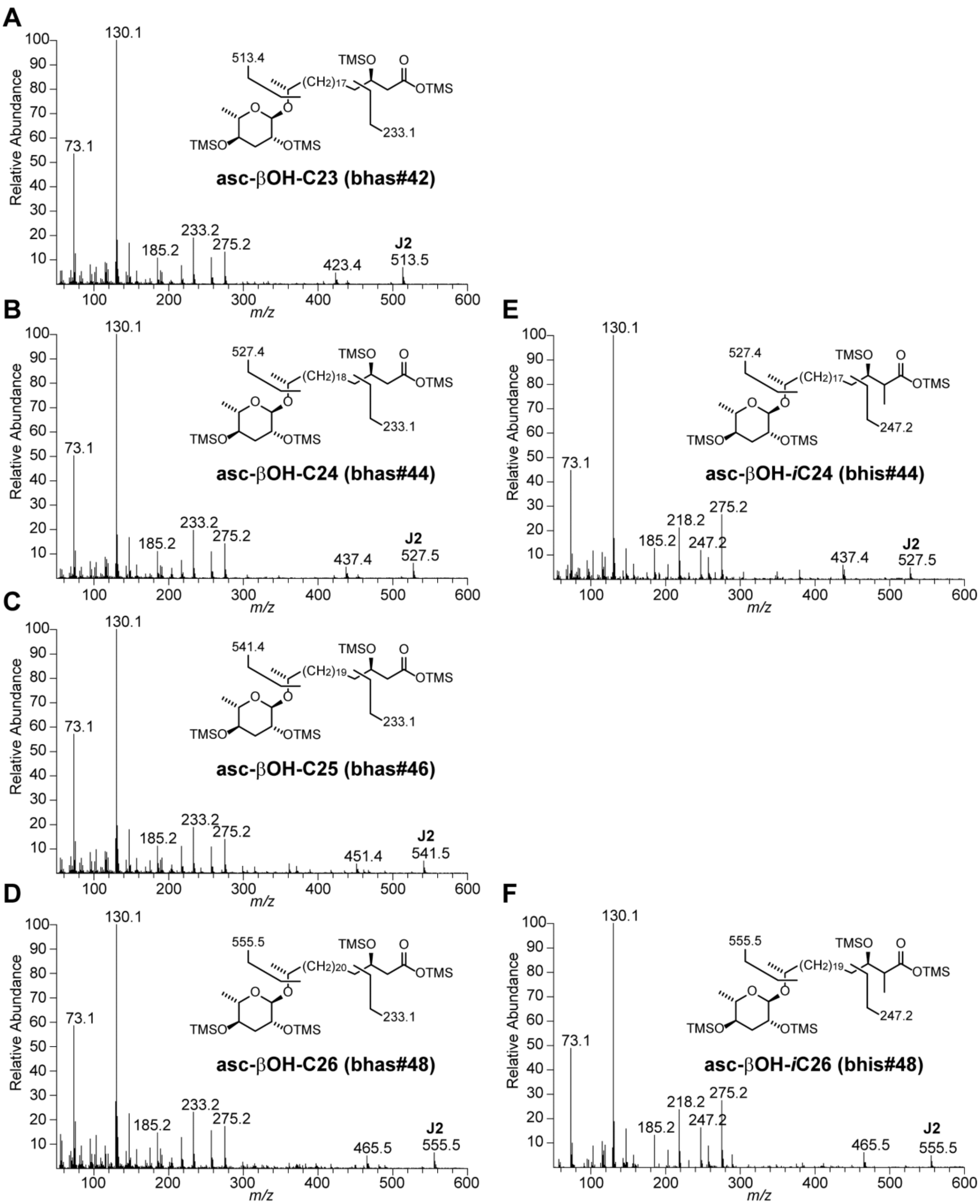

Figure S9: Assignment of acyl ascarosides (asc-C#) along with their α-methyl isomers (asc-*i*C24 and asc-*i*C26). (A): EIC for the K1-fragment at *m/z* 130.1 $[C_6H_{14}OSi]^{+\bullet}$ shows diverse ascarosides in a *daf-22 exo*-metabolome fraction; (B) EICs for J1 fragments at [M-173] show (ω-1)- and (ω)-linked long chain ascarosides; (C) EICs for J2 fragments at [M-291] show almost exclusively (ω-1)-linked long chain ascarosides along with two α-methyl branched isomers, asc-*i*C24 (iscr#44) and asc-*i*C26 (iscr#48); (D) EICs for enoyl ascarosides reveal signals for asc-Δ*i*C24 (iscr#43) and asc-Δ*i*C26 (iscr#47).

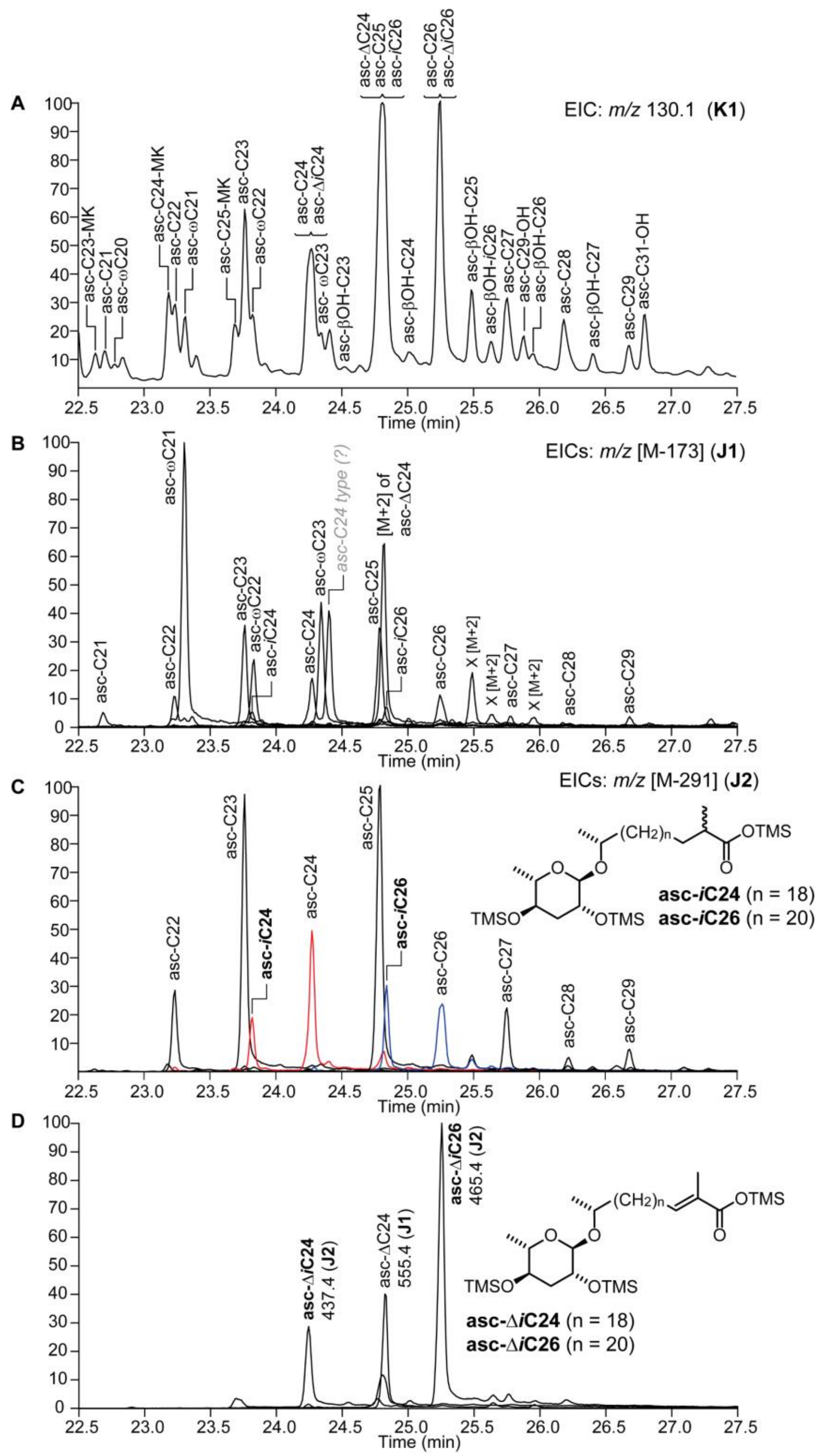

Figure S10: GC-EIMS spectra of TMS-derivatized α-methyl branched *iso*-enoyl ascarosides, asc-Δ*i*C24 (iscr#43) and asc-Δ*i*C26 (iscr#47).

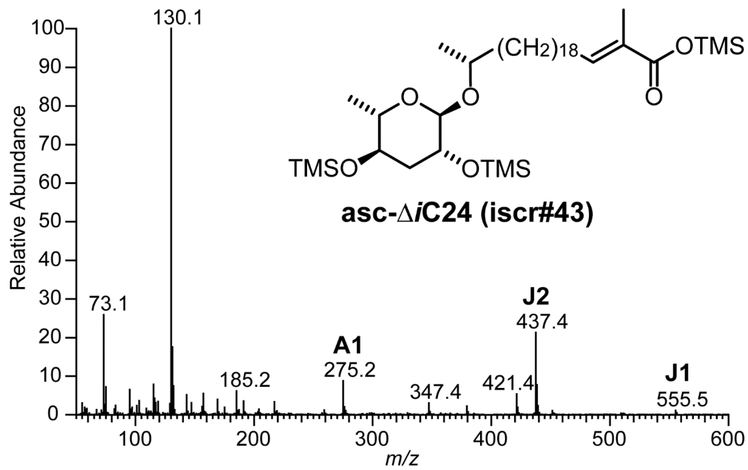

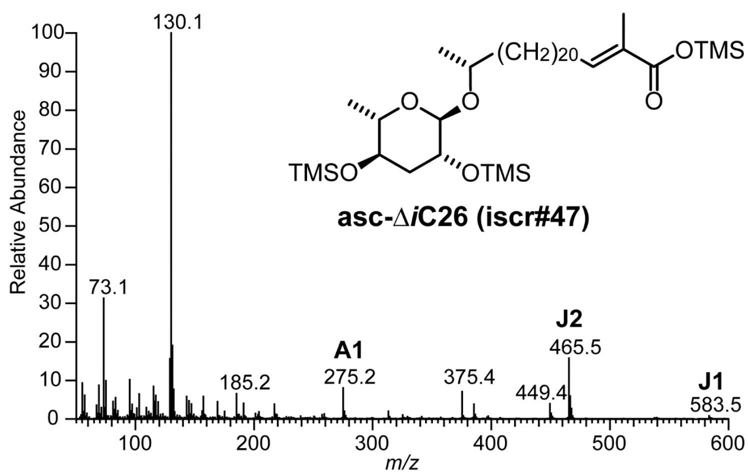

Figure S11: Assignment of β-hydroxyacyl ascaroside ethanolamide and an α-methyl derivative based on combined screening for (A): the ascaroside-specific K1-fragment at *m/z* 130.1 $[C_6H_{14}OSi]^{+\bullet}$, along with (B): *m/z* 276.2 $[C_{11}H_{26}NO_3Si_2]^+$ and *m/z* 290.2 $[C_{12}H_{28}NO_3Si_2]^+$ as well as (C): *m/z* 348.2 $[C_{14}H_{34}NO_3Si_3]^+$ and *m/z* 362.2 $[C_{15}H_{36}NO_3Si_3]^+$ from α-cleavage, and (D): the J2-fragment ion signals at *m/z* 584.5 $[C_{33}H_{70}NO_3Si_2]^+$ and *m/z* 598.5 $[C_{34}H_{72}NO_3Si_2]^+$. EIMS spectra of TMS-derivatized asc-βOH-C25-EA (ebha#46) (E) and the α-methyl homolog asc-βOH-*i*C26-EA (ebhi#48) (F).

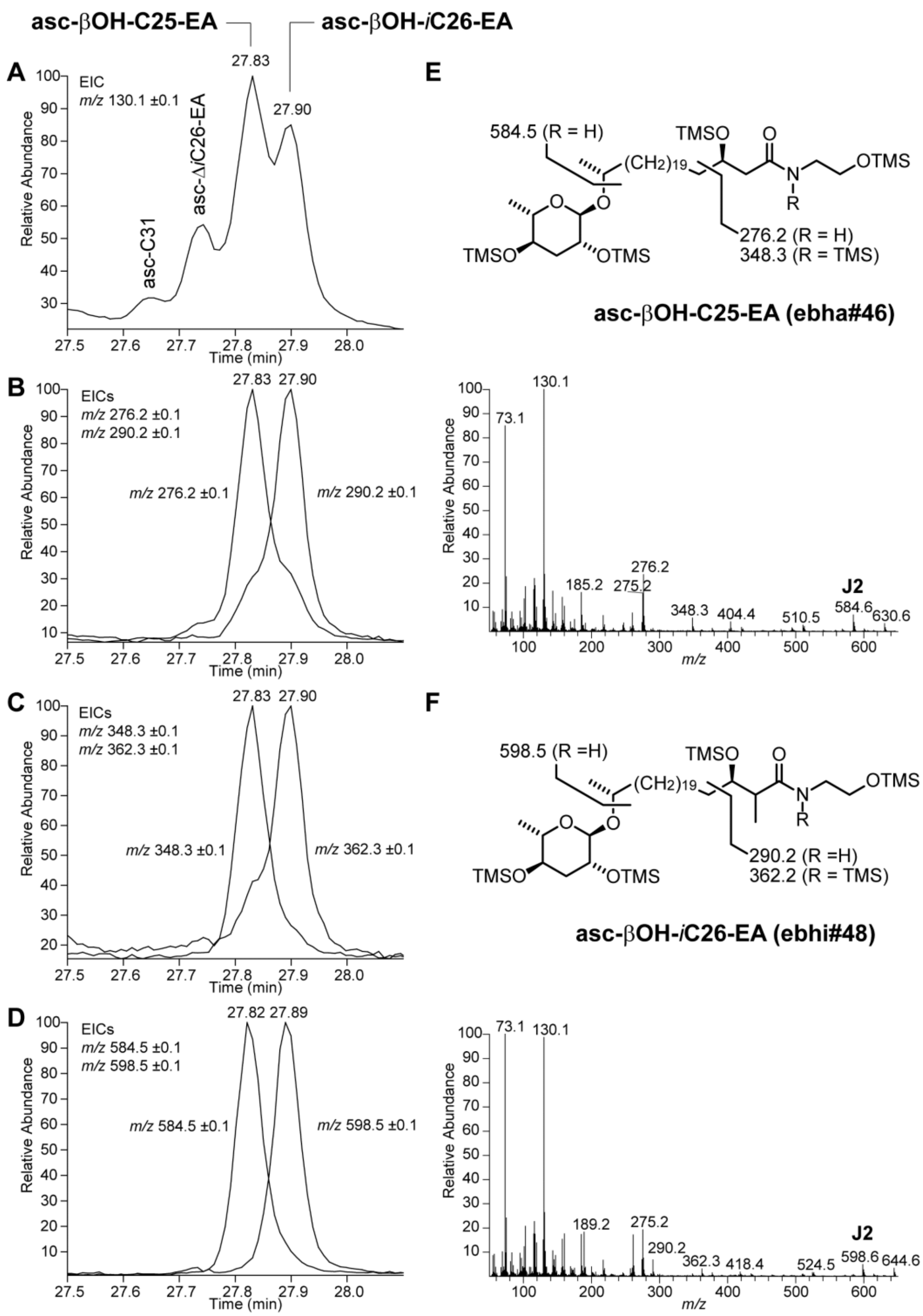

Figure S12: EIMS spectra of TMS-derivatized enoyl ascaroside ethanolamides.

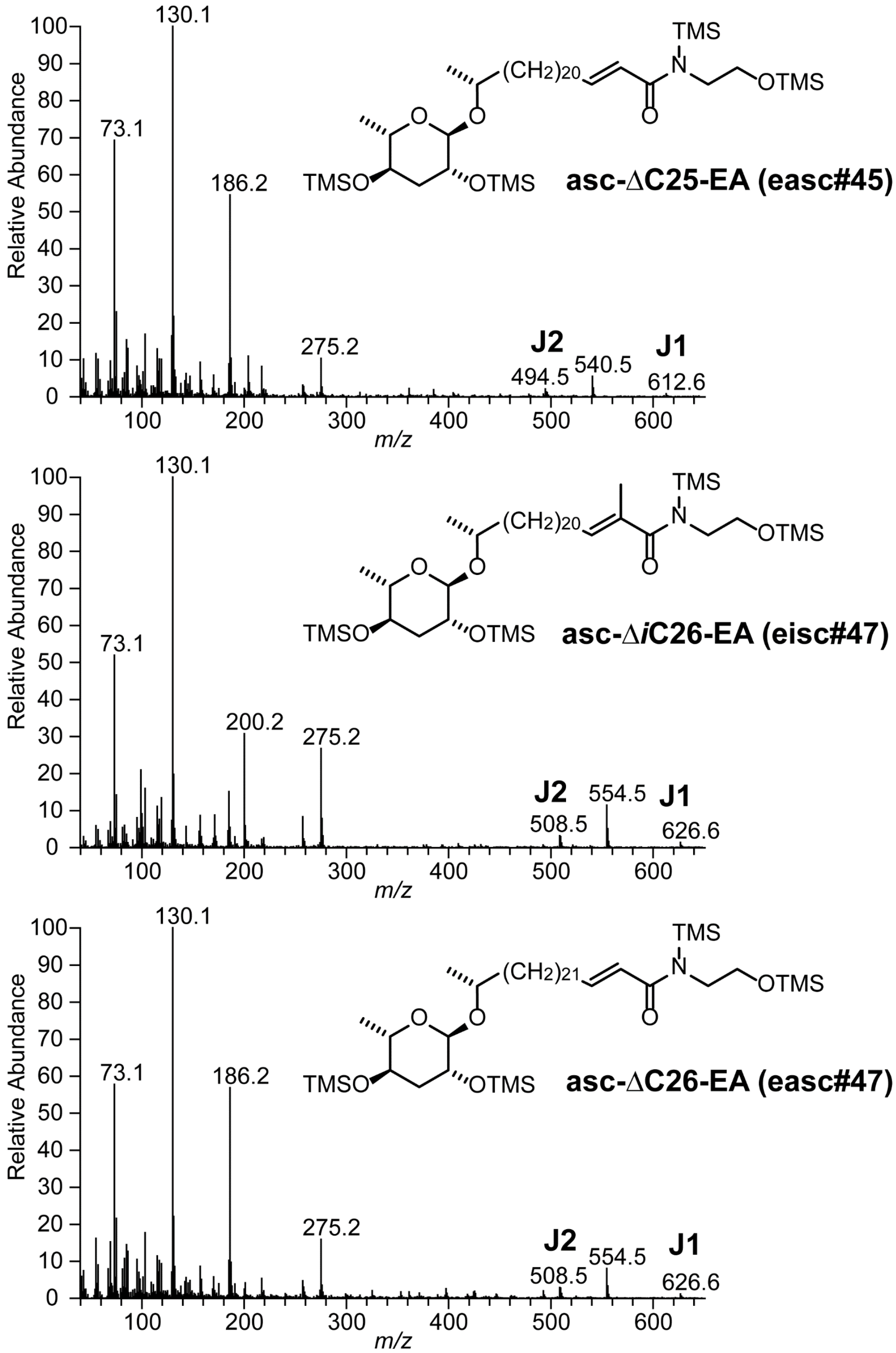

Figure S13a: EIMS spectra of TMS-derivatized (ω)- and (ω-1)-acyl ascarosides.

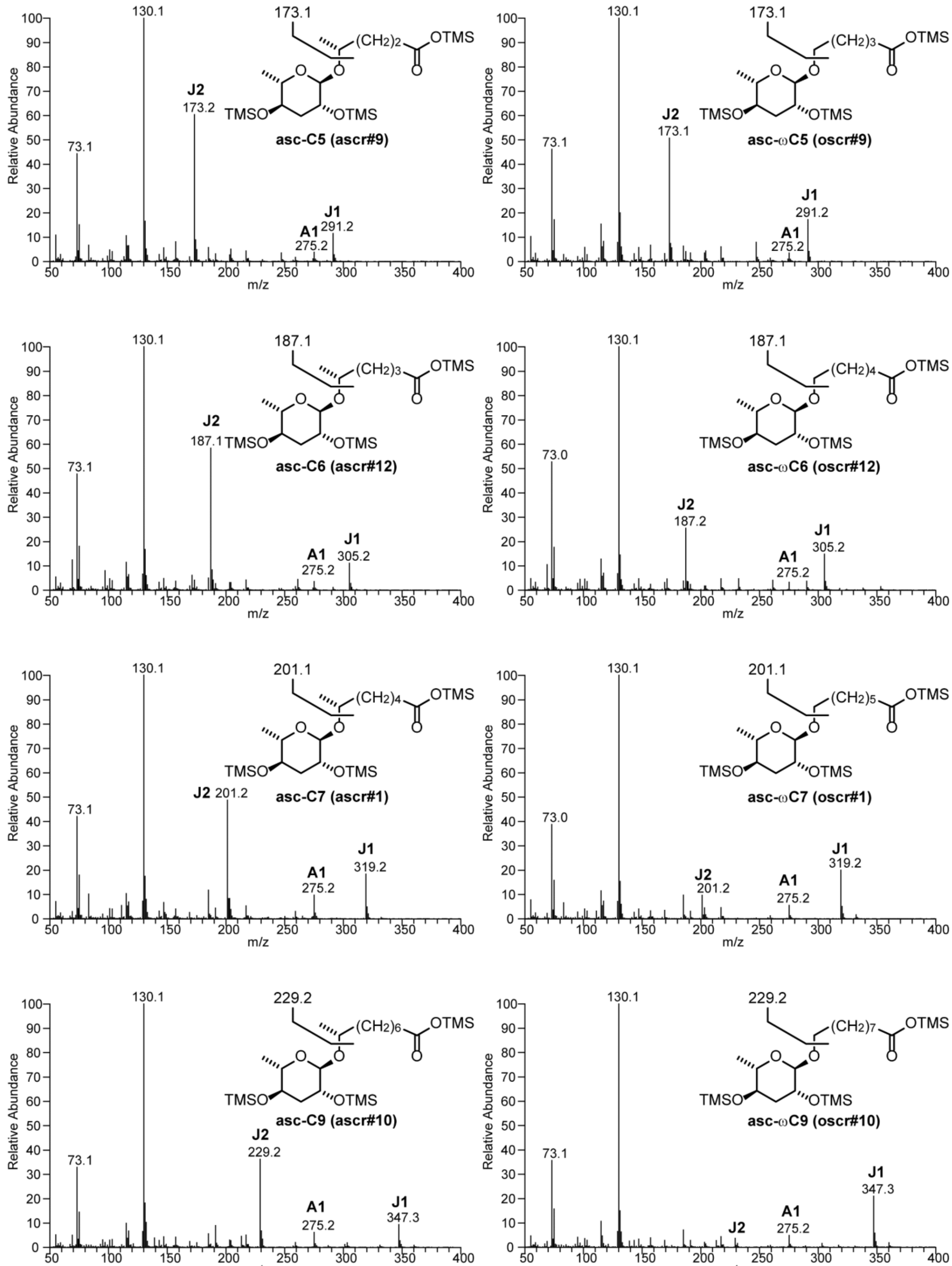

Figure S13b: EIMS spectra of TMS-derivatized (ω)- and (ω-1)-acyl and β-hydroxyacyl ascarosides

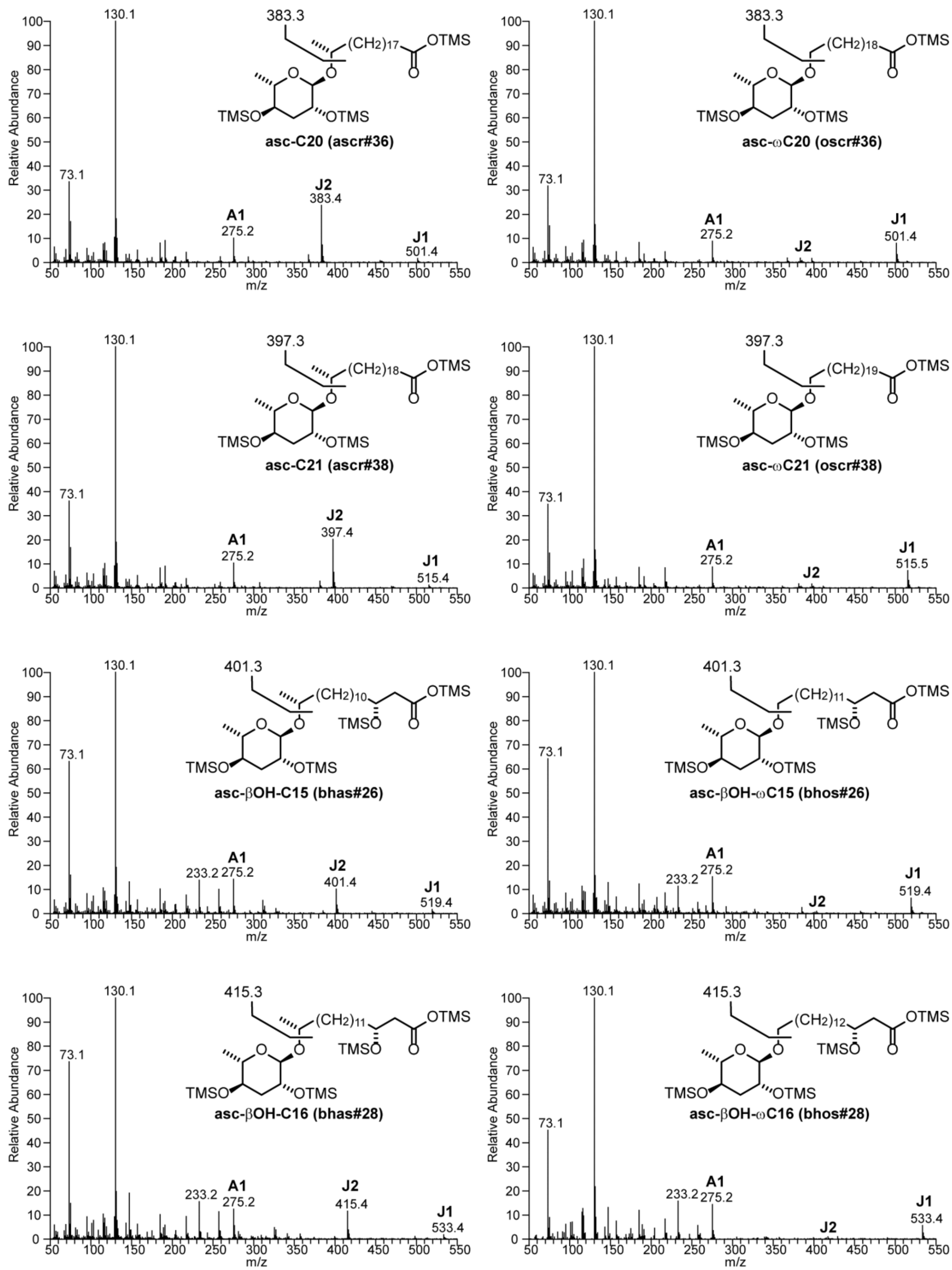

Figure S14: Ascaroside profiling of lipophilic *exo*-metabolome fractions of *C. elegans* wild type and peroxisomal β-oxidation mutants using the K1-fragment at *m/z* 130.1 $[C_6H_{14}OSi]^{+\bullet}$ shows that the production of very long chain 2-hydroxyalkyl ascarosides with asc-C31-OH as the dominating component is independent of *aocx-1*, *maoc-1*, *dhs-28*, and *daf-22*.

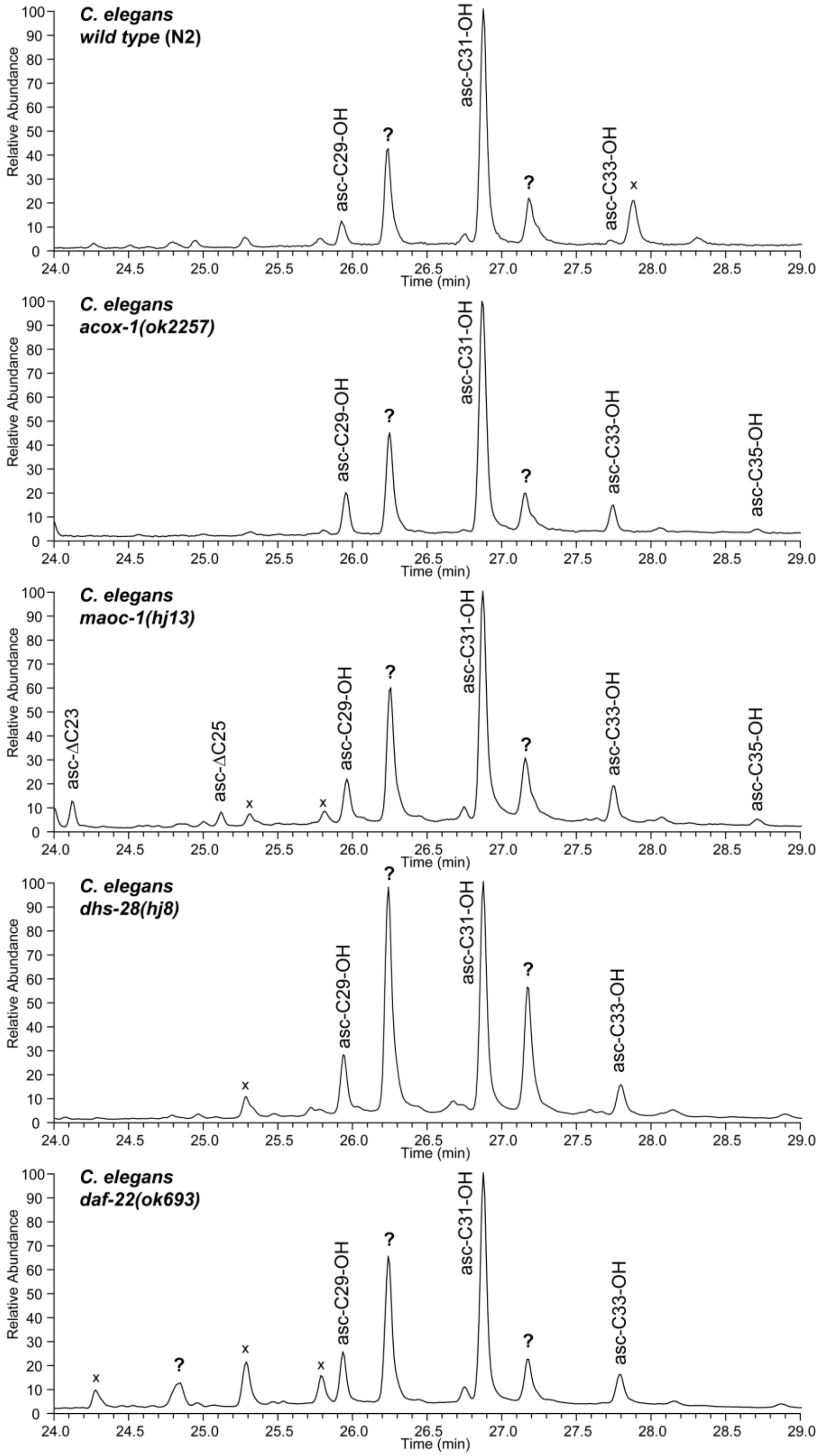

Table S1: Characteristic EIMS fragment ion signals and GC Kovats retention indices for TMS-derivatized (ω-1)-linked acyl ascarosides (**asc-C#**) detected by combined screening for the K1-fragment at *m/z* 130.1 $[C_6H_{14}OSi]^{+\bullet}$ and the J1 and J2 fragment ion signals.

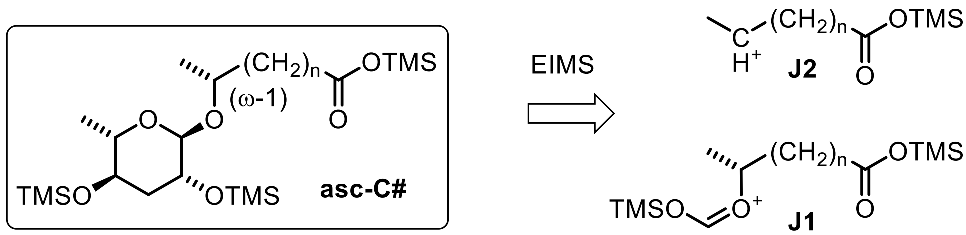

SMID	n	side chain	J1 *m/z* [M-173]	J2 *m/z* [M-291]	Kovats RI	WT	*acox-1*	*maoc-1*	*dhs-28*	*daf-22*
*none**§	0	C3	263.1	(145.1)	1818	-	-	-	-	-
ascr#11*	1	C4	277.1	159.1	1912	+	-	-	-	-
ascr#9*	2	C5	291.1	173.1	2003	+	+	-	-	-
ascr#12	3	C6	305.2	187.1	2099	+	+	-	-	-
ascr#1*	4	C7	319.2	201.1	2190	+	+	-	-	-
ascr#14	5	C8	333.2	215.1	2278	+	+	-	-	-
ascr#10*	6	C9	347.2	229.2	2372	+	+	+	+	-
ascr#16	7	C10	361.2	243.2	2464	+	+	+	+	+
ascr#18*	8	C11	375.2	257.2	2557	+	+	+	+	+
ascr#20*	9	C12	389.3	271.2	2653	+	+	+	+	+
ascr#22*	10	C13	403.3	285.2	2747	+	+	+	+	+
ascr#24	11	C14	417.3	299.2	2843	-	+	+	+	+
ascr#26	12	C15	431.3	313.3	2939	+	+	+	+	+
ascr#28	13	C16	445.3	327.3	3035	-	+	+	+	+
ascr#30	14	C17	459.3	341.3	3130	+	+	+	+	+
ascr#32*	15	C18	473.3	355.3	3228	-	+	+	+	+
ascr#34	16	C19	487.4	369.3	3322	-	+	+	+	+
ascr#36	17	C20	501.4	383.3	3419	-	-	+	+	+
ascr#38	18	C21	515.4	397.3	3517	-	+	+	+	+
ascr#40	19	C22	529.4	411.4	3613	-	-	-	+	+
ascr#42	20	C23	543.4	425.4	3710	-	-	+	+	+
ascr#44	21	C24	557.4	439.4	3806	-	-	-	+	+
ascr#46	22	C25	571.5	453.4	3904	-	-	+	+	+
ascr#48	23	C26	585.5	467.4	(>4000)	-	-	-	-	+
ascr#50	24	C27	599.5	481.4	(>4000)	-	-	-	+	+
ascr#52	25	C28	613.5	495.5	(>4000)	-	-	-	-	+
ascr#54	26	C29	627.5	509.5	(>4000)	-	-	-	-	+
ascr#56	27	C30	641.5	523.5	(>4000)	-	-	-	-	+
ascr#58	28	C31	(655.6)	537.5	(>4000)	-	-	-	-	+
ascr#60	29	C32	(669.6)	551.5	(>4000)	-	-	-	-	+
ascr#62	30	C33	(683.6)	565.5	(>4000)	-	-	-	-	+

[*]: confirmed using an authentic standard, [§]: not identified as natural product

Table S2: Characteristic EIMS fragment ion signals and GC Kovats retention indices for TMS-derivatized (ω)-linked acyl ascarosides (**asc-ωC#**) detected by combined screening for the K1-fragment at *m/z* 130.1 $[C_6H_{14}OSi]^{+\bullet}$ and the J1 (and J2) fragment ion signals.

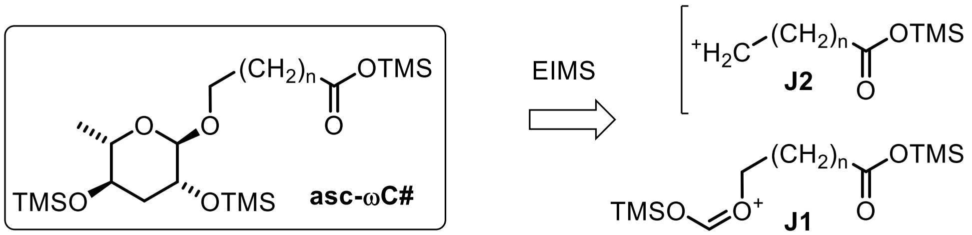

SMID	n	side chain	J1 *m/z* [M-173]	J2[a] *m/z* [M-291]	Kovats RI	WT	*acox-1*	*maoc-1*	*dhs-28*	*daf-22*
ascr#5*	1	ωC3	263.1	(145.1)	1920	+	-	-	-	-
oscr#11	2	ωC4	277.1	159.1	*nd*	-	-	-	-	-
oscr#9*	3	ωC5	291.1	173.1	2102	+	+	-	-	-
oscr#12	4	ωC6	305.2	187.1	2193	+	+	-	-	-
oscr#1	5	ωC7	319.2	201.1	2285	+	+	-	-	-
oscr#14	6	ωC8	333.2	215.1	*nd*	-	-	-	-	-
oscr#10*	7	ωC9	347.2	229.2	2475	+	+	+	+	-
oscr#16	8	ωC10	361.2	243.2	2569	-	+	+	+	+
oscr#18	9	ωC11	375.2	257.2	2665	+	+	+	+	+
oscr#20	10	ωC12	389.3	271.2	2760	-	+	+	+	+
oscr#22	11	ωC13	403.3	285.2	2857	-	+	+	+	+
oscr#24	12	ωC14	417.3	299.2	2952	-	+	+	+	+
oscr#26	13	ωC15	431.3	313.3	3049	-	+	+	+	+
oscr#28	14	ωC16	445.3	327.3	3143	-	-	+	+	+
oscr#30	15	ωC17	459.3	341.3	3241	-	+	+	+	+
oscr#32	16	ωC18	473.3	355.3	3336	-	-	+	+	+
oscr#34	17	ωC19	487.4	369.3	3433	-	+	+	+	+
oscr#36*	18	ωC20	501.4	383.3	3529	-	-	+	+	+
oscr#38	19	ωC21	515.4	397.3	3625	-	-	+	+	+
oscr#40	20	ωC22	529.4	411.4	3722	-	-	+	+	+
oscr#42	21	ωC23	543.4	425.4	3817	-	-	+	+	+

[*]: confirmed using an authentic standard; [a]: low intensity.

Table S3: Characteristic EIMS fragment ion signals and GC Kovats retention indices for TMS-derivatized α-methyl-branched (ω-1)-linked *iso*-acyl ascarosides (**asc-*iC#***) detected by combined screening for *m/z* 130.1 $[C_6H_{14}OSi]^{+\bullet}$ and the J1 and J2 fragment ion signals (Figure S9).

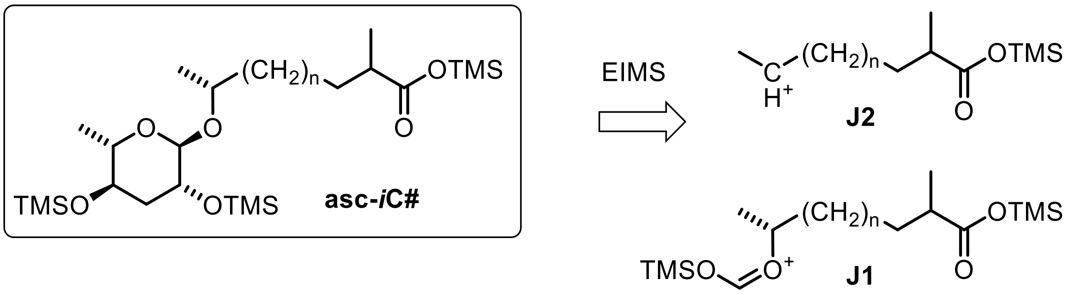

SMID	n	side chain	J1 *m/z* [M-173]	J2 *m/z* [M-291]	Kovats RI	WT	*acox-1*	*maoc-1*	*dhs-28*	*daf-22*
iscr#44	18	*i*C24	557.4	439.4	3723	-	-	-	-	+
iscr#48	20	*i*C26	585.5	467.4	3918	-	-	-	-	+

Table S4: Characteristic EIMS fragment ion signals and GC Kovats retention indices for TMS-derivatized (ω-1)-linked enoyl ascarosides (**asc-ΔC#**) detected by combined screening for the K1-fragment at *m/z* 130.1 $[C_6H_{14}OSi]^{+\bullet}$ and the J1 and J2 fragment ion signals.

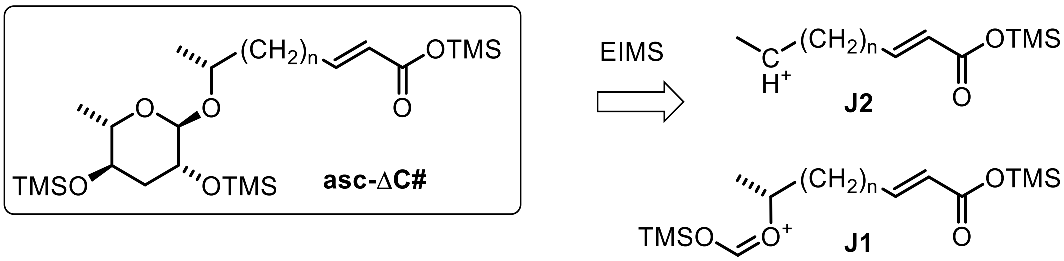

SMID	n	side chain	J1 *m/z* [M-173]	J2 *m/z* [M-291]	Kovats RI	WT	*acox-1*	*maoc-1*	*dhs-28*	*daf-22*
none	1	ΔC6	303.1	185.1	2144	+	-	-	-	-
ascr#7*	2	ΔC7	317.2	199.1	2245	+	-	-	-	-
ascr#13	3	ΔC8	331.2	213.1	2343	+	-	-	-	-
ascr#3*	4	ΔC9	345.2	227.1	2447	+	+	+	-	-
ascr#15	5	ΔC10	359.2	241.2	2549	-	-	+	-	-
ascr#17	6	ΔC11	373.2	255.2	2643	+	-	+	+	-
ascr#19	7	ΔC12	387.2	269.2	2731	-	-	+	+	-
ascr#21	8	ΔC13	401.3	283.2	2832	-	-	+	+	-
ascr#23	9	ΔC14	415.3	297.2	2928	-	-	+	+	-
ascr#25	10	ΔC15	429.3	311.2	3025	-	+	+	+	+
ascr#27	11	ΔC16	443.3	325.3	3121	-	-	+	+	+
ascr#29	12	ΔC17	457.3	339.3	3215	-	+	+	+	+
ascr#31	13	ΔC18	471.3	353.3	3315	-	-	+	+	+
ascr#33	14	ΔC19	485.3	367.3	3405	-	-	+	+	+
ascr#35	15	ΔC20	499.4	381.3	3509	-	-	+	+	+
ascr#37	16	ΔC21	513.4	395.3	3606	-	-	+	+	+
ascr#39	17	ΔC22	527.4	409.3	3704	-	-	+	+	+
ascr#41	18	ΔC23	541.4	423.4	3798	-	-	+	+	+
ascr#43	19	ΔC24	555.4	437.4	3896	-	-	+	+	+
ascr#45	20	ΔC25	569.4	451.4	3992	-	-	+	+	+

[*]: confirmed using an authentic standard

Table S5: Characteristic EIMS fragment ion signals and GC Kovats retention indices for TMS-derivatized (ω)-linked enoyl ascarosides (**asc-ωΔC#**) detected by combined screening for the K1-fragment at *m/z* 130.1 $[C_6H_{14}OSi]^{+\bullet}$ and the J1 (and J2)[a] fragment ion signals.

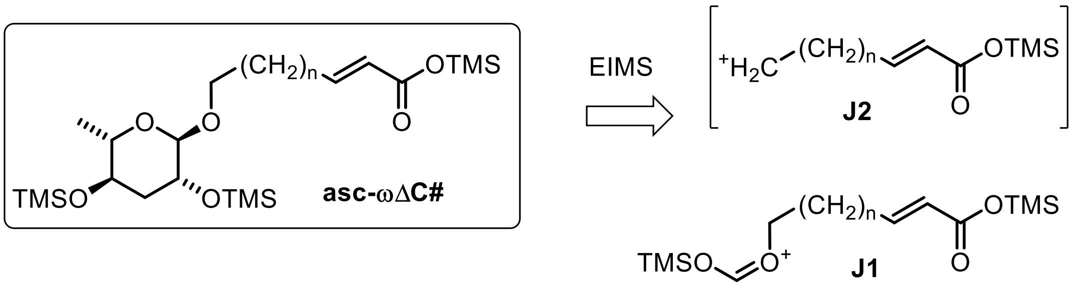

SMID	n	side chain	J1 *m/z* [M-173]	J2[a] *m/z* [M-291]	Kovats RI	WT	*acox-1*	*maoc-1*	*dhs-28*	*daf-22*
oscr#7	3	ωΔC7	317.2	199.1	2342	-	+	-	-	-
oscr#13	4	ωΔC8	331.2	213.1	2421	-	-	-	-	-
oscr#3	5	ωΔC9	345.2	227.1	2509	-	+	+	-	-
oscr#15	6	ωΔC10	359.2	241.2	2605	-	-	+	-	-
oscr#17	7	ωΔC11	373.2	255.2	2698	-	+	+	+	-
oscr#19	8	ωΔC12	387.2	269.2	2794	-	-	+	-	-
oscr#21	9	ωΔC13	401.3	283.2	2893	-	-	+	+	-
oscr#23	10	ωΔC14	415.3	297.2	2988	-	-	+	+	-
oscr#25	11	ωΔC15	429.3	311.2	3084	-	-	+	+	-
oscr#27	12	ωΔC16	443.3	325.3	3181	-	-	+	+	-
oscr#29	13	ωΔC17	457.3	339.3	3278	-	-	+	+	+
oscr#31	14	ωΔC18	471.3	353.3	3375	-	-	+	+	-
oscr#33	15	ωΔC19	485.3	367.3	3470	-	-	+	+	+
oscr#35	16	ωΔC20	499.4	381.3	3569	-	-	+	-	-
oscr#37	17	ωΔC21	513.4	395.3	3665	-	-	+	+	+
oscr#39	18	ωΔC22	527.4	409.3	3760	-	-	+	-	-
oscr#41	19	ωΔC23	541.4	423.4	3856	-	-	+	-	-

[a]: low intensity

Table S6: Characteristic EIMS fragment ion signals and GC Kovats retention indices for TMS-derivatized α-methyl-branched (ω-1)-linked *iso*-enoyl ascarosides (**asc-Δ*i*C#**) detected by combined screening for the K1-fragment at *m/z* 130.1 $[C_6H_{14}OSi]^{+\bullet}$ and the J1 and J2 fragment ion signals (Figure S9-10).

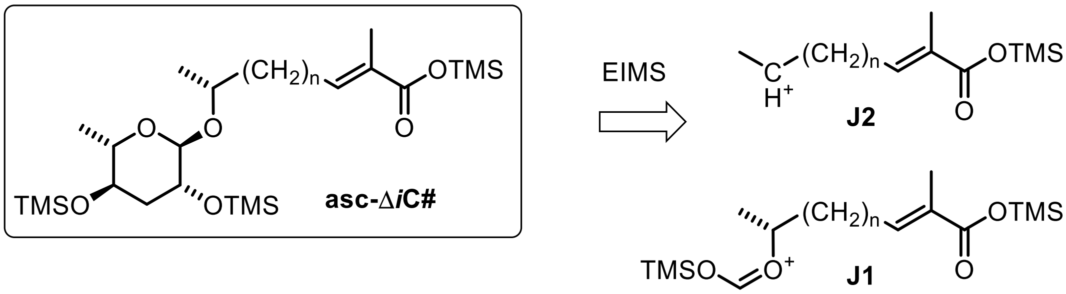

SMID	n	side chain	J1 *m/z* [M-173]	J2 *m/z* [M-291]	Kovats RI	**WT**	***acox-1***	***maoc-1***	***dhs-28***	***daf-22***
iscr#43	18	Δ*i*C24	555.4	437.4	3801	-	-	-	-	+
iscr#47	20	Δ*i*C26	583.5	465.4	(>4000)	-	-	-	-	+

Table S7: Characteristic EIMS fragment ion signals and GC Kovats retention indices for TMS-derivatized (ω-1)-linked β-hydroxyacyl ascarosides (**asc-βOH-C#**) detected by combined screening for the K1-fragment at *m/z* 130.1 $[C_6H_{14}OSi]^{+\bullet}$ and *m/z* 233.1 $[C_9H_{21}O_3Si_2]^+$ from α-cleavage, as well as the J1 and J2 fragment ion signals (Figure S8).

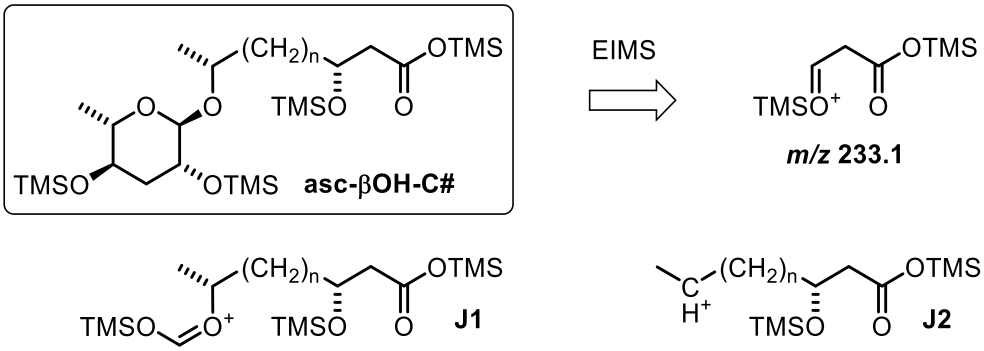

SMID	n	side chain	J1 *m/z* [M-173]	J2 *m/z* [M-291]	Kovats RI	**WT**	***acox-1***	***maoc-1***	***dhs-28***	***daf-22***
bhas#12	1	βOH-C6	393.2	275.1	2221	-	+	-	-	-
bhas#1	2	βOH-C7	407.2	289.2	2333	-	+	-	-	-
bhas#14	3	βOH-C8	421.2	303.2	*nd*	-	-	-	-	-
bhas#10	4	βOH-C9	435.2	317.2	2529	-	+	-	-	-
bhas#16	5	βOH-C10	449.3	331.2	*nd*	-	-	-	-	-
bhas#18	6	βOH-C11	463.3	345.2	2717	-	+	+	+	-
bhas#20	7	βOH-C12	477.3	359.2	2813	-	-	+	+	-
bhas#22*	8	βOH-C13	491.3	373.3	2908	-	+	+	+	-
bhas#24	9	βOH-C14	505.3	387.3	2999	-	-	+	+	+
bhas#26	10	βOH-C15	519.3	401.3	3094	-	+	+	+	+
bhas#28	11	βOH-C16	533.4	415.3	3187	-	-	+	+	+
bhas#30	12	βOH-C17	547.4	429.3	3282	-	+	+	+	+
bhas#32	13	βOH-C18	561.4	443.3	3376	-	-	+	+	+
bhas#34	14	βOH-C19	575.4	457.4	3471	-	-	+	+	+
bhas#36	15	βOH-C20	589.4	471.4	3568	-	-	+	+	+
bhas#38	16	βOH-C21	603.4	485.4	3664	-	-	+	+	+
bhas#40	17	βOH-C22	617.4	499.4	3757	-	-	-	+	+
bhas#42	18	βOH-C23	631.5	513.4	3852	-	-	+	+	+
bhas#44	19	βOH-C24	645.5	527.4	3947	-	-	-	-	+
bhas#46	20	βOH-C25	(659.5)	541.4	(>4000)	-	-	-	+	+
bhas#48	21	βOH-C26	(673.5)	555.5	(>4000)	-	-	-	-	+
bhas#50	22	βOH-C27	(687.5)	569.5	(>4000)	-	-	-	-	+

[*]: confirmed using an authentic standard

Table S8: Characteristic EIMS fragment ion signals and GC Kovats retention indices for TMS-derivatized (ω)-linked β-hydroxyacyl ascarosides (**asc-βOH-ωC#**) detected by combined screening for the K1-fragment at *m/z* 130.1 $[C_6H_{14}OSi]^{+\bullet}$ and *m/z* 233.1 $[C_9H_{21}O_3Si_2]^+$ from α-cleavage, as well as the J1 (and J2)[a] fragment ion signals (Figure S8).

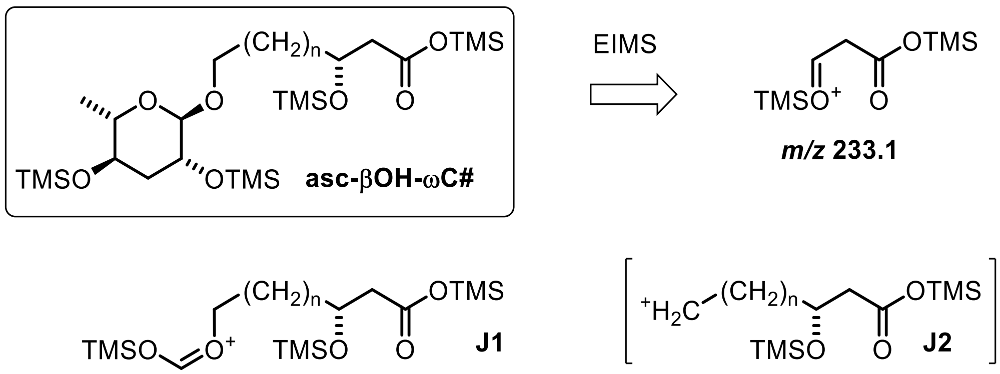

SMID	n	side chain	J1 *m/z* [M-173]	J2[a] *m/z* [M-291]	Kovats RI	WT	*acox-1*	*maoc-1*	*dhs-28*	*daf-22*
bhos#10	5	βOH-ωC9	435.2	317.2	2607	-	+	-	-	-
bhos#16	6	βOH-ωC10	449.3	331.2	*nd*	-	-	-	-	-
bhos#18	7	βOH-ωC11	463.3	345.2	*nd*	-	-	-	-	-
bhos#20	8	βOH-ωC12	477.3	359.2	*nd*	-	-	-	-	-
bhos#22	9	βOH-ωC13	491.3	373.3	3012	-	-	-	+	+
bhos#24	10	βOH-ωC14	505.3	387.3	3106	-	-	-	+	+
bhos#26*	11	βOH-ωC15	519.3	401.3	3202	-	-	-	+	+
bhos#28	12	βOH-ωC16	533.4	415.3	3295	-	-	-	+	+
bhos#30	13	βOH-ωC17	547.4	429.3	3390	-	-	-	+	+
bhos#32	14	βOH-ωC18	561.4	443.3	3485	-	-	-	+	+
bhos#34	15	βOH-ωC19	575.4	457.4	3580	-	-	-	+	+
bhos#36	16	βOH-ωC20	589.4	471.4	3675	-	-	-	+	+
bhos#38	17	βOH-ωC21	603.4	485.4	3769	-	-	-	+	+
bhos#40	18	βOH-ωC22	617.4	499.4	3864	-	-	-	-	+
bhos#42	19	βOH-ωC23	631.5	513.4	3959	-	-	-	-	+

[*]: confirmed using an authentic standard, [a]: low intensity

Table S9: Characteristic EIMS fragment ion signals and GC Kovats retention indices for TMS-derivatized α-methyl-branched (ω-1)-linked β-hydroxy-*iso*-acyl ascarosides (**asc-βOH-*i*C#**) detected by combined screening for the K1-fragment at *m/z* 130.1 $[C_6H_{14}OSi]^{+\bullet}$, *m/z* 247.1 $[C_{10}H_{23}O_3Si_2]^+$ from α-cleavage, and *m/z* 218.1 $[C_9H_{22}O_2Si_2]^+$ from McLafferty-type TMS-rearrangement, as well as the J1 and J2 fragment ion signals (Figure S8).

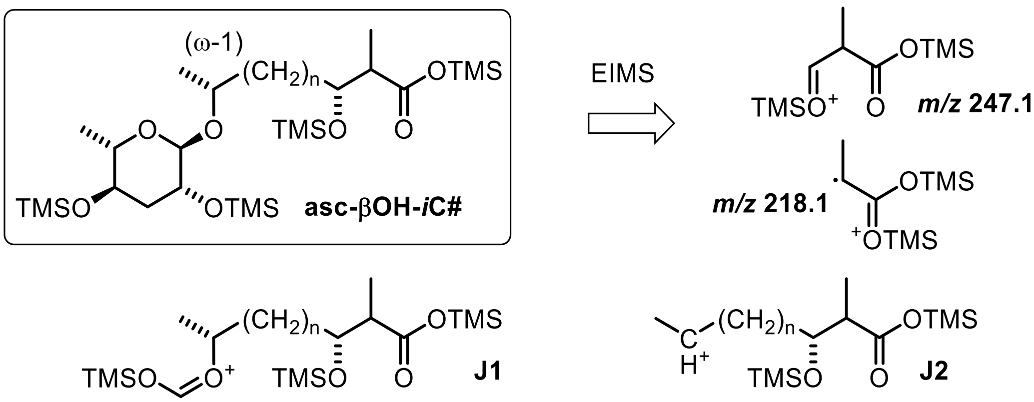

SMID	n	side chain	J1 *m/z* [M-173]	J2 *m/z* [M-291]	Kovats RI	WT	*acox-1*	*maoc-1*	*dhs-28*	*daf-22*
bhis#44	18	βOH-*i*C24	645.5	527.4	(>4000)	-	-	-	-	+
bhis#48	20	βOH-*i*C26	(673.5)	555.5	(>4000)	-	-	-	-	+

Table S10: Characteristic EIMS fragment ion signals and GC Kovats retention indices for TMS-derivatized (ω-1)-linked 2-hydroxyalkyl ascarosides (**asc-C#-OH**) detected by combined screening for the K1-fragment at *m/z* 130.1 $[C_6H_{14}OSi]^{+\bullet}$ and *m/z* 117.1 $[C_5H_{13}OSi]^{+}$ from α-cleavage, as well as the (J1)[a], J2, and [J2 – TMSOH]-fragment ion signals.

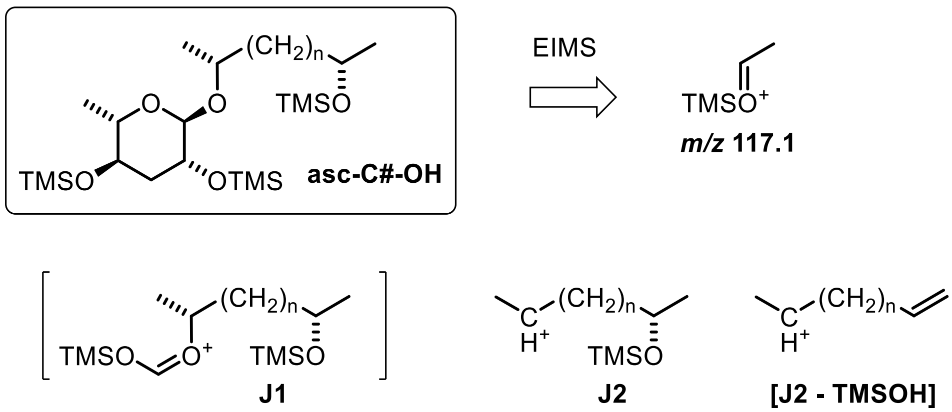

SMID	n	side chain	J1 *m/z* [M-173]	J2 *m/z* [M-291]	Kovats RI	WT	*acox-1*	*maoc-1*	*dhs-28*	*daf-22*
ascr#6.1*	2	C6-OH	291.2[a]	173.1 83.1[b]	1940	+	-	-	-	-
none	25	C29-OH	613.5[*nd*]	495.5[a] 405.4[b]	(>4000)	+	+	+	+	+
none	27	C31-OH	(655.6)	523.5[a] 433.5[b]	(>4000)	+	+	+	+	+
none	29	C33-OH	(683.6)	551.6[a] 461.5[b]	(>4000)	+	+	+	+	+

[*]: confirmed using an authentic standard; [a]: very low intensity, [b]: [J2 – TMSOH], *nd* = not detected.

Table S11: Characteristic EIMS fragment ion signals and GC Kovats retention indices for TMS-derivatized (ω-1)-linked 2-oxoalkyl ascarosides (**asc-C#-MK**) detected by combined screening for the K1-fragment at *m/z* 130.1 $[C_6H_{14}OSi]^{+\bullet}$ and the J1 and J2 fragment ion signals.

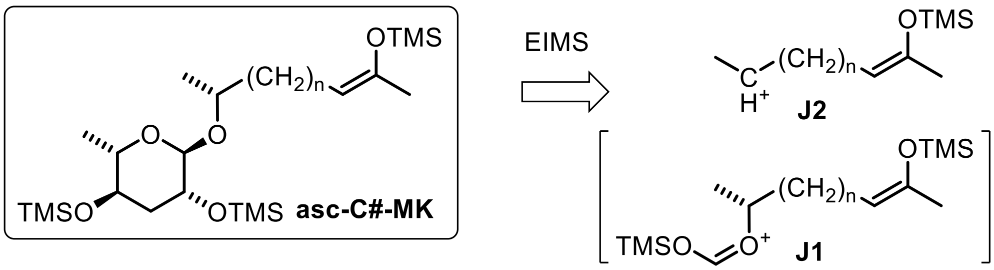

SMID	n	side chain	J1 *m/z* [M-173]	J2 *m/z* [M-291]	Kovats RI	WT	*acox-1*	*maoc-1*	*dhs-28*	*daf-22*
ascr#2*	1	C6-MK	217.1	99.1	1869	+	-	-	-	-
mkas#14	3	C8-MK	245.2	127.1	2060	-	+	-	-	-
mkas#26	10	C15-MK	415.4[nd] 343.3[a]	297.3 225.3[b]	2723	-	-	-	-	+
mkas#28	11	C16-MK	429.4[nd] 357.3[a]	311.3 239.3[b]	2820	-	-	-	-	+
mkas#30	12	C17-MK	443.4[nd] 371.3[a]	325.3 253.3[b]	2916	-	-	-	-	+
mkas#32	13	C18-MK	457.4[nd] 385.3[a]	339.3 267.3[b]	3014	-	-	-	-	+
mkas#34	14	C19-MK	471.4[nd] 399.3[a]	353.3 281.3[b]	3111	-	-	-	-	+
mkas#36	15	C20-MK	485.4[nd] 413.3[a]	367.3 295.3[b]	3210	-	-	-	-	+
mkas#38	16	C21-MK	499.4[nd] 427.4[a]	381.4 309.3[b]	3309	-	-	-	-	+
mkas#40	17	C22-MK	513.4[nd] 441.4[a]	395.4 323.3[b]	3407	-	-	-	-	+
mkas#42	18	C23-MK	527.4[nd] 455.4[a]	409.4 337.3[b]	3505	-	-	-	-	+
mkas#44	19	C24-MK	541.5[nd] 469.4[a]	423.4 351.4[b]	3604	-	-	-	-	+
mkas#46	20	C25-MK	555.5[nd] 483.4[a]	437.4 365.4[b]	3695	-	-	-	-	+
mkas#48	21	C26-MK	569.5[nd] 497.4[a]	451.4 379.4[b]	3800	-	-	-	-	+
mkas#50	22	C27-MK	583.5[nd] 511.5[a]	465.4 393.4[b]	3910	-	-	-	-	+
mkas#52	23	C28-MK	597.5[nd] 525.5[a]	479.5 407.4[b]	3998	-	-	-	-	+

[*]: confirmed using an authentic standard; [a]: very low intensity, [b]: [J2 – TMSOH], *nd* = not detected

Table S12: Characteristic EIMS fragment ion signals and GC Kovats retention indices for TMS-derivatized (ω)-linked 2-oxoalkyl ascarosides (**asc-ωC#-MK**) detected by combined screening for the K1-fragment at *m/z* 130.1 $[C_6H_{14}OSi]^{+\bullet}$ and the (J1)[a] and J2 fragment ion signals.

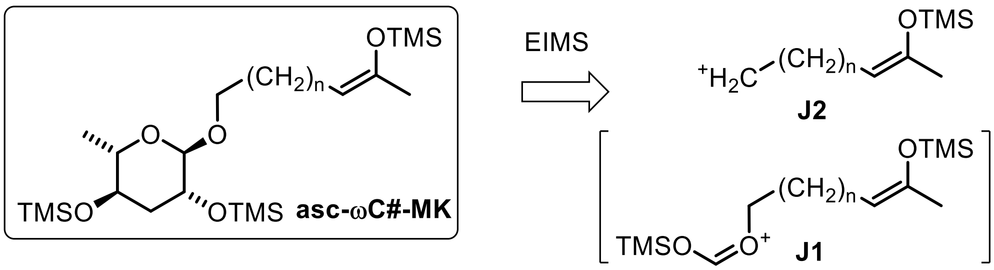

SMID	n	side chain	J1 *m/z* [M-173]	J2 *m/z* [M-291]	Kovats RI	WT	*acox-1*	*maoc-1*	*dhs-28*	*daf-22*
mkos#30	13	ωC17-MK	443.4[nd] 371.3[a]	325.3 253.3[b]	3300	-	-	-	-	+
mkos#32	14	ωC18-MK	457.4[nd] 385.3[a]	339.3 267.3[b]	3397	-	-	-	-	+
mkos#34	15	ωC19-MK	471.4[nd] 399.3[a]	353.3 281.3[b]	3492	-	-	-	-	+
mkos#36	16	ωC20-MK	485.4[nd] 413.3[a]	367.3 295.3[b]	3589	-	-	-	-	+
mkos#38	17	ωC21-MK	499.4[nd] 427.4[a]	381.4 309.3[b]	3685	-	-	-	-	+
mkos#40	18	ωC22-MK	513.4[nd] 441.4[a]	395.4 323.3[b]	3783	-	-	-	-	+

[a]: [J1 – C_3H_8Si] with very low intensity; [b]: [J2 – C_3H_8Si]; *nd* = not detected

Table S13: Characteristic EIMS fragment ion signals and GC Kovats retention indices for TMS-derivatized (ω-1)-linked acyl ascaroside ethanol amides (**asc-C#-EA**) detected by combined screening for the K1-fragment at *m/z* 130.1 $[C_6H_{14}OSi]^{+\bullet}$ and the J1 and J2 fragment ion signals (Figure S3).

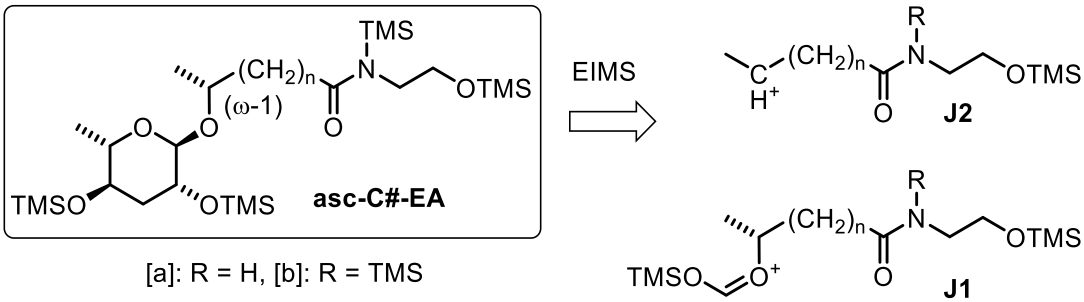

[a]: R = H, [b]: R = TMS

SMID	n	side chain	J1 *m/z* [M-173]	J2 *m/z* [M-291]	Kovats RI	WT	*acox-1*	*maoc-1*	*dhs-28*	*daf-22*
easc#9	2	C5-EA	334.3[a] 406.2[b]	216.2[a] 288.2[b]	2444	[c]	-	-	-	-
easc#18*	8	C11-EA	418.3[a] 490.3[b]	300.3[a] 372.3[b]	3042	[d]	+	-	-	-
easc#20	9	C12-EA	432.3[a] 504.3[b]	314.3[a] 386.3[b]	3134	-	+	-	-	-
easc#22	10	C13-EA	446.3[a] 518.3[b]	328.3[a] 400.3[b]	3248	-	+	-	-	-
easc#24	11	C14-EA	460.3[a] 532.3[b]	342.3[a] 414.3[b]	3346	-	+	-	-	-

[*]: confirmed with authentic standard, [a]: R = H, [b]: R = TMS, [c]: observed in *Caenorhabditis portoensis*, [d]: observed in *Heterorhabditis bacteriophora*

Table S14: Characteristic EIMS fragment ion signals and GC Kovats retention indices for TMS-derivatized (ω-1)-linked enoyl ascaroside ethanol amides (**asc-ΔC#-EA**) detected by combined screening for the K1-fragment at *m/z* 130.1 $[C_6H_{14}OSi]^{+\bullet}$ and *m/z* 186.1 $[C_8H_{16}NO_2Si]^+$, as well as the J1 and J2 fragment ion signals (Figure S12).

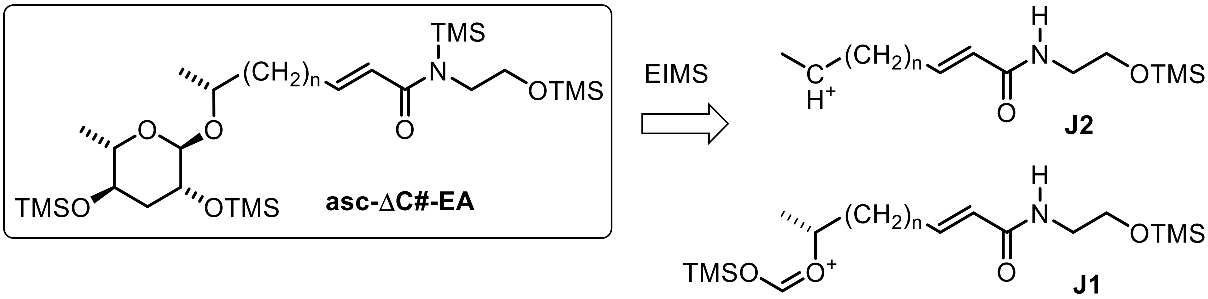

SMID	n	side chain	J1 *m/z* [M-173]	J2 *m/z* [M-291]	RI RT [min]	WT	*acox-1*	*maoc-1*	*dhs-28*	*daf-22*
easc#45	20	ΔC25-EA	612.5 540.4[a]	494.4	(>4000) 26.21	-	-	-	-	+
easc#47	21	ΔC26-EA	626.5 554.5[a]	508.5	(>4000) 26.67	-	-	-	-	+
easc#49	22	ΔC27-EA	640.5 568.5[a]	522.5	(>4000) 27.13	-	-	-	-	+
easc#51	23	ΔC28-EA	(654.5) 582.5[a]	536.5	(>4000) 27.63	-	-	-	-	+
easc#53	24	ΔC29-EA	(668.5) 596.5[a]	550.5	(>4000) 28.21	-	-	-	-	+

[a]: [J1 – C_3H_8Si]

Table S15: Characteristic EIMS fragment ion signals and GC Kovats retention indices for TMS-derivatized α-methyl-branched (ω-1)-linked *iso*-enoyl ascaroside ethanol amides (**asc-Δ*i*C#-EA**) detected by combined screening for the K1-fragment at *m/z* 130.1 $[C_6H_{14}OSi]^{+\bullet}$ and *m/z* 200.1 $[C_9H_{18}NO_2Si]^{+}$, as well as the J1 and J2 fragment ion signals (Figure S12).

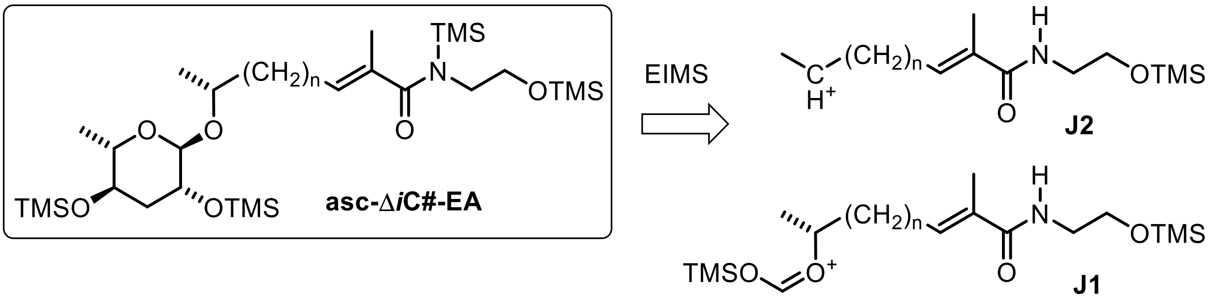

SMID	n	side chain	J1 *m/z* [M-173]	J2 *m/z* [M-291]	Kovats RI RT [min]	WT	*acox-1*	*maoc-1*	*dhs-28*	*daf-22*
eisc#47	20	Δ*i*C26-EA	626.5 554.4[a]	508.5	(>4000) 26.34	-	-	-	-	+

[a]: $[J1 – C_3H_8Si]$

Table S16: Characteristic EIMS fragment ion signals and GC Kovats retention indices for TMS-derivatized (ω-1)-linked β-hydroxyacyl ascaroside ethanolamides (**asc-βOH-C#-EA**) detected by combined screening for the K1-fragment at *m/z* 130.1 $[C_6H_{14}OSi]^{+\bullet}$ along with *m/z* 348.2 $[C_{14}H_{34}NO_3Si_3]^+$ and *m/z* 276.1 $[C_{11}H_{26}NO_3Si_2]^+$ from α-cleavage, as well as the J1 and J2 fragment ion signals (Figure S11).

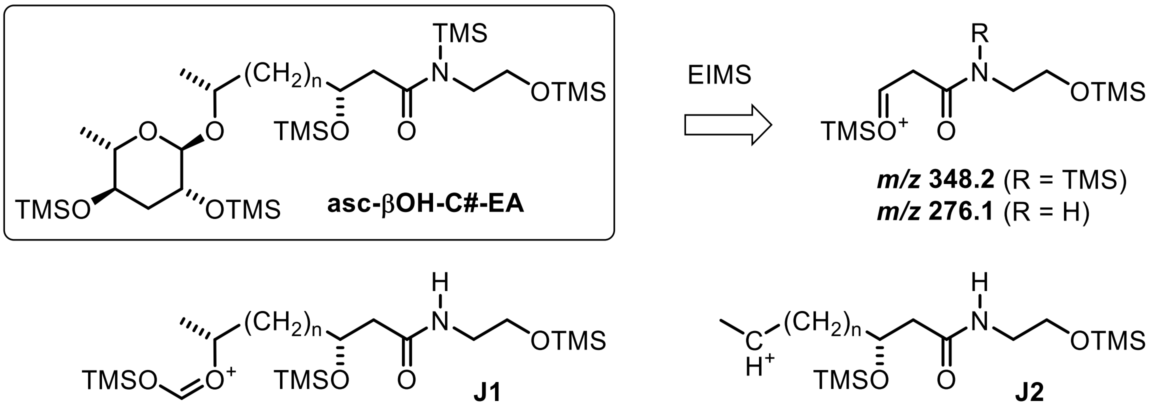

SMID	n	side chain	J1 *m/z* [M-173]	J2 *m/z* [M-291]	Kovats RI RT [min]	WT	*acox-1*	*maoc-1*	*dhs-28*	*daf-22*
ebha#30	12	βOH-C17-EA	590.4 518.4[b]	472.4	3741 23.93	-	-	-	-	+
ebha#32	13	βOH-C18-EA	604.4 532.4[b]	486.4	3835 24.43	-	-	-	-	+
ebha#34	14	βOH-C19-EA	618.4 546.4[b]	500.4	3933 24.94	-	-	-	-	+
ebha#36	15	βOH-C20-EA	632.5 560.4[b]	514.4	(>4000) 25.44	-	-	-	-	+
ebha#38	16	βOH-C21-EA	646.5 574.4[b]	528.4	(>4000) 25.91	-	-	-	-	+
ebha#40	17	βOH-C22-EA	(660.5) 588.4[b]	542.4	(>4000) 26.38	-	-	-	-	+
ebha#42	18	βOH-C23-EA	(674.5) 602.5[b]	556.5	(>4000) 26.84	-	-	-	-	+
ebha#44	19	βOH-C24-EA	(688.5) 616.5[b]	570.5	(>4000) 27.31	-	-	-	-	+
ebha#46	20	βOH-C25-EA	(702.5) 630.5[b]	584.5	(>4000) 27.82	-	-	-	-	+
ebha#48	21	βOH-C26-EA	(716.5) 644.5[b]	598.5	(>4000) 28.41	-	-	-	-	+
ebha#50	22	βOH-C27-EA	(730.6) (658.5)	612.5	(>4000) 29.08	-	-	-	-	+

[b]: [J1 – C_3H_8Si]

Table S17: Characteristic EIMS fragment ion signals and GC Kovats retention indices for TMS-derivatized (ω)-linked β-hydroxyacyl ascaroside ethanolamides (**asc-βOH-ωC#-EA**) detected by combined screening for the K1-fragment at *m/z* 130.1 $[C_6H_{14}OSi]^{+\bullet}$ along with *m/z* 348.2 $[C_{14}H_{34}NO_3Si_3]^+$ and *m/z* 276.1 $[C_{11}H_{26}NO_3Si_2]^+$ from α-cleavage, as well as the J1 (and J2)[a] fragment ion signals.

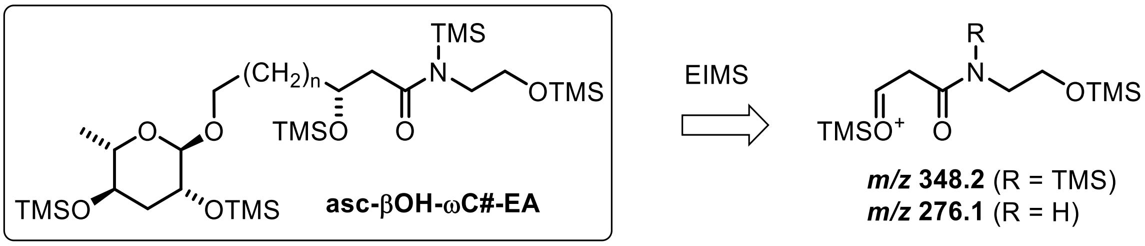

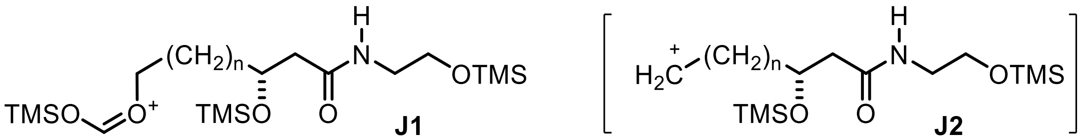

SMID	n	side chain	J1 *m/z* [M-173]	J2[a] *m/z* [M-291]	Kovats RI RT [min]	WT	*acox-1*	*maoc-1*	*dhs-28*	*daf-22*
ebho#24	10	βOH-ωC14-EA	548.4 476.3[b]	430.3 358.3[c]	3562.5 22.95	-	-	-	-	+
ebho#26	11	βOH-ωC15-EA	562.4 490.3[b]	444.3 372.3[c]	3660.0 23.49	-	-	-	-	+
ebho#28	12	βOH-ωC16-EA	576.4 504.4[b]	458.3 386.3[c]	3751.9 23.99	-	-	-	-	+
ebho#30	13	βOH-ωC17-EA	590.4 518.4[b]	472.4 400.3[c]	3850.0 24.51	-	-	-	-	+
ebho#32	14	βOH-ωC18-EA	604.4 532.4[b]	486.4 414.3[c]	3945.1 25.00	-	-	-	-	+
ebho#34	15	βOH-ωC19-EA	618.4 546.4[b]	500.4 428.4[c]	(>4000) 25.49	-	-	-	-	+
ebho#36	16	βOH-ωC20-EA	632.5 560.4[b]	514.4 442.4[c]	(>4000) 25.97	-	-	-	-	+
ebho#38	17	βOH-ωC21-EA	646.5 574.4[b]	528.4 456.4[c]	(>4000) 26.45	-	-	-	-	+
ebho#40	18	βOH-ωC22-EA	(660.5) 588.4[b]	542.4 470.4[c]	(>4000) 26.90	-	-	-	-	+
ebho#42	19	βOH-ωC23-EA	(674.5) 602.4[b]	556.5 484.4[c]	(>4000) 27.36	-	-	-	-	+

[a]: low intensity, [b]: $[J1 – C_3H_8Si]$, [c]: $[J2 – C_3H_8Si]$

Table S18: Characteristic EIMS fragment ion signals and GC Kovats retention indices for TMS-derivatized (ω-1)-linked α-methyl-β-hydroxyacyl ascaroside ethanolamides (**asc-βOH-*iC#*-EA**) detected by combined screening for the K1-fragment at *m/z* 130.1 $[C_6H_{14}OSi]^{+\bullet}$ along with *m/z* 362.3 $[C_{15}H_{36}NO_3Si_3]^+$ and *m/z* 290.2 $[C_{12}H_{28}NO_3Si_2]^+$ from α-cleavage, as well as the J1 and J2 fragment ion signals (Figure S11).

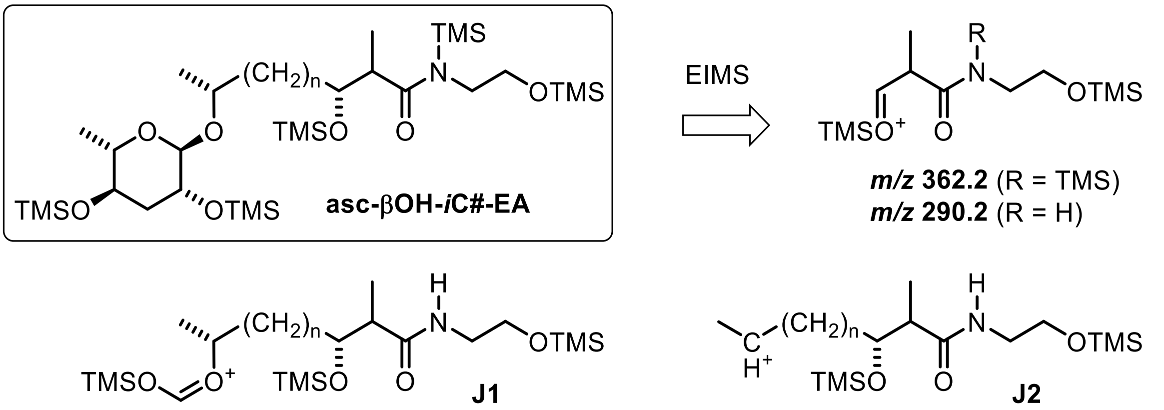

SMID	n	side chain	J1 *m/z* [M-173]	J2 *m/z* [M-291]	Kovats RI RT [min]	WT	*acox-1*	*maoc-1*	*dhs-28*	*daf-22*
ebhi#44	18	βOH-*i*C24-EA	(688.6) 616.5[a]	570.5 498.5[b]	(>4000) 26.89	-	-	-	-	+
ebhi#48	20	βOH-*i*C26-EA	(716.6) 644.5[a]	598.5 526.5[b]	(>4000) 27.89	-	-	-	-	+

[a]: [J1 – C_3H_8Si], [b]: [J2 – C_3H_8Si]

Table S19: Characteristic EIMS fragment ion signals and GC Kovats retention indices for TMS-derivatized (ω-1)-linked acyl ascaroside methyl esters (**asc-C#-OMe**) detected by combined screening for the K1-fragment at *m/z* 130.1 $[C_6H_{14}OSi]^{+\bullet}$ and the J1 and J2 fragment ion signals.

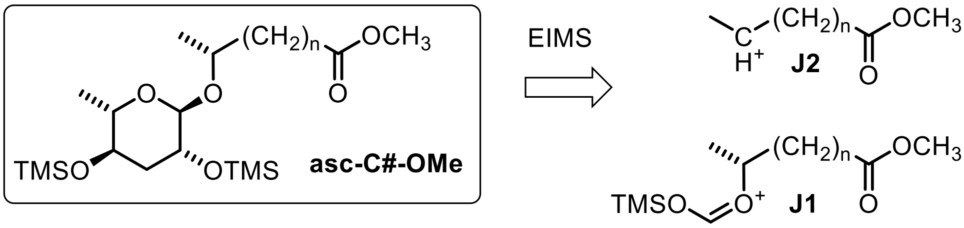

SMID	n	side chain	J1 *m/z* [M-173]	J2 *m/z* [M-291]	Kovats RI	WT	*acox-1*	*maoc-1*	*dhs-28*	*daf-22*
asom#9*	2	C5-OMe	233.1	115.1	1906	-	+	-	-	-
asom#12	3	C6-OMe	247.1	129.1	1995	-	+	-	-	-
asom#1	4	C7-OMe	261.2	143.1	2086	+	+	-	-	-
asom#14	5	C8-OMe	275.2	157.1	2175	-	+	-	-	-
asom#10	6	C9-OMe	289.2	171.1	2268	-	+	-	-	-
asom#16	7	C10-OMe	303.2	185.2	*nd*	-	-	-	-	-
asom#18*	8	C11-OMe	317.2	199.2	2457	-	+	+	-	-
asom#20*	9	C12-OMe	331.2	213.2	2552	-	-	+	-	-
asom#22*	10	C13-OMe	345.2	227.2	2649	-	-	+	+	-
asom#24	11	C14-OMe	359.3	241.2	2749	-	-	-	+	+
asom#26	12	C15-OMe	373.3	255.2	2847	-	-	+	+	+
asom#28	13	C16-OMe	387.3	269.2	2946	-	-	-	+	+
asom #30	14	C17-OMe	401.3	283.3	3043	-	-	+	+	+
asom #32	15	C18-OMe	415.3	297.3	3142	-	-	-	+	+

[*]: confirmed using an authentic standard

Table S21: ESI-(-)-HR-MS/MS data for (ω-1)-linked acyl ascarosides (**asc-C#**).

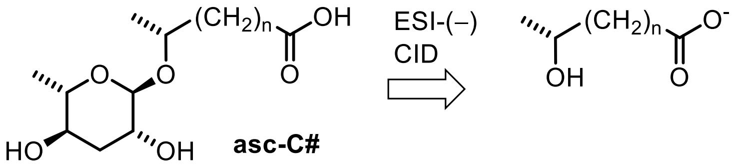

SMID	n	Side chain	Molecular formula	*m/z* obs	*m/z* calc	Δ [ppm]	
none	0	C3	$C_9H_{15}O_6$ ($C_3H_5O_3$)	219.0875 (*nd*)	219.0874 (89.0244)	0.5 -	$[M-H]^-$ $[M-C_6H_{11}O_3]^-$
ascr#11	1	C4	$C_{10}H_{17}O_6$ ($C_4H_7O_3$)	233.1033 (*nd*)	233.1031 (103.0401)	0.9 -	$[M-H]^-$ $[M-C_6H_{11}O_3]^-$
ascr#9	2	C5	$C_{11}H_{19}O_6$ ($C_5H_9O_3$)	247.1187 (*nd*)	247.1187 (117.0557)	0.1 -	$[M-H]^-$ $[M-C_6H_{11}O_3]^-$
ascr#12	3	C6	$C_{12}H_{21}O_6$ ($C_6H_{11}O_3$)	261.1342 (*nd*)	261.1344 (131.0714)	0.6 -	$[M-H]^-$ $[M-C_6H_{11}O_3]^-$
ascr#1	4	C7	$C_{13}H_{23}O_6$ ($C_7H_{13}O_3$)	275.1500 (145.0872)	275.1500 (145.0870)	0.1 1.1	$[M-H]^-$ $[M-C_6H_{11}O_3]^-$
ascr#14	5	C8	$C_{14}H_{25}O_6$ ($C_8H_{15}O_3$)	289.1656 (*nd*)	289.1657 (159.1027)	0.4 -	$[M-H]^-$ $[M-C_6H_{11}O_3]^-$
ascr#10	6	C9	$C_{15}H_{27}O_6$ ($C_9H_{17}O_3$)	303.1818 (173.1181)	303.1813 (173.1183)	1.7 1.4	$[M-H]^-$ $[M-C_6H_{11}O_3]^-$
ascr#16	7	C10	$C_{16}H_{29}O_6$ ($C_{10}H_{19}O_3$)	317.1969 (187.1343)	317.1970 (187.1340)	0.3 1.8	$[M-H]^-$ $[M-C_6H_{11}O_3]^-$
ascr#18	8	C11	$C_{17}H_{31}O_6$ ($C_{11}H_{21}O_3$)	331.2132 (201.1497)	331.2126 (201.1496)	1.8 0.6	$[M-H]^-$ $[M-C_6H_{11}O_3]^-$
ascr#20	9	C12	$C_{18}H_{33}O_6$ ($C_{12}H_{23}O_3$)	345.2283 (215.1655)	345.2283 (215.1653)	0.2 1.3	$[M-H]^-$ $[M-C_6H_{11}O_3]^-$
ascr#22	10	C13	$C_{19}H_{35}O_6$ ($C_{13}H_{25}O_3$)	359.2439 (229.1811)	359.2439 (229.1809)	0.1 0.9	$[M-H]^-$ $[M-C_6H_{11}O_3]^-$
ascr#24	11	C14	$C_{20}H_{37}O_6$ ($C_{14}H_{27}O_3$)	373.2597 (243.1966)	373.2596 (243.1966)	0.4 0.1	$[M-H]^-$ $[M-C_6H_{11}O_3]^-$
ascr#26	12	C15	$C_{21}H_{39}O_6$ ($C_{15}H_{29}O_3$)	387.2756 (257.2124)	387.2752 (257.2122)	1.0 0.5	$[M-H]^-$ $[M-C_6H_{11}O_3]^-$
ascr#28	13	C16	$C_{22}H_{41}O_6$ ($C_{16}H_{31}O_3$)	401.2908 (271.2276)	401.2909 (271.2279)	0.1 1.0	$[M-H]^-$ $[M-C_6H_{11}O_3]^-$
ascr#30	14	C17	$C_{23}H_{43}O_6$ ($C_{17}H_{33}O_3$)	415.3061 (285.2433)	415.3065 (285.2435)	1.0 0.9	$[M-H]^-$ $[M-C_6H_{11}O_3]^-$
ascr#32	15	C18	$C_{24}H_{45}O_6$ ($C_{18}H_{35}O_3$)	429.3218 (299.2593)	429.3222 (299.2592)	0.7 0.6	$[M-H]^-$ $[M-C_6H_{11}O_3]^-$
ascr#34	16	C19	$C_{25}H_{47}O_6$ ($C_{19}H_{37}O_3$)	443.3377 (313.2749)	443.3378 (313.2748)	0.3 0.2	$[M-H]^-$ $[M-C_6H_{11}O_3]^-$
ascr#36	17	C20	$C_{26}H_{49}O_6$ ($C_{20}H_{39}O_3$)	457.3532 (327.2903)	457.3535 (327.2905)	0.5 0.5	$[M-H]^-$ $[M-C_6H_{11}O_3]^-$
ascr#38	18	C21	$C_{27}H_{51}O_6$ ($C_{21}H_{41}O_3$)	471.3687 (341.3063)	471.3691 (341.3061)	0.9 0.7	$[M-H]^-$ $[M-C_6H_{11}O_3]^-$
ascr#40	19	C22	$C_{28}H_{53}O_6$ ($C_{22}H_{43}O_3$)	485.3838 (355.3211)	485.3848 (355.3218)	1.9 1.9	$[M-H]^-$ $[M-C_6H_{11}O_3]^-$
ascr#42	20	C23	$C_{29}H_{55}O_6$ ($C_{23}H_{45}O_3$)	499.4000 (369.3369)	499.4004 (369.3374)	0.9 1.4	$[M-H]^-$ $[M-C_6H_{11}O_3]^-$
ascr#44	21	C24	$C_{30}H_{57}O_6$ ($C_{24}H_{47}O_3$)	513.4156 (383.3527)	513.4161 (383.3531)	0.9 0.9	$[M-H]^-$ $[M-C_6H_{11}O_3]^-$
ascr#46	22	C25	$C_{31}H_{59}O_6$ ($C_{25}H_{49}O_3$)	527.4320 (397.3686)	527.4317 (397.3687)	0.8 0.3	$[M-H]^-$ $[M-C_6H_{11}O_3]^-$
ascr#48	23	C26	$C_{32}H_{61}O_6$ ($C_{26}H_{51}O_3$)	541.4469 (411.3839)	541.4474 (411.3844)	0.9 1.1	$[M-H]^-$ $[M-C_6H_{11}O_3]^-$
ascr#50	24	C27	$C_{33}H_{63}O_6$ ($C_{27}H_{53}O_3$)	555.4627 (425.3993)	555.4630 (425.4000)	0.6 1.6	$[M-H]^-$ $[M-C_6H_{11}O_3]^-$
ascr#52	25	C28	$C_{34}H_{65}O_6$ ($C_{28}H_{55}O_3$)	569.4782 (439.4163)	569.4787 (439.4157)	0.8 1.4	$[M-H]^-$ $[M-C_6H_{11}O_3]^-$
ascr#54	26	C29	$C_{35}H_{67}O_6$ ($C_{29}H_{57}O_3$)	583.4937 (453.4306)	583.4943 (453.4313)	1.0 1.6	$[M-H]^-$ $[M-C_6H_{11}O_3]^-$

SMID	n	Side chain	Molecular formula	*m/z* obs	*m/z* calc	Δ [ppm]	
ascr#56	27	C30	$C_{36}H_{69}O_6$ ($C_{30}H_{59}O_3$)	597.5091 (467.4462)	597.5100 (467.4470)	1.4 1.6	$[M-H]^-$ $[M-C_6H_{11}O_3]^-$
ascr#58	28	C31	$C_{37}H_{71}O_6$ ($C_{31}H_{61}O_3$)	611.5253 (481.4621)	611.5256 (481.4626)	0.5 1.1	$[M-H]^-$ $[M-C_6H_{11}O_3]^-$
ascr#60	29	C32	$C_{38}H_{73}O_6$ ($C_{32}H_{63}O_3$)	625.5401 (*nd*)	625.5413 (495.4783)	1.9 -	$[M-H]^-$ $[M-C_6H_{11}O_3]^-$
ascr#62	30	C33	$C_{39}H_{75}O_6$ ($C_{33}H_{65}O_3$)	639.5560 (*nd*)	639.5569 (509.4923)	1.4 -	$[M-H]^-$ $[M-C_6H_{11}O_3]^-$

Table S22: ESI-(-)-HR-MS/MS data for (ω)-linked acyl ascarosides (**asc-ωC#**).

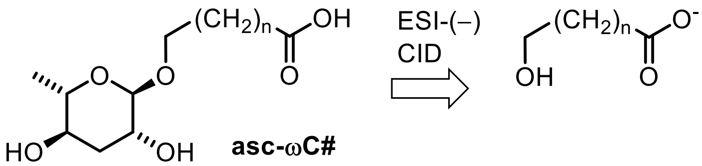

SMID	n	Side chain	Molecular formula	*m/z* obs	*m/z* calc	Δ [ppm]	
ascr#5	1	ωC3	$C_9H_{15}O_6$ ($C_3H_5O_3$)	219.0877 (*nd*)	219.0874 (89.0244)	1.4 -	$[M-H]^-$ $[M-C_6H_{11}O_3]^-$
oscr#11	2	ωC4	$C_{10}H_{17}O_6$ ($C_4H_7O_3$)	(*nd*) (*nd*)	233.1031 (103.0401)	(*nd*) -	$[M-H]^-$ $[M-C_6H_{11}O_3]^-$
oscr#9	3	ωC5	$C_{11}H_{19}O_6$ ($C_5H_9O_3$)	247.1189 (*nd*)	247.1187 (117.0557)	0.8 -	$[M-H]^-$ $[M-C_6H_{11}O_3]^-$
oscr#12	4	ωC6	$C_{12}H_{21}O_6$ ($C_6H_{11}O_3$)	261.1344 (*nd*)	261.1344 (131.0714)	0.2 -	$[M-H]^-$ $[M-C_6H_{11}O_3]^-$
oscr#1	5	ωC7	$C_{13}H_{23}O_6$ ($C_7H_{13}O_3$)	275.1504 (145.0873)	275.1500 (145.0870)	1.4 2.1	$[M-H]^-$ $[M-C_6H_{11}O_3]^-$
oscr#14	6	ωC8	$C_{14}H_{25}O_6$ ($C_8H_{15}O_3$)	289.1659 (*nd*)	289.1657 (159.1027)	0.8 -	$[M-H]^-$ $[M-C_6H_{11}O_3]^-$
oscr#10	7	ωC9	$C_{15}H_{27}O_6$ ($C_9H_{17}O_3$)	303.1817 (173.1186)	303.1813 (173.1183)	1.4 1.7	$[M-H]^-$ $[M-C_6H_{11}O_3]^-$
oscr#16	8	ωC10	$C_{16}H_{29}O_6$ ($C_{10}H_{19}O_3$)	317.1975 (*nd*)	317.1970 (187.1340)	1.5 -	$[M-H]^-$ $[M-C_6H_{11}O_3]^-$
oscr#18	9	ωC11	$C_{17}H_{31}O_6$ ($C_{11}H_{21}O_3$)	331.2130 (201.1498)	331.2126 (201.1496)	1.2 1.1	$[M-H]^-$ $[M-C_6H_{11}O_3]^-$
oscr#20	10	ωC12	$C_{18}H_{33}O_6$ ($C_{12}H_{23}O_3$)	345.2289 (*nd*)	345.2283 (215.1653)	1.7 -	$[M-H]^-$ $[M-C_6H_{11}O_3]^-$
oscr#22	11	ωC13	$C_{19}H_{35}O_6$ ($C_{13}H_{25}O_3$)	359.2434 (229.1806)	359.2439 (229.1809)	1.4 1.0	$[M-H]^-$ $[M-C_6H_{11}O_3]^-$
oscr#24	12	ωC14	$C_{20}H_{37}O_6$ ($C_{14}H_{27}O_3$)	373.2597 (243.1967)	373.2596 (243.1966)	0.4 0.4	$[M-H]^-$ $[M-C_6H_{11}O_3]^-$
oscr#26	13	ωC15	$C_{21}H_{39}O_6$ ($C_{15}H_{29}O_3$)	387.2755 (257.2120)	387.2752 (257.2122)	0.7 0.7	$[M-H]^-$ $[M-C_6H_{11}O_3]^-$
oscr#28	14	ωC16	$C_{22}H_{41}O_6$ ($C_{16}H_{31}O_3$)	401.2912 (271.2282)	401.2909 (271.2279)	0.9 0.5	$[M-H]^-$ $[M-C_6H_{11}O_3]^-$
oscr#30	15	ωC17	$C_{23}H_{43}O_6$ ($C_{17}H_{33}O_3$)	415.3064 (285.2434)	415.3065 (285.2435)	0.2 0.4	$[M-H]^-$ $[M-C_6H_{11}O_3]^-$
oscr#32	16	ωC18	$C_{24}H_{45}O_6$ ($C_{18}H_{35}O_3$)	429.3224 (299.2589)	429.3222 (299.2592)	0.5 0.9	$[M-H]^-$ $[M-C_6H_{11}O_3]^-$
oscr#34	17	ωC19	$C_{25}H_{47}O_6$ ($C_{19}H_{37}O_3$)	443.3374 (313.2744)	443.3378 (313.2748)	0.8 0.3	$[M-H]^-$ $[M-C_6H_{11}O_3]^-$
oscr#36	18	ωC20	$C_{26}H_{49}O_6$ ($C_{20}H_{39}O_3$)	457.3526 (327.2900)	457.3535 (327.2905)	1.8 1.5	$[M-H]^-$ $[M-C_6H_{11}O_3]^-$
oscr#38	19	ωC21	$C_{27}H_{51}O_6$ ($C_{21}H_{41}O_3$)	471.3684 (341.3056)	471.3691 (341.3061)	1.4 1.5	$[M-H]^-$ $[M-C_6H_{11}O_3]^-$
oscr#40	20	ωC22	$C_{28}H_{53}O_6$ ($C_{22}H_{43}O_3$)	485.3840 (355.3213)	485.3848 (355.3218)	1.5 1.4	$[M-H]^-$ $[M-C_6H_{11}O_3]^-$
oscr#42	21	ωC23	$C_{29}H_{55}O_6$ ($C_{23}H_{45}O_3$)	499.3997 (369.3368)	499.4004 (369.3374)	1.4 1.1	$[M-H]^-$ $[M-C_6H_{11}O_3]^-$

Table S23: ESI-(-)-HR-MS/MS data for α-methyl-branched (ω-1)-linked *iso*-acyl ascarosides (**asc-*iC#***).

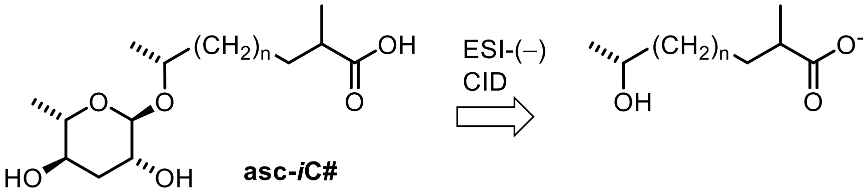

asc-*iC#*

SMID	n	Side chain	Molecular formula	*m/z* obs	*m/z* calc	Δ [ppm]	
iscr#44	18	*i*C24	$C_{30}H_{57}O_6$ ($C_{24}H_{47}O_3$)	513.4156 (383.3538)	513.4161 (383.3531)	0.9 1.8	$[M-H]^-$ $[M-C_6H_{11}O_3]^-$
iscr#48	20	*i*C26	$C_{32}H_{61}O_6$ ($C_{26}H_{51}O_3$)	541.4470 (411.3838)	541.4474 (411.3844)	0.7 1.4	$[M-H]^-$ $[M-C_6H_{11}O_3]^-$

Table S24: ESI-(-)-HR-MS/MS data for (ω-1)-linked enoyl ascarosides (**asc-ΔC#**).

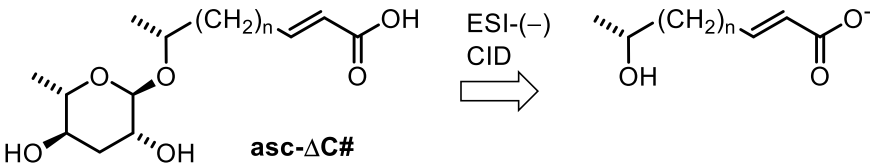

asc-ΔC#

SMID	n	Side chain	Molecular formula	*m/z* obs	*m/z* calc	Δ [ppm]	
none	1	ΔC6	$C_{12}H_{19}O_6$ ($C_6H_9O_3$)	259.1182 (*nd*)	259.1187 (129.0557)	2.0 -	$[M-H]^-$ $[M-C_6H_{11}O_3]^-$
ascr#7	2	ΔC7	$C_{13}H_{21}O_6$ ($C_7H_{11}O_3$)	273.1343 (143.0712)	273.1344 (143.0714)	0.4 1.5	$[M-H]^-$ $[M-C_6H_{11}O_3]^-$
ascr#13	3	ΔC8	$C_{14}H_{23}O_6$ ($C_8H_{13}O_3$)	287.1497 (*nd*)	287.1500 (157.0870)	1.1 -	$[M-H]^-$ $[M-C_6H_{11}O_3]^-$
ascr#3	4	ΔC9	$C_{15}H_{25}O_6$ ($C_9H_{15}O_3$)	301.1655 (171.1022)	301.1657 (171.1027)	0.7 2.6	$[M-H]^-$ $[M-C_6H_{11}O_3]^-$
ascr#15	5	ΔC10	$C_{16}H_{27}O_6$ ($C_{10}H_{17}O_3$)	315.1814 (*nd*)	315.1813 (185.1183)	0.2 -	$[M-H]^-$ $[M-C_6H_{11}O_3]^-$
ascr#17	6	ΔC11	$C_{17}H_{29}O_6$ ($C_{11}H_{19}O_3$)	329.1964 (199.1338)	329.1970 (199.1340)	1.6 1.1	$[M-H]^-$ $[M-C_6H_{11}O_3]^-$
ascr#19	7	ΔC12	$C_{18}H_{31}O_6$ ($C_{12}H_{21}O_3$)	343.2124 (213.1511)	343.2126 (213.1496)	0.7 2.3	$[M-H]^-$ $[M-C_6H_{11}O_3]^-$
ascr#21	8	ΔC13	$C_{19}H_{33}O_6$ ($C_{13}H_{23}O_3$)	357.2280 (227.1648)	357.2283 (227.1653)	0.8 2.2	$[M-H]^-$ $[M-C_6H_{11}O_3]^-$
ascr#23	9	ΔC14	$C_{20}H_{35}O_6$ ($C_{14}H_{25}O_3$)	371.2436 (241.1805)	371.2439 (241.1809)	0.9 1.7	$[M-H]^-$ $[M-C_6H_{11}O_3]^-$
ascr#25	10	ΔC15	$C_{21}H_{37}O_6$ ($C_{15}H_{27}O_3$)	385.2592 (255.1961)	385.2596 (255.1966)	0.9 2.0	$[M-H]^-$ $[M-C_6H_{11}O_3]^-$
ascr#27	11	ΔC16	$C_{22}H_{49}O_6$ ($C_{16}H_{39}O_3$)	399.2748 (269.2119)	399.2752 (269.2122)	1.1 1.1	$[M-H]^-$ $[M-C_6H_{11}O_3]^-$
ascr#29	12	ΔC17	$C_{23}H_{41}O_6$ ($C_{17}H_{31}O_3$)	413.2902 (283.2274)	413.2909 (283.2279)	1.6 1.8	$[M-H]^-$ $[M-C_6H_{11}O_3]^-$
ascr#31	13	ΔC18	$C_{24}H_{43}O_6$ ($C_{18}H_{33}O_3$)	427.3057 (297.2429)	427.3065 (297.2435)	1.9 2.0	$[M-H]^-$ $[M-C_6H_{11}O_3]^-$
ascr#33	14	ΔC19	$C_{25}H_{45}O_6$ ($C_{19}H_{35}O_3$)	441.3218 (311.2587)	441.3222 (311.2592)	0.8 1.6	$[M-H]^-$ $[M-C_6H_{11}O_3]^-$
ascr#35	15	ΔC20	$C_{26}H_{47}O_6$ ($C_{20}H_{37}O_3$)	455.3370 (325.2739)	455.3378 (325.2748)	1.8 2.8	$[M-H]^-$ $[M-C_6H_{11}O_3]^-$
ascr#37	16	ΔC21	$C_{27}H_{49}O_6$ ($C_{21}H_{39}O_3$)	469.3530 (339.2898)	469.3535 (339.2905)	1.0 2.1	$[M-H]^-$ $[M-C_6H_{11}O_3]^-$
ascr#39	17	ΔC22	$C_{28}H_{51}O_6$ ($C_{22}H_{41}O_3$)	483.3685 (353.3053)	483.3691 (353.3061)	1.2 2.3	$[M-H]^-$ $[M-C_6H_{11}O_3]^-$

SMID	n	Side chain	Molecular formula	*m/z* obs	*m/z* calc	Δ [ppm]	
ascr#41	18	ΔC23	$C_{29}H_{53}O_6$ ($C_{23}H_{43}O_3$)	497.3849 (367.3211)	497.3848 (367.3218)	0.2 1.9	$[M-H]^-$ $[M-C_6H_{11}O_3]^-$
ascr#43	19	ΔC24	$C_{30}H_{55}O_6$ ($C_{24}H_{45}O_3$)	511.3999 (381.3371)	511.4004 (381.3374)	1.1 0.8	$[M-H]^-$ $[M-C_6H_{11}O_3]^-$
ascr#45	20	ΔC25	$C_{31}H_{57}O_6$ ($C_{25}H_{47}O_3$)	525.4157 (395.3525)	525.4161 (395.3531)	0.8 1.5	$[M-H]^-$ $[M-C_6H_{11}O_3]^-$

Table S25: ESI-(-)-HR-MS data for (ω)-linked enoyl ascarosides (**asc-ωΔC#**).

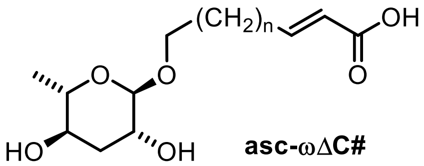

asc-ωΔC#

SMID	n	Side chain	Molecular formula	*m/z* obs	*m/z* calc	Δ [ppm]	
oscr#7	3	ωΔC7	$C_{13}H_{21}O_6$	273.1351	273.1344	2.6	$[M-H]^-$
oscr#13	4	ωΔC8	$C_{14}H_{23}O_6$	*nd*	287.1500	-	$[M-H]^-$
oscr#3	5	ωΔC9	$C_{15}H_{25}O_6$	301.1655	301.1657	0.7	$[M-H]^-$
oscr#15	6	ωΔC10	$C_{16}H_{27}O_6$	315.1810	315.1813	1.1	$[M-H]^-$
oscr#17	7	ωΔC11*	$C_{17}H_{29}O_6$	329.1966	329.1970	1.2	$[M-H]^-$
oscr#19	8	ωΔC12	$C_{18}H_{31}O_6$	343.2124	343.2126	0.5	$[M-H]^-$
oscr#21	9	ωΔC13	$C_{19}H_{33}O_6$	357.2275	357.2283	2.1	$[M-H]^-$
oscr#23	10	ωΔC14	$C_{20}H_{35}O_6$	371.2437	371.2439	0.6	$[M-H]^-$
oscr#25	11	ωΔC15	$C_{21}H_{37}O_6$	385.2588	385.2596	1.9	$[M-H]^-$
oscr#27	12	ωΔC16	$C_{22}H_{49}O_6$	399.2760	399.2752	1.5	$[M-H]^-$
oscr#29	13	ωΔC17	$C_{23}H_{41}O_6$	413.2913	413.2909	1.0	$[M-H]^-$
oscr#31	14	ωΔC18	$C_{24}H_{43}O_6$	427.3068	427.3065	0.7	$[M-H]^-$
oscr#33	15	ωΔC19	$C_{25}H_{45}O_6$	441.3229	441.3222	1.6	$[M-H]^-$
oscr#35	16	ωΔC20	$C_{26}H_{47}O_6$	455.3381	455.3378	0.7	$[M-H]^-$
oscr#37	17	ωΔC21	$C_{27}H_{49}O_6$	469.3538	469.3535	0.6	$[M-H]^-$
oscr#39	18	ωΔC22	$C_{28}H_{51}O_6$	483.3690	483.3691	0.2	$[M-H]^-$
oscr#41	19	ωΔC23	$C_{29}H_{53}O_6$	497.3836	497.3848	2.4	$[M-H]^-$

Table S26: ESI-(-)-HR-MS/MS data for α-methyl-branched (ω)-linked *iso*-enoyl ascarosides (**asc-Δ*i*C#**).

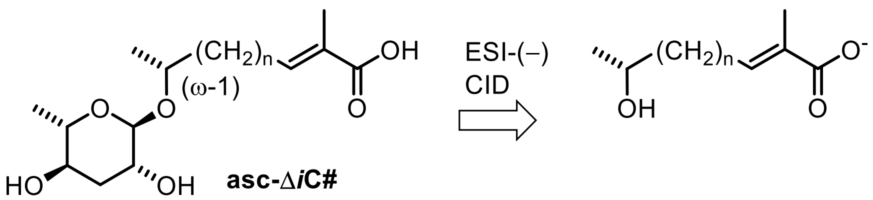

asc-Δ*i*C#

SMID	n	Side chain	Molecular formula	*m/z* obs	*m/z* calc	Δ [ppm]	
iscr#43	18	Δ*i*C24	$C_{30}H_{55}O_6$ ($C_{24}H_{45}O_3$)	511.4000 (381.3374)	511.4004 (381.3374)	0.8 0.1	$[M-H]^-$ $[M-C_6H_{11}O_3]^-$
iscr#47	20	Δ*i*C26	$C_{32}H_{59}O_6$ ($C_{26}H_{49}O_3$)	539.4317 (409.3689)	539.4317 (409.3687)	0.0 0.4	$[M-H]^-$ $[M-C_6H_{11}O_3]^-$

Table S27: ESI-(-)-HR-MS data for (ω-1)-linked β-hydroxyacyl ascarosides (**asc-βOH-C#**).

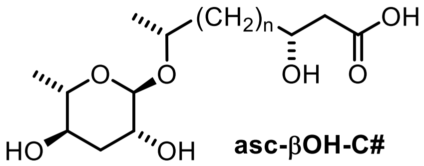

asc-βOH-C#

SMID	n	Side chain	Molecular formula	*m/z* obs	*m/z* calc	Δ [ppm]	
bhas#12	1	βOH-C6	$C_{12}H_{21}O_7$	277.1304	277.1293	4.0	$[M-H]^-$
bhas#1	2	βOH-C7	$C_{13}H_{23}O_7$	291.1457	291.1449	2.8	$[M-H]^-$
bhas#14	3	βOH-C8	$C_{14}H_{25}O_7$	*nd*	305.1606	-	$[M-H]^-$
bhas#10	4	βOH-C9	$C_{15}H_{27}O_7$	319.1764	319.1762	0.5	$[M-H]^-$
bhas#16	5	βOH-C10	$C_{16}H_{29}O_7$	333.1916	333.1919	0.7	$[M-H]^-$
bhas#18	6	βOH-C11	$C_{17}H_{31}O_7$	347.2076	347.2075	0.1	$[M-H]^-$
bhas#20	7	βOH-C12	$C_{18}H_{33}O_7$	361.2231	361.2232	0.2	$[M-H]^-$
bhas#22	8	βOH-C13	$C_{19}H_{35}O_7$	375.2391	375.2388	0.8	$[M-H]^-$
bhas#24	9	βOH-C14	$C_{20}H_{37}O_7$	389.2545	389.2545	0.0	$[M-H]^-$
bhas#26	10	βOH-C15	$C_{21}H_{39}O_7$	403.2702	403.2701	0.3	$[M-H]^-$
bhas#28	11	βOH-C16	$C_{22}H_{41}O_7$	417.2860	417.2858	0.6	$[M-H]^-$
bhas#30	12	βOH-C17	$C_{23}H_{43}O_7$	431.3021	431.3014	1.5	$[M-H]^-$
bhas#32	13	βOH-C18	$C_{24}H_{45}O_7$	445.3171	445.3171	0.0	$[M-H]^-$
bhas#34	14	βOH-C19	$C_{25}H_{47}O_7$	459.3329	459.3327	0.3	$[M-H]^-$
bhas#36	15	βOH-C20	$C_{26}H_{49}O_7$	473.3488	473.3484	0.9	$[M-H]^-$
bhas#38	16	βOH-C21	$C_{27}H_{51}O_7$	487.3643	487.3640	0.6	$[M-H]^-$
bhas#40	17	βOH-C22	$C_{28}H_{53}O_7$	501.3797	501.3797	0.0	$[M-H]^-$
bhas#42	18	βOH-C23	$C_{29}H_{55}O_7$	515.3959	515.3953	1.1	$[M-H]^-$
bhas#44	19	βOH-C24	$C_{30}H_{57}O_7$	529.4105	529.4110	0.9	$[M-H]^-$
bhas#46	20	βOH-C25	$C_{31}H_{59}O_7$	543.4266	543.4266	0.1	$[M-H]^-$
bhas#48	21	βOH-C26	$C_{32}H_{61}O_7$	557.4415	557.4423	1.3	$[M-H]^-$
bhas#50	22	βOH-C27	$C_{33}H_{63}O_7$	571.4577	571.4579	0.4	$[M-H]^-$

Table S28: ESI-(-)-HR-MS data for (ω)-linked β-hydroxyacyl ascarosides (**asc-βOH-ωC#**).

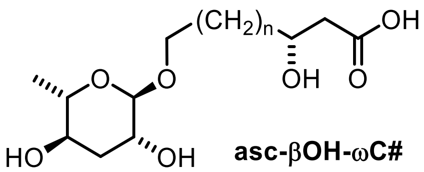

asc-βOH-ωC#

SMID	n	Side chain	Molecular formula	*m/z* obs	*m/z* calc	Δ [ppm]	
bhos#22	9	βOH-ωC13	$C_{19}H_{35}O_7$	375.2387	375.2388	0.3	$[M-H]^-$
bhos#24	10	βOH-ωC14	$C_{20}H_{37}O_7$	389.2545	389.2545	0.1	$[M-H]^-$
bhos#26	11	βOH-ωC15	$C_{21}H_{39}O_7$	403.2704	403.2701	0.7	$[M-H]^-$
bhos#28	12	βOH-ωC16	$C_{22}H_{41}O_7$	417.2863	417.2858	1.2	$[M-H]^-$
bhos#30	13	βOH-ωC17	$C_{23}H_{43}O_7$	431.3013	431.3014	0.2	$[M-H]^-$
bhos#32	14	βOH-ωC18	$C_{24}H_{45}O_7$	445.3173	445.3171	0.6	$[M-H]^-$
bhos#34	15	βOH-ωC19	$C_{25}H_{47}O_7$	459.3331	459.3327	0.9	$[M-H]^-$
bhos#36	16	βOH-ωC20	$C_{26}H_{49}O_7$	473.3487	473.3484	0.7	$[M-H]^-$
bhos#38	17	βOH-ωC21	$C_{27}H_{51}O_7$	487.3641	487.3640	0.1	$[M-H]^-$
bhos#40	18	βOH-ωC22	$C_{28}H_{53}O_7$	501.3792	501.3797	0.9	$[M-H]^-$
bhos#42	19	βOH-ωC23	$C_{29}H_{55}O_7$	515.3948	515.3953	1.1	$[M-H]^-$

Table S29: ESI-(-)-HR-MS data for α-methyl-branched (ω-1)-linked β-hydroxy *iso*-acyl ascarosides (**asc-βOH-*i*C#**)

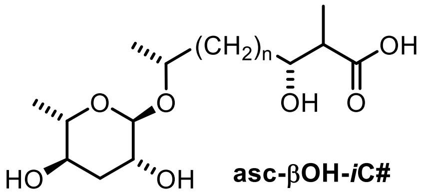

SMID	n	Side chain	Molecular formula	*m/z* obs	*m/z* calc	Δ [ppm]	
bhis#44	18	βOH-*i*C24	$C_{30}H_{57}O_7$	529.4099	529.4110	1.8	$[M-H]^-$
bhis#48	20	βOH-*i*C26	$C_{32}H_{61}O_7$	557.4412	557.4423	2.0	$[M-H]^-$

Table S30: ESI-(+)-HR-MS data for (ω-1)-linked 2-hydroxyalkyl ascarosides (**asc-C#-OH**)

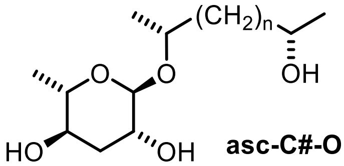

SMID	n	Side chain	Molecular formula	*m/z* obs	*m/z* calc	Δ [ppm]	
ascr#6.1	2	C6-OH	$C_{12}H_{24}NaO_5$	271.1520	271.1516	1.5	$[M+Na]^+$
none	25	C29-OH	$C_{35}H_{71}O_5$ $C_{35}H_{70}NaO_5$	571.5291 593.5116	571.5296 593.5115	0.9 0.1	$[M+H]^+$ $[M+Na]^+$
none	27	C31-OH	$C_{37}H_{75}O_5$ $C_{37}H_{74}NaO_5$	599.5614 621.5435	599.5609 621.5428	0.8 1.0	$[M+H]^+$ $[M+Na]^+$
none	29	C33-OH	$C_{39}H_{79}O_5$ $C_{39}H_{78}NaO_5$	627.5931 649.5747	627.5922 649.5741	1.4 0.9	$[M+H]^+$ $[M+Na]^+$

Table S31: ESI-(+)-HR-MS/MS data for (ω-1)-linked 2-oxoalkyl ascarosides (**asc-C#-MK**).

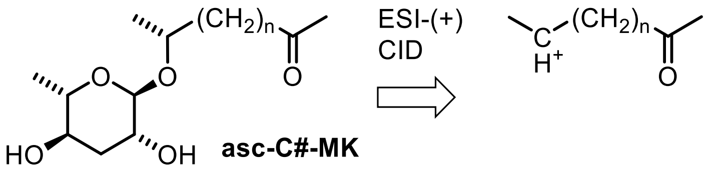

SMID	n	Side chain	Molecular formula	*m/z* obs	*m/z* calc	Δ [ppm]	
ascr#2	2	C6-MK	$C_{12}H_{22}NaO_5$	269.1361	269.1359	0.7	$[M+Na]^+$
mkas#14	4	C8-MK	$C_{14}H_{26}NaO_5$	297.1675	297.1672	1.0	$[M+Na]^+$
mkas#26	11	C15-MK	$C_{21}H_{44}NO_5$ $(C_{15}H_{31}O)$	390.3216 (243.2323)	390.3214 243.2319	0.6 0.9	$[M+NH_4]^+$ $[M-C_6H_9O_3]^+$
mkas#28	12	C16-MK	$C_{22}H_{46}NO_5$ $(C_{16}H_{33}O)$	404.3368 (257.2471)	404.3371 257.2475	0.7 1.6	$[M+NH_4]^+$ $[M-C_6H_9O_3]^+$
mkas#30	13	C17-MK	$C_{23}H_{48}NO_5$ $(C_{17}H_{35}O)$	418.3530 (271.2626)	418.3540 271.2632	2.6 0.3	$[M+NH_4]^+$ $[M-C_6H_9O_3]^+$
mkas#32	14	C18-MK	$C_{24}H_{50}NO_5$ $(C_{18}H_{37}O)$	432.3686 (285.2781)	432.3684 285.2788	0.7 2.5	$[M+NH_4]^+$ $[M-C_6H_9O_3]^+$

SMID	n	Side chain	Molecular formula	*m/z* obs	*m/z* calc	Δ [ppm]	
mkas#34	15	C19-MK	$C_{25}H_{52}NO_5$ ($C_{19}H_{39}O$)	446.3846 (299.2940)	446.3840 299.2945	1.4 1.7	$[M+NH_4]^+$ $[M-C_6H_9O_3]^+$
mkas#36	16	C20-MK	$C_{26}H_{54}NO_5$ ($C_{20}H_{41}O$)	460.3995 (313.3095)	460.3997 313.3101	0.2 1.9	$[M+NH_4]^+$ $[M-C_6H_9O_3]^+$
mkas#38	17	C21-MK	$C_{27}H_{56}NO_5$ ($C_{21}H_{43}O$)	474.4143 (309.3144)	474.4153 (309.3152)	2.0 2.7	$[M+NH_4]^+$ $[M-C_6H_9O_3]^+$
mkas#40	18	C22-MK	$C_{28}H_{58}NO_5$ ($C_{22}H_{43}O$)	488.4297 (323.3298)	488.4310 (323.3308)	2.6 3.2	$[M+NH_4]^+$ $[M-C_6H_9O_3]^+$
mkas#42	19	C23-MK	$C_{29}H_{60}NO_5$ ($C_{23}H_{45}O$)	502.4458 (337.3458)	502.4466 (337.3465)	1.5 2.2	$[M+NH_4]^+$ $[M-C_6H_9O_3]^+$
mkas#44	20	C24-MK	$C_{30}H_{62}NO_5$ ($C_{24}H_{47}O$)	516.4618 (351.3615)	516.4623 (351.3621)	0.8 1.8	$[M+NH_4]^+$ $[M-C_6H_9O_3]^+$
mkas#46	21	C25-MK	$C_{31}H_{64}NO_5$ ($C_{25}H_{49}O$)	530.4773 (365.3772)	530.4779 (365.3778)	1.1 1.6	$[M+NH_4]^+$ $[M-C_6H_9O_3]^+$
mkas#48	22	C26-MK	$C_{32}H_{66}NO_5$ ($C_{26}H_{51}O$)	544.4935 (379.3929)	544.4936 (379.3934)	0.1 1.4	$[M+NH_4]^+$ $[M-C_6H_9O_3]^+$
mkas#50	23	C27-MK	$C_{33}H_{68}NO_5$ ($C_{27}H_{53}O$)	558.5083 (393.4083)	558.5092 (393.4091)	1.6 2.1	$[M+NH_4]^+$ $[M-C_6H_9O_3]^+$
mkas#52	24	C28-MK	$C_{34}H_{70}NO_5$ ($C_{28}H_{55}O$)	572.5234 (407.4239)	572.5249 407.4247	2.6 2.0	$[M+NH_4]^+$ $[M-C_6H_9O_3]^+$

Table S32: ESI-(+)-HR-MS/MS data for (ω)-linked 2-oxoalkyl ascarosides (**asc-ωC#-MK**).

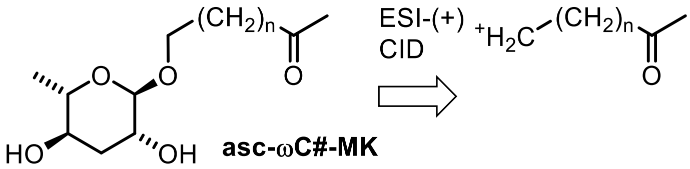

asc-ωC#-MK

SMID	n	Side chain	Molecular formula	*m/z* obs	*m/z* calc	Δ [ppm]	
mkos#26	12	ωC15-MK	$C_{21}H_{44}NO_5$ ($C_{15}H_{31}O$)	390.3203 (243.2311)	390.3214 243.2319	2.8 3.3	$[M+NH_4]^+$ $[M-C_6H_9O_3]^+$
mkos#28	13	ωC16-MK	$C_{22}H_{46}NO_5$ ($C_{16}H_{33}O$)	404.3356 (257.2469)	404.3371 257.2475	3.7 2.3	$[M+NH_4]^+$ $[M-C_6H_9O_3]^+$
mkos#30	14	ωC17-MK	$C_{23}H_{48}NO_5$ ($C_{17}H_{35}O$)	418.3528 (271.2629)	418.3540 271.2632	1.3 1.1	$[M+NH_4]^+$ $[M-C_6H_9O_3]^+$
mkos#32	15	C18-MK	$C_{24}H_{50}NO_5$ ($C_{18}H_{37}O$)	432.3678 (285.2775)	432.3684 285.2788	1.4 4.6	$[M+NH_4]^+$ $[M-C_6H_9O_3]^+$
mkos#34	16	ωC19-MK	$C_{25}H_{52}NO_5$ ($C_{19}H_{39}O$)	446.3842 (299.2937)	446.3840 299.2945	0.4 2.7	$[M+NH_4]^+$ $[M-C_6H_9O_3]^+$
mkos#36	17	ωC20-MK	$C_{26}H_{54}NO_5$ ($C_{20}H_{41}O$)	460.3989 (313.3090)	460.3997 313.3101	1.7 3.5	$[M+NH_4]^+$ $[M-C_6H_9O_3]^+$
mkos#38	18	ωC21-MK	$C_{27}H_{56}NO_5$ ($C_{21}H_{43}O$)	474.4148 (309.3145)	474.4153 (309.3152)	1.1 2.3	$[M+NH_4]^+$ $[M-C_6H_9O_3]^+$
mkos#40	19	ωC22-MK	$C_{28}H_{58}NO_5$ ($C_{22}H_{43}O$)	488.4299 (323.3296)	488.4310 (323.3308)	2.3 3.7	$[M+NH_4]^+$ $[M-C_6H_9O_3]^+$
mkos#42	20	ωC23-MK	$C_{29}H_{60}NO_5$ ($C_{23}H_{45}O$)	502.4451 (337.3459)	502.4466 (337.3465)	3.0 1.8	$[M+NH_4]^+$ $[M-C_6H_9O_3]^+$

Table S33: ESI-(+)-HR-MS/MS data for (ω-1)-linked acyl ascaroside ethanolamides (**asc-C#-EA**)

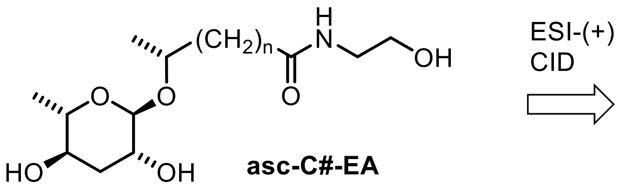

asc-C#-EA

SMID	n	Side chain	Molecular formula	*m/z* obs	*m/z* calc	Δ [ppm]	
easc#9	2	C5-EA[a]	$C_{13}H_{28}NO_6$	294.1909	294.1911	0.7	$[M+H]^+$
easc#18	8	C11-EA*[b]	$C_{19}H_{38}NO_6$ ($C_{13}H_{28}NO_3$)	376.2690 246.2058	376.2694 246.2064	1.1 2.4	$[M+H]^+$ $[M-C_6H_9O_3]^+$
easc#20	9	C12-EA	$C_{20}H_{40}NO_6$	390.2854	390.2850	1.0	$[M+H]^+$
easc#22	10	C13-EA	$C_{21}H_{42}NO_6$	404.3015	404.3007	2.0	$[M+H]^+$
easc#24	11	C14-EA	$C_{22}H_{44}NO_6$	418.3170	418.3163	1.7	$[M+H]^+$

[a]: *Caenorhabditis portoensis*, [b]: *Heterorhabditis bacteriophora*, [*]: synthetic standard

Table S34: ESI-(+)-HR-MS data for (ω-1)-linked enoyl ascaroside ethanol amides (**asc-ΔC#-EA**)

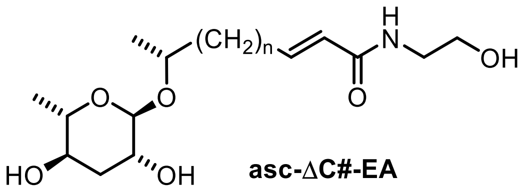

asc-ΔC#-EA

SMID	n	Side chain	Molecular formula	*m/z* obs	*m/z* calc	Δ [ppm]	
easc#45	20	ΔC25-EA	$C_{33}H_{63}NNaO_6$	592.4552	592.4548	0.7	$[M+Na]^+$
easc#47	21	ΔC26-EA	$C_{34}H_{65}NNaO_6$	606.4709	606.4704	0.8	$[M+Na]^+$
easc#49	22	ΔC27-EA	$C_{35}H_{67}NNaO_6$	620.4865	620.4861	0.6	$[M+Na]^+$
easc#51	23	ΔC28-EA	$C_{36}H_{69}NNaO_6$	634.5026	634.5017	1.4	$[M+Na]^+$
easc#53	24	ΔC29-EA	$C_{37}H_{71}NNaO_6$	648.5181	648.5174	1.1	$[M+Na]^+$

Table S35: ESI-(+)-HR-MS data for α-methyl-branched (ω-1)-linked *iso*-enoyl ascaroside ethanol amide (**asc-Δ*i*C#-EA**)

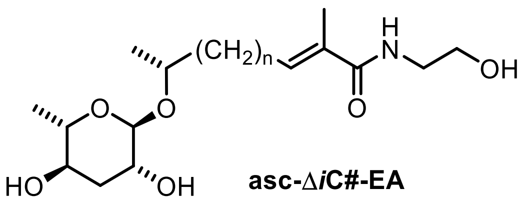

asc-Δ*i*C#-EA

SMID	n	Side chain	Molecular formula	*m/z* obs	*m/z* calc	Δ [ppm]	
eisc#47	20	Δ*i*C26-EA	$C_{34}H_{65}NNaO_6$ $C_{34}H_{66}NO_6$	606.4707 584.4887	606.4704 584.4885	0.5 0.4	$[M+Na]^+$ $[M+H]^+$

Table S36: ESI-(+)-HR-MS/MS data for (ω-1)-linked β-hydroxyacyl ascaroside ethanolamides (**asc-βOH-C#-EA**)

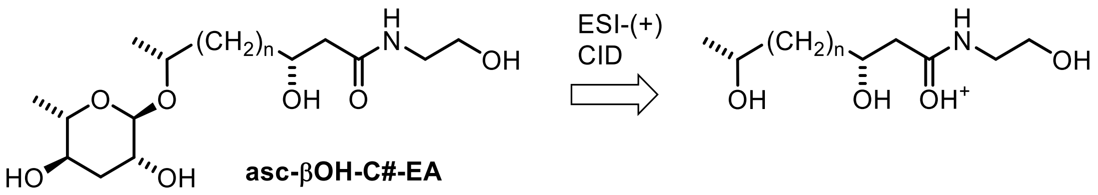

SMID	n	Side chain	Molecular formula	*m/z* obs	*m/z* calc	Δ [ppm]	
ebha#30	12	βOH-C17-EA	$C_{25}H_{50}NO_7$ ($C_{19}H_{40}NO_4$)	476.3583 (346.2951)	476.3582 (346.2955)	0.2 0.2	$[M+H]^+$ $[M-C_6H_9O_3]^+$
ebha#32	13	βOH-C18-EA	$C_{26}H_{52}NO_7$ ($C_{20}H_{42}NO_4$)	490.3738 (360.3106)	490.3738 (360.3108)	0.0 0.3	$[M+H]^+$ $[M-C_6H_9O_3]^+$
ebha#34	14	βOH-C19-EA	$C_{27}H_{54}NO_7$ ($C_{21}H_{44}NO_4$)	504.3899 (374.3267)	504.3895 (374.3265)	0.8 0.5	$[M+H]^+$ $[M-C_6H_9O_3]^+$
ebha#36	15	βOH-C20-EA	$C_{28}H_{56}NO_7$ ($C_{22}H_{46}NO_4$)	518.4058 (388.3427)	518.4051 (388.3421)	1.4 1.4	$[M+H]^+$ $[M-C_6H_9O_3]^+$
ebha#38	16	βOH-C21-EA	$C_{29}H_{58}NO_7$ ($C_{23}H_{48}NO_4$)	532.4217 (402.3585)	532.4208 (402.3578)	1.8 1.9	$[M+H]^+$ $[M-C_6H_9O_3]^+$
ebha#40	17	βOH-C22-EA	$C_{30}H_{60}NO_7$ ($C_{24}H_{50}NO_4$)	546.4371 (416.3739)	546.4364 (416.3734)	1.2 1.2	$[M+H]^+$ $[M-C_6H_9O_3]^+$
ebha#42	18	βOH-C23-EA	$C_{31}H_{62}NO_7$ ($C_{25}H_{52}NO_4$)	560.4528 (430.3896)	560.4521 (430.3891)	1.2 1.2	$[M+H]^+$ $[M-C_6H_9O_3]^+$
ebha#44	19	βOH-C24-EA	$C_{32}H_{64}NO_7$ ($C_{26}H_{54}NO_4$)	574.4677 (444.4046)	574.4677 (444.4047)	0.1 0.4	$[M+H]^+$ $[M-C_6H_9O_3]^+$
ebha#46	20	βOH-C25-EA	$C_{33}H_{66}NO_7$ ($C_{27}H_{56}NO_4$)	588.4832 (458.4204)	588.4834 (458.4204)	0.2 0.0	$[M+H]^+$ $[M-C_6H_9O_3]^+$
ebha#48	21	βOH-C26-EA	$C_{34}H_{68}NO_7$ ($C_{28}H_{58}NO_4$)	602.4984 (472.4352)	602.4990 (472.4360)	1.0 1.7	$[M+H]^+$ $[M-C_6H_9O_3]^+$
ebha#50	22	βOH-C27-EA	$C_{35}H_{70}NO_7$ ($C_{29}H_{60}NO_4$)	616.5139 (486.4506)	616.5160 (486.4517)	1.2 2.3	$[M+H]^+$ $[M-C_6H_9O_3]^+$

Table S37: ESI-(+)-HR-MS/MS data for (ω)-linked β-hydroxyacyl ascaroside ethanolamides (**asc-βOH-ωC#-EA**)

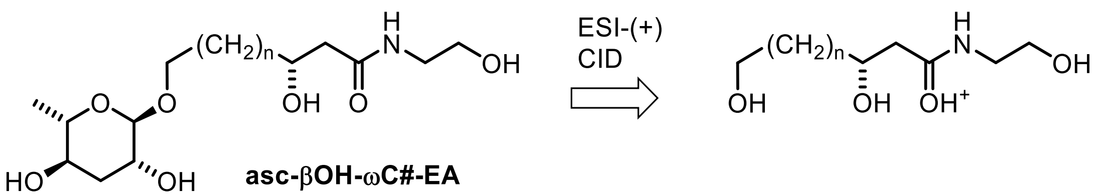

SMID	n	Side chain	Molecular formula	*m/z* obs	*m/z* calc	Δ [ppm]	
ebho#24	10	βOH-ωC14-EA	$C_{22}H_{44}NO_7$ ($C_{16}H_{34}NO_4$)	434.3118 (304.2489)	434.3112 (304.2482)	1.4 2.3	$[M+H]^+$ $[M-C_6H_9O_3]^+$
ebho#26	11	βOH-ωC15-EA	$C_{23}H_{46}NO_7$ ($C_{17}H_{36}NO_4$)	448.3271 (318.2647)	448.3269 (318.2639)	0.4 2.5	$[M+H]^+$ $[M-C_6H_9O_3]^+$
ebho#28	12	βOH-ωC16-EA	$C_{24}H_{48}NO_7$ ($C_{18}H_{38}NO_4$)	462.3429 (332.2800)	462.3425 (332.2795)	0.9 1.5	$[M+H]^+$ $[M-C_6H_9O_3]^+$
ebho#30	13	βOH-ωC17-EA	$C_{25}H_{50}NO_7$ ($C_{19}H_{40}NO_4$)	476.3576 (346.2959)	476.3582 (346.2952)	1.3 2.0	$[M+H]^+$ $[M-C_6H_9O_3]^+$
ebho#32	14	βOH-ωC18-EA	$C_{26}H_{52}NO_7$ ($C_{20}H_{42}NO_4$)	490.3738 (360.3107)	490.3738 (360.3108)	0.0 0.3	$[M+H]^+$ $[M-C_6H_9O_3]^+$
ebho#34	15	βOH-ωC19-EA	$C_{27}H_{54}NO_7$ ($C_{21}H_{44}NO_4$)	504.3893 (374.3266)	504.3895 (374.3265)	0.3 0.2	$[M+H]^+$ $[M-C_6H_9O_3]^+$
ebho#36	16	βOH-ωC20-EA	$C_{28}H_{56}NO_7$ ($C_{22}H_{46}NO_4$)	518.4052 (388.3424)	518.4051 (388.3421)	0.1 0.7	$[M+H]^+$ $[M-C_6H_9O_3]^+$

SMID	n	Side chain	Molecular formula	*m/z* obs	*m/z* calc	Δ [ppm]	
ebho#38	17	βOH-ωC21-EA	$C_{29}H_{58}NO_7$ ($C_{23}H_{48}NO_4$)	532.4220 (402.3583)	532.4208 (402.3578)	2.2 1.3	$[M+H]^+$ $[M-C_6H_9O_3]^+$
ebho#40	18	βOH-ωC22-EA	$C_{30}H_{60}NO_7$ ($C_{24}H_{50}NO_4$)	546.4369 (416.3737)	546.4364 (416.3734)	0.8 0.7	$[M+H]^+$ $[M-C_6H_9O_3]^+$
ebho#42	19	βOH-ωC23-EA	$C_{31}H_{62}NO_7$ ($C_{25}H_{52}NO_4$)	560.4523 (430.3891)	560.4521 (430.3891)	0.4 0.0	$[M+H]^+$ $[M-C_6H_9O_3]^+$

Table S38: ESI-(+)-HR-MS/MS data for (ω-1)-linked α-methyl-β-hydroxyacyl ascaroside ethanolamides (**asc-βOH-*i*C#-EA**)

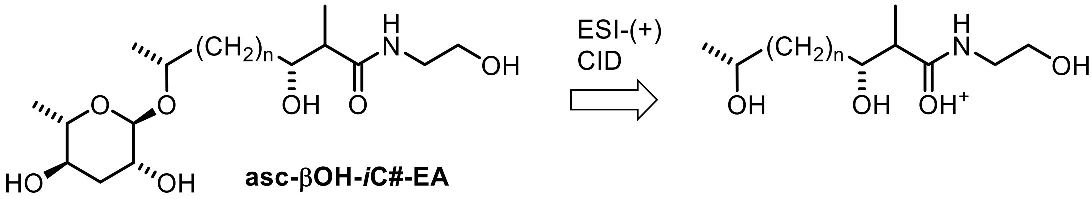

SMID	n	Side chain	Molecular formula	*m/z* obs	*m/z* calc	Δ [ppm]	
ebhi#44	18	βOH-*i*C24-EA	$C_{32}H_{64}NO_7$ ($C_{26}H_{54}NO_4$)	574.4682 (444.4053)	574.4677 (444.4047)	0.8 1.4	$[M+H]^+$ $[M-C_6H_9O_3]^+$
ebhi#48	20	βOH-*i*C26-EA	$C_{34}H_{68}NO_7$ ($C_{28}H_{58}NO_4$)	602.4983 (472.4354)	602.4990 (472.4360)	1.1 1.4	$[M+H]^+$ $[M-C_6H_9O_3]^+$

4. Synthesis of ascaroside standards

Authentic reference standards of asc-ωC3 (ascr#5),[3] asc-C5 (ascr#9),[4] asc-ωC5 (oscr#9),[5] asc-C6-OH (ascr#6.1),[6,7] asc-C7 (ascr#1),[8] asc-ΔC7 (ascr#7),[6] asc-C9 (ascr#10),[4] asc-ωC9 (oscr#10),[5] asc-ΔC9 (ascr#3),[8,9] asc-C6-MK (ascr#2),[7,8] asc-C11 (ascr18),[10] asc-βOH-C13 (bhas#22),[5] HB-asc-ΔC9 (hbas#3),[5] IC-asc-ΔC9 (icas#3),[4] IC-asc-C6-MK (icas#2)[7] were synthesized as previously described (Figure S1). Reference standards of asc-C3, asc-C4 (ascr#11), asc-C18 (ascr#32), asc-ωC20 (oscr#36), and asc-C11-EA (easc#18) were prepared as described in the following sections.

4.1. Synthesis of asc-C3

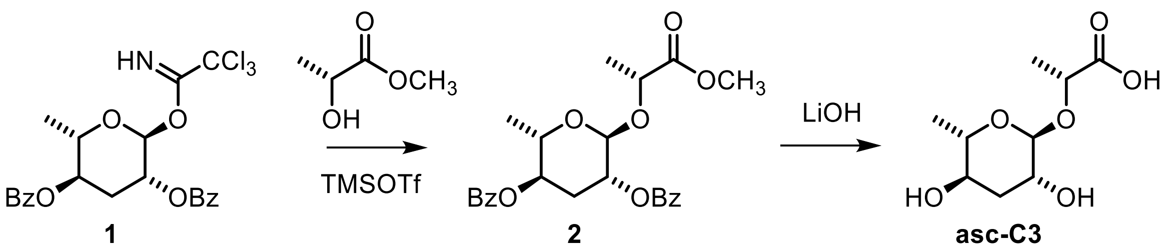

4.1.1. Synthesis of methyl (2*R*)-[(2,4-di-*O*-benzoyl-3,6-dideoxy-α-L-*arabino*-hexopyranosyl)oxy]propanoate (2)

A solution of 66 mg 1-[2,4-di-*O*-benzoyl-3,6-dideoxy-α-L-*arabino*-hexopyranosyl]-2,2,2-trichloroacetimidate (**1**)[11] (132 µmol) in 10 ml dry DCM was treated with 32 µL methyl (2*R*)-hydroxypropanoate (330 µmol) in 200 µL dry dichloromethane and 5 µL trimethylsilyl triflate at 0 °C. After 1 h at 0 °C the reaction was concentrated in vacuum and purified by column chromatography on silica gel to afford 35.1 mg methyl (2*R*)-[(2,4-di-*O*-benzoyl-3,6-dideoxy-α-L-*arabino*-hexopyranosyl)oxy]propanoate (**2**) (79 µmol, 60% yield) as a colorless oil.

^{1}H NMR (400 MHz, CD_3OD): δ (ppm) 1.18 (3H, d, *J* = 6.2 Hz), 1.44 (3H, d, *J* = 6.7 Hz), 2.23 (1H, m), 2.41 (1H, ddd, *J* = 13.5 Hz, *J* = 3.7 Hz, *J* = 3.7 Hz), 3.76 (3H, s), 4.28 (2H, m), 4.94 (1H, s), 5.12 (1H, ddd, *J* = 10.7 Hz, *J* = 10.2 Hz, *J* = 4.4 Hz), 5.19 (1H, br s), 7.50 (4H, m), 7.63 (2H, m), 8.02 (2H, d, *J* = 7.1 Hz), 8.09 (2H, d, *J* = 8.1 Hz) - (Fig. S17)
^{13}C NMR (100 MHz, $CDCl_3$): δ (ppm) 18.0, 18.6, 30.6, 52.6, 68.8, 71.8, 72.1, 75.2, 98.3, 129.7 (2), 129.7 (2), 130.6 (2), 130.7 (2), 131.1, 131.1, 134.5, 134.6, 166.9, 167.1, 174.8 - (Fig. S18)

4.1.2. Synthesis of (2*R*)-[(3,6-dideoxy-α-L-*arabino*-hexopyranosyl)oxy] propanoic acid (asc-C3)

A solution of 35.1 mg methyl (2*R*)-[(2,4-di-*O*-benzoyl-3,6-dideoxy-α-L-*arabino*-hexopyranosyl)oxy]propanoate (**2**) (79 µmol) in 350 µl of methanol was treated with 380 µl saturated LiOH solution (2.22 mmol) and stirred for 12 h. The reaction was quenched with acetic acid, concentrated to dryness and chromatographed on silica gel using a gradient of 40-100% methanol in DCM to afford 11 mg (2*R*)-[(3,6-dideoxy-α-L-*arabino*-hexopyranosyl)oxy]-propanoic acid (**asc-C3**) as a colorless oil (47.2 µmol, 60% yield).

^{1}H NMR (400 MHz, CD_3OD): δ (ppm) 1.18 (3H, d, *J* = 6.2 Hz), 1.36 (3H, d, *J* = 6.7 Hz), 1.93 (2H, m), 3.49 (1H, m), 3.75 (1H, dq, *J* = 9.2 Hz, *J* = 6.3 Hz), 3.83 (1H, s br), 4.13 (1H, q, *J* = 6.7 Hz), 4.62 (1H, s) - (Fig. S19)
^{13}C NMR (100 MHz, CD_3OD): δ (ppm) 18.0, 18.5, 35.9, 68.6, 69.6, 71.4, 74.6, 99.4, *Cq* not observed - (Fig. S20)
ESI-(-)-HR-MS obs. *m/z* 219.0873, calc. *m/z* 219.0869 for $C_9H_{15}O_6$, Δ 1.8 ppm.

4.2. Synthesis of asc-C4 (ascr#11)

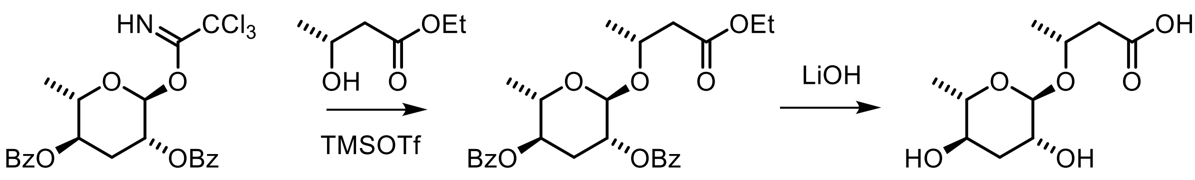

4.2.1. Synthesis of ethyl (3*R*)-[(2,4-di-*O*-benzoyl-3,6-dideoxy-α-L-*arabino*-hexopyranosyl)oxy]butanoate (3)

A solution of 466 mg 1-[2,4-di-*O*-benzoyl-3,6-dideoxy-α-L-*arabino*-hexopyranosyl]-2,2,2-trichloroacetimidate (**1**)[11] (934 µmol) in 12 ml dry DCM was treated with 182 µL ethyl (3*R*)-hydroxybutanoate (1.4 mmol) in 200 µL dry dichloromethane and 10 µL trimethylsilyl triflate at 0 °C. After 2 h at 0 °C the reaction was concentrated in vacuum and purified by column chromatography on silica gel to afford 310 mg ethyl (3*R*)-[(2,4-di-*O*-benzoyl-3,6-dideoxy-α-L-*arabino*-hexopyranosyl)oxy]butanoate (**3**) (659 µmol, 71% yield) as a colorless oil.

^{1}H NMR (400 MHz, CD_3OD): δ (ppm) 1.26 (3H, d *J* = 6.3 Hz), 1.28 (3H, d, *J* = 6.1 Hz), 1.32 (3H, t, *J* = 7.1 Hz), 2.14 (1H, m), 2.50 (1H, m), 2.60 (2H, m), 4.19 (3H, m), 4.37 (1H, m), 5.00 (1H, s), 5.08 (1H, s.br), 5.11 (1H, m), 7.52 (4H, m), 7.65 (2H, m), 8.01 (2H, d, *J* = 8.2 Hz), 8.10 (2H, d, *J* = 8.3 Hz) - (Fig. S21)

^{13}C NMR (100 MHz, CD_3OD): δ (ppm) 14.4, 17.9, 19.2, 29.8, 42.7, 60.7, 67.1, 69.3, 70.7, 71.1, 93.6, 128.59 (2), 128.61 (2), 129.7 (2), 129.97, 130.0 (2), 130.2, 133.33, 133.42, 165.8, 165.9, 171.4 - (Fig. S22)

4.2.2. Synthesis of (2*R*)-[(3,6-dideoxy-α-L-*arabino*-hexopyranosyl)oxy]butanoic acid (asc-C4)

A solution of 130 mg ethyl (3*R*)-[(2,4-di-*O*-benzoyl-3,6-dideoxy-α-L-*arabino*-hexopyranosyl) oxy]butanoate (**3**) (276 µmol) in 1.3 ml methanol was treated with 1.55 ml saturated LiOH solution (8.28 mmol) and stirred for 12 h. The reaction was quenched with acetic acid, concentrated to dryness and chromatographed on silica gel using a 10% methanol with 0.5% acetic acid in DCM to afford 62 mg (2*R*)-[(3,6-dideoxy-α-L-*arabino*-hexopyranosyl)oxy] butanoic acid (**asc-C4**) as a colorless oil (265 µmol, 96% yield).

^{1}H NMR (400 MHz, CD_3OD): δ (ppm) 1.21 (6H, m), 1.75 (1H, m), 1.92 (1H, td, *J* = 13.0 Hz, *J* = 3.9 Hz), 2.42 (1H, m), 2.52 (1H, m), 3.50 (1H, ddd, *J* = 10.6 Hz, *J* = 10.2 Hz, *J* = 4.4), 3.66 (1H, tq, *J* = 7.5 Hz, *J* = 6.1 Hz), 3.72 (1H, br s), 4.25 (1H, m), 4.66 (1H, s) - (Fig. S23)
^{13}C NMR (100 MHz, CD_3OD): δ (ppm) 18.0, 19.2, 35.9, 44.1, 68.4, 69.9, 70.0, 71.1, 97.5, *Cq* not observed - (Fig. S24)
ESI-(-)-HR-MS obs. *m/z* 233.1037, calc. *m/z* 233.1031 for $C_{10}H_{17}O_6$, Δ 2.6 ppm.

4.3. Synthesis of asc-C18 (ascr#32)

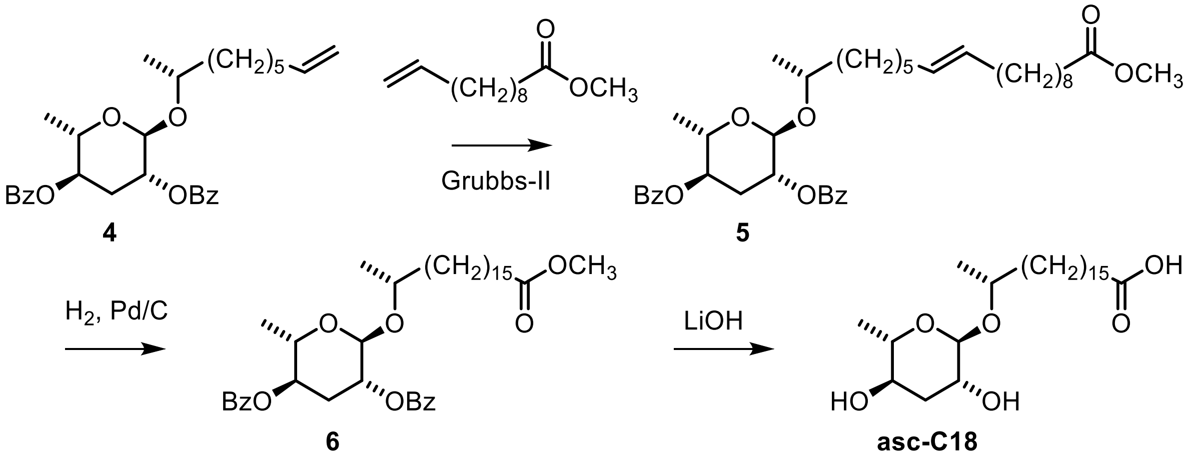

4.3.1. Synthesis of methyl (17*R*)-[(2,4-di-*O*-benzoyl-3,6-dideoxy-α-L-*arabino*-hexopyranosyl)oxy]-(10*E*)-octadecenoate (5).

A stirred solution of 10 mg (8*R*)-[(2,4-di-*O*-benzoyl-3,6-dideoxy-α-L-*arabino*-hexopyranosyl) oxy]-1-nonene (**4**)[5] (20.8 µmol) in 10 ml dry DCM was treated with 23.4 µL methyl 10-undecenoate (100.9 µmol) in 200 µL dry dichloromethane and 1.8 mg Grubbs 2nd generation catalyst (2.1 µmol) and heated under argon to 40 °C. After 6 h the catalyst was filtered off, the solution concentrated and the product isolated by column chromatography on silica gel using 7% ethyl acetate in hexane to afford 7 mg methyl (17*R*)-[(2,4-di-*O*-benzoyl-3,6-dideoxy-α-L-*arabino*-hexopyranosyl)oxy]-(10*E*)-octadecenoate (**5**) (10.8 µmol, 52% yield) as a colorless oil.

^{1}**H NMR** (400 MHz, CD_3OD): δ (ppm) 1.10 (3H, d, *J* = 6.1 Hz), 1.16 (3H, d, *J* = 6.4 Hz), 1.21 (8H, m), 1.32 (6H, m), 1.48 (6H, m), 1.88 (2H, m), 1.94 (2H, m), 2.11 (1H, m), 2.19 (2H, m), 2.31 (1H, ddd, *J* = 13.4 Hz, *J* = 4.1 Hz, *J* = 4.1 Hz), 3.54 (3H, s), 3.79 (1H, dt, *J* = 5.8 Hz, *J* = 3.6 Hz), 4.07 (1H, dq, *J* = 9.5 Hz, *J* = 6.4 Hz), 4.87 (1H, s), 4.99 (2H, m), 5.03 (2H, m), 5.30 (2H, m), 7.43 (4H, m), 7.54 (4H, m), 7.92 (2H, d, *J* = 7.5 Hz), 8.01 (2H, d, *J* = 7.7 Hz) - (Fig. S25-26)

^{13}**C NMR** (100 MHz, CD_3OD): δ (ppm) 18.2, 19.5, 26.0, 26.7, 30.0, 30.1, 30.2, 30.3, 30.4, 30.6, 30.7, 30.7, 33.5, 33.6, 34.8, 38.2, 51.9, 68.3, 72.1, 72.8, 73.8, 95.1, 129.7 (4C), 130.6 (2C), 130.7 (2C), 131.2, 131.2, 131.4, 131.7, 134.5, 134.6, 167.1, 167.1, 176.0 - (Fig. S27-28)

4.3.2. Synthesis of methyl (17*R*)-[(2,4-di-*O*-benzoyl-3,6-dideoxy-α-L-*arabino*-hexopyranosyl)oxy]octadecanoate (6)

A stirred solution of 7 mg methyl (17*R*)-[(2,4-di-*O*-benzoyl-3,6-dideoxy-α-L-*arabino*-hexopyranosyl)oxy]-(10*E*)-octadecenoate (**5**) (10.8 µmol) in 10 ml methanol was treated with 5 mg 10% palladium on carbon and hydrogenated for 12 h to afford after filtration 6.8 mg of methyl (17*R*)-[(2,4-di-*O*-benzoyl-3,6-dideoxy-α-L-*arabino*-hexopyranosyl)oxy]octadecanoate (**6**) (10.4 µmol, 96% yield) as a colorless oil.

^{1}**H NMR** (400 MHz, CD_3OD): δ (ppm) 1.10 (3H, d, *J* = 6.1 Hz), 1.16 (3H, d, *J* = 5.9 Hz), 1.27 (20H, m), 1.48 (8H, m), 2.11 (1H, m), 2.20 (2H, m), 2.31 (1H, ddd, *J* = 13.8 Hz, *J* = 3.9 Hz, *J* = 3.7 Hz), 3.54 (3H, s), 3.79 (1H, m), 4.07 (1H, dq, *J* = 10.1 Hz, *J* = 5.9 Hz), 4.87 (1H, s), 4.99 (1H, br s), 5.04 (1H, m), 7.42 (4H, m), 7.55 (2H, m), 7.92 (2H, d, *J* = 7.3 Hz), 8.01 (2H, d, *J* = 7.5 Hz) - (Fig. S29-30)

^{13}C NMR (100 MHz, CD_3OD): δ (ppm) 17.9, 19.3, 25.7(2C), 30.3, 30.4 (11C), 34.6, 37.9, 51.6, 68.1, 72.5 (2C), 73.7, 95.0, 129.5 (4C), 130.3 (2C), 130.5(2C), 134.3 (2C), 169.5 - (Fig. S31)

4.3.3. Synthesis of (17*R*)-[(3,6-dideoxy-α-L-*arabino*-hexopyranosyl)oxy]octadecanoic acid (asc-C18)

A stirred solution of 6.8 mg of methyl (17*R*)-[(2,4-di-*O*-benzoyl-3,6-dideoxy-α-L-*arabino*-hexopyranosyl)oxy]octadecanoate (**6**) (10.4 µmol) in 70 µl methanol was treated with 25 µl of a saturated aqueous LiOH solution (312 µmol) and stirred for 12 h. The mixture was acidified with acetic acid and concentrated in vacuum. Column chromatography on silica gel using 5% methanol with 1% acetic acid in DCM afforded 1.3 mg (17*R*)-[(3,6-dideoxy-α-L-*arabino*-hexopyranosyl)oxy]octadecanoic acid (**asc-C18**) (3.0 µmol, 29% yield) as a as a waxy solid.

^{1}H NMR (400 MHz, CD_3OD): δ (ppm) 1.12 (3H, d, *J* = 6.0 Hz), 1.21 (3H, d, *J* = 6.2 Hz), 1.30 (22H, s), 1.58 (4H, m), 1.77 (1H, m), 1.97 (3H, m), 2.23 (2H, t, *J* = 7.5 Hz), 3.52 (1H, ddd, *J* = 10.5 Hz, *J* = 10.4 Hz, *J* = 4.4 Hz), 3.63 (1H, dq, *J* = 8.2 Hz, *J* = 6.6 Hz), 3.71 (1H, br s), 3.77 (1H, m), 4.64 (1H, s) - (Fig. S32)
^{13}C NMR (100 MHz, CD_3OD): δ (ppm) 18.1, 19.4, 26.1, 26.7, 29.9, 30.1 (2C), 30.3 (2C), 30.5 (2C), 30.6, 30.7 (4C), 36.0, 38.4, 68.4, 70.0, 71.2, 72.6, 97.7, *Cq* not observed - (Fig. S33)

The product was analyzed by HPLC-ESI-(-)-HR-MS to show a homologous mixture of long chain ascarosides dominated by asc-C18 (Figure S15).

	obs. *m/z* [M – H]	**calc. *m/z* [M – H]**	**Molecular formula**	**Δ [ppm]**
asc-C18	429.3219	429.3222	$C_{24}H_{45}O_6$	0.7
asc-C17	415.3062	415.3065	$C_{23}H_{43}O_6$	0.6
asc-C16	401.2903	401.2909	$C_{22}H_{41}O_6$	1.4
asc-C15	387.2746	387.2752	$C_{21}H_{39}O_6$	1.7

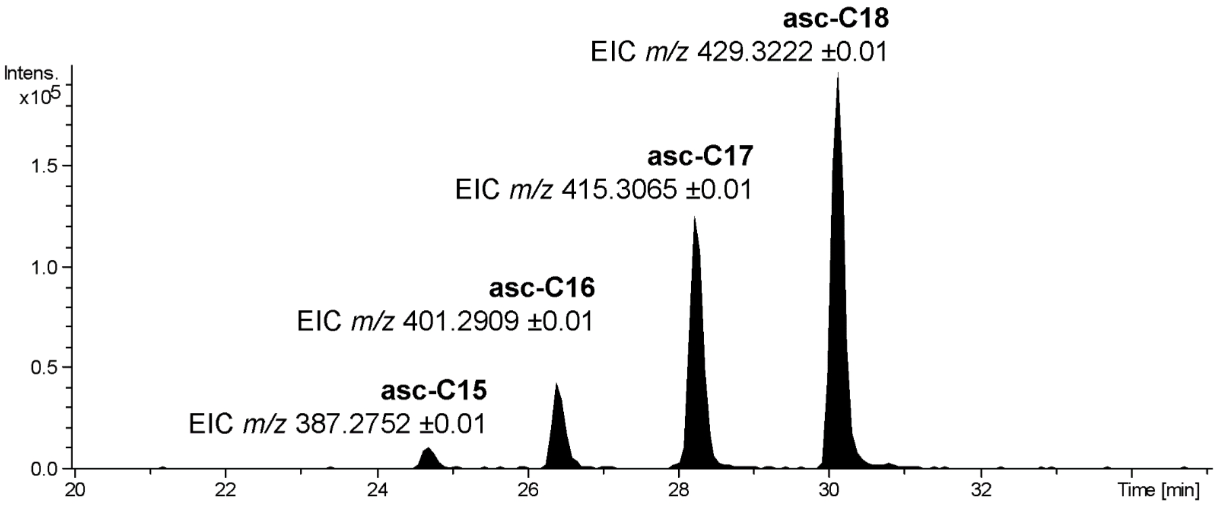

Figure S15: HPLC-ESI-(-)-HRMS extracted ion chromatograms for the homologous series of ascarosides produced by metathesis with asc-C18 as the dominating compound.

4.4. Synthesis of asc-ωC20 (oscr#36)

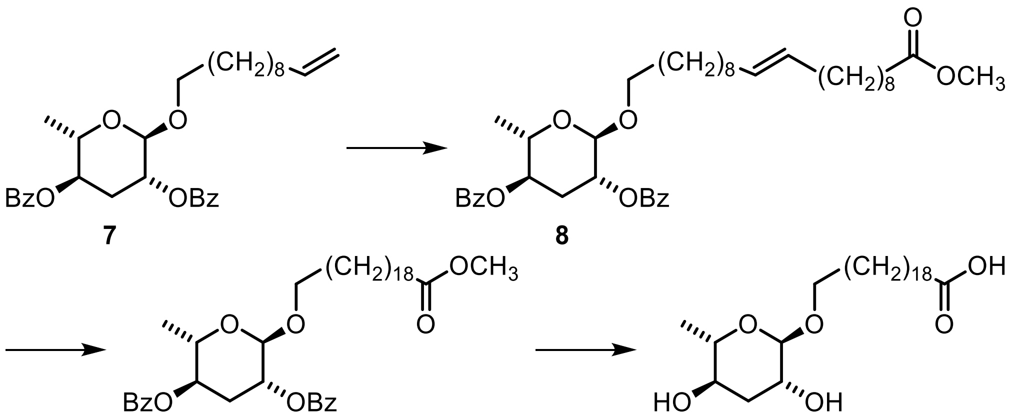

4.4.1. Synthesis of methyl 20-[(2,4-di-*O*-benzoyl-3,6-dideoxy-α-L-*arabino*-hexopyranosyl)oxy]-(10*E*)-eicosenoate (8)

A stirred solution of 10 mg 11-[(2,4-di-*O*-benzoyl-3,6-dideoxy-α-L-*arabino*-hexopyranosyl)oxy]-1-undecene (**7**)[5] (19.7 μmol) in 10 ml dry DCM was treated with 22.1 μL methyl 10-undecenoate (98.3 μmol) in 200 μL dry dichloromethane and 1.7 mg Grubbs 2nd generation catalyst (2.0 μmol) and heated under argon to 40 °C. After 6 h the catalyst was filtered off, the solution concentrated and the product isolated by column chromatography on silica gel using 7% ethyl acetate in hexane to afford 6 mg methyl 20-[(2,4-di-*O*-benzoyl-3,6-dideoxy-α-L-*arabino*-hexopyranosyl)oxy]-(10*E*)-eicosenoate (**8**) (8.8 μmol, 45% yield) as a colorless oil.

^{1}H NMR (400 MHz, CD_3OD): δ (ppm) 1.27 (3H, d, *J* = 6.6 Hz), 1.32 (20H, m), 1.46 (2H, m), 1.59 (2H, m), 1.67 (2H, m), 1.99 (4H, m), 2.21 (1H, m), 2.30 (2H, t), 2.41 (1H, ddd, *J* = 13.7 Hz, *J* = 3.9 Hz, *J* = 3.6 Hz), 3.55 (1H, dt, *J* = 9.5 Hz, *J* = 6.3 Hz), 3.64 (3H, s), 3.80 (1H, dt, *J* = 9.2 Hz, *J* = 6.8 Hz), 4.11 (1H, dq, *J* = 9.8 Hz, *J* = 6.2 Hz), 4.83 (1H, s), 5.13 (2H, m), 5.35 (2H, m), 7.52 (4H, m), 7.65 (2H, m), 8.02 (2H, d, *J* = 7.7 Hz), 8.10 (2H, d, *J* = 7.7 Hz) - (Fig. S34-35)
^{13}C NMR (100 MHz, CD_3OD): δ (ppm) 18.2, 26.0, 27.3, 27.3, 30.1, 30.1, 30.2, 30.2, 30.3, 30.4, 30.4, 30.5, 30.6, 30.7, 30.7, 30.7, 33.6, 34.8, 51.9, 68.1, 68.9, 72.0, 72.2, 97.7, 129.7, 30.6, 130.7, 131.5, 134.5, 134.6,167.7, 173.2, 173.3 - (Fig. S36)

4.4.2. Synthesis of methyl 20-[(2,4-di-*O*-benzoyl-3,6-dideoxy-α-L-*arabino*-hexopyranosyl)oxy]eicosanoate (9)

A stirred solution of 6 mg methyl 20-[(2,4-di-*O*-benzoyl-3,6-dideoxy-α-L-*arabino*-hexopyranosyl)oxy]-(10*E*)-eicosenoate (**8**) (8.8 µmol) in 10 ml methanol was treated with 5 mg 10% Pd on carbon and hydrogenated for 12 h to afford after filtration 5.8 mg of methyl 20-[(2,4-di-*O*-benzoyl-3,6-dideoxy-α-L-*arabino*-hexopyranosyl)oxy]eicosanoate (**9**) (8.5 µmol, 96% yield) as a colorless oil.

^{1}H NMR (400 MHz, CD_3OD): δ (ppm) 1.28 (26H, m), 1.46 (2H, m), 1.59 (2H, m), 1.68 (2H, m), 2.21 (1H, m), 2.30 (2H, t, *J* = 7.3 Hz), 2.41 (1H, m), 3.55 (1H, dt, *J* = 9.7 Hz, *J* = 6.1 Hz), 3.65 (3H, s), 3.80 (1H, dt, *J* = 9.1 Hz, *J* = 6.8 Hz), 4.12 (1H, dq, *J* = 9.7 Hz, *J* = 6.1 Hz), 4.85 (1H, s), 5.13 (2H, m), 7.52 (4H, m), 7.66 (2H, m), 8.02 (2H, d, *J* = 7.8 Hz), 8.10 (2H, d, *J* = 7.6 Hz) - (Fig. S37-38)
^{13}C NMR (100 MHz, CD_3OD): δ (ppm) 17.9, 25.7, 26.9, 30.1 (13C), 30.3, 30.4, 34.6, 51.6, 67.9, 68.8, 68.9, 72.0 (2C), 97.5, 129.5 (4C), 130.4 (2C), 130.4 (2C), 134.2 (2C), *Cq* not observed - (Fig. S39)

4.4.3. Synthesis of 20-[(3,6-dideoxy-α-L-*arabino*-hexopyranosyl)oxy]eicosanoic acid (asc-ωC20)

A stirred solution of 5.8 mg of methyl 20-[(2,4-di-*O*-benzoyl-3,6-dideoxy-α-L-*arabino*-hexopyranosyl)oxy]eicosanoate (**9**) (8.5 µmol) in 60 µl methanol was treated with 23 µl of a saturated aqueous LiOH solution (298 µmol) and stirred for 12 h. The mixture was acidified with acetic acid and concentrated under reduced pressure. Column chromatography on silica gel using 5% methanol with 1% acetic acid in DCM afforded 1.3 mg 20-[(3,6-dideoxy-α-L-*arabino*-hexopyranosyl)oxy]eicosanoic acid (**asc-ωC20**) (2.8 µmol, 33% yield) as a waxy solid.

^{1}H NMR (400 MHz, CD_3OD): δ (ppm) 1.22 (3H, d, *J* = 5.8 Hz), 1.29 (30H, m), 1.60 (4H, m), 1.77 (1H, m), 1.95 (1H, ddd, *J* = 13.2 Hz, *J* = 3.6 Hz, *J* = 3.7 Hz), 2.26 (2H, t, *J* = 7.2 Hz), 3.41 (1H, m), 3.54 (2H, m), 3.68 (1H, dt, *J* = 9.3 Hz, *J* = 6.8 Hz), 3.76 (1H, br s), 4.49 (1H, s) - (Fig. S40)
^{13}C NMR (100 MHz, CD_3OD): δ (ppm) 18.1, 26.4, 27.4, 30.3, 30.4, 30.5, 30.6, 30.71 (5C), 30.74 (8C), 36.0, 68.4 (2C), 69.5, 70.9, 100.4, *Cq* not observed - (Fig. S41)

The product was analyzed by HPLC-ESI-(-)-HR-MS to show a homologous mixture of long chain ascarosides dominated by asc-ωC20 (Fig. S16).

	obs. *m/z* [M – H]	calc. *m/z* [M – H]	Molecular formula	Δ [ppm]
asc-ωC20	457.3534	457.3535	$C_{26}H_{49}O_6$	0.1
asc-ωC19	443.3375	443.3378	$C_{25}H_{47}O_6$	0.7
asc-ωC18	429.3218	429.3222	$C_{24}H_{45}O_6$	0.9
asc-ωC17	415.3066	415.3065	$C_{23}H_{43}O_6$	0.1

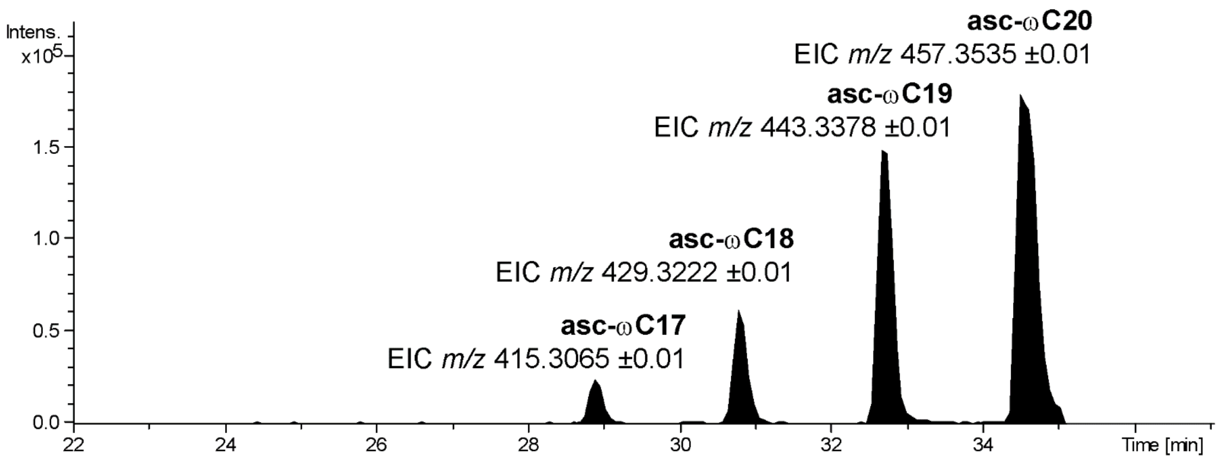

Figure S16: HPLC-ESI-(-)-HRMS extracted ion chromatograms for the homologous series of ascarosides produced by metathesis with asc-ωC20 as the dominating compound.

4.5. Synthesis of asc-C11-EA (easc#18)

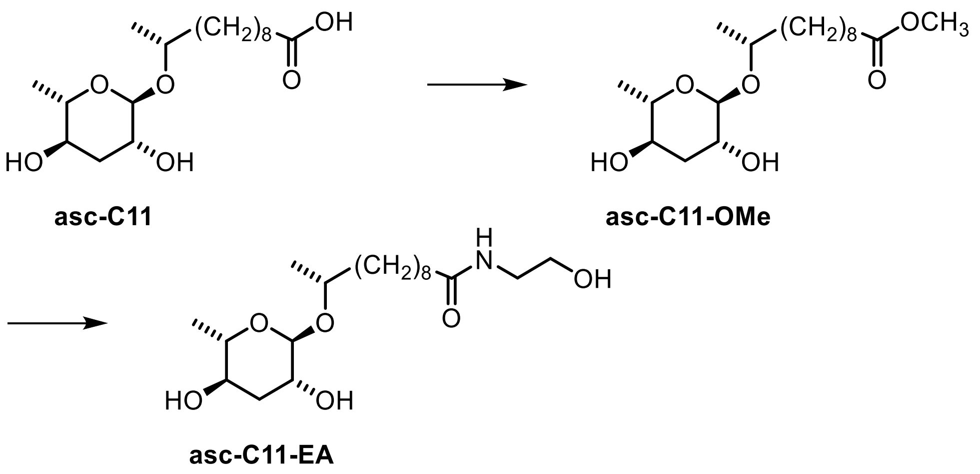

4.5.1. Synthesis of methyl (10*R*)-[(3,6-dideoxy-α-L-*arabino*-hexopyranosyl)oxy] undecanoate (asc-C11-OMe)

A solution of 1 mg (10*R*)-[(3,6-dideoxy-α-L-*arabino*-hexopyranosyl)oxy] undecanoic acid (**asc-C11**, 3 µmol)[10] in 300 µl methanol was treated with 15 µl of 1.0 M trimethylsilyl diazomethane (15 µmol) in diethyl ether. After stirring for 1 h excess reagent was destroyed by addition of 15 µl acetic acid and the solution concentrated in vacuum to give methyl (10*R*)-[(3,6-dideoxy-α-L-*arabino*-hexopyranosyl)oxy]undecanoate (**asc-C11-OMe**) that was directly used for the next step without any further purification.

^{1}H NMR (400 MHz, CD_3OD) δ 1.12 (3H, d, *J* = 6.1 Hz), 1.21 (3H, d, *J* = 6.2 Hz), 1.76 (1H, ddd, *J* = 13.2 Hz, J = 11.3 Hz, J = 3.2 Hz), 1.95 (1H, dt, J = 13.2 Hz, *J* = 3.7 Hz), 2.32 (2H, t, *J* = 7.4 Hz), 3.52 (1H, ddd, 11.2 Hz, 9.5 Hz4.5 Hz), 3.63 (1H, dq, *J* = 6.2 , *J* = 3.4 Hz), 3.65 (3H, s), 3.71 (1H, m), 3.777 (1H, m), 4.64 (1H, s.br) - (Fig. S42)

4.5.2. Synthesis of *N*-(2-hydroxyethyl) (10*R*)-[(3,6-dideoxy-α-L-*arabino*-hexopyranosyl) oxy]undecanamide (asc-C11-EA)

The crude residue of the methyl (10*R*)-[(3,6-dideoxy-α-L-*arabino*-hexopyranosyl)oxy] undecanoate (**asc-C11-OMe**) was dissolved in 100 µl ethanolamine (freshly distilled from KOH under argon). After 3 days the solution was concentrated under reduced pressure and the product was isolated by RP-SPE on a 500 mg C18 Chromabond column using a 10% incremental increase of methanol in water as eluent to afford 0.7 mg of *N*-(2-hydroxyethyl) (10*R*)-[(3,6-dideoxy-α-L-*arabino*-hexopyranosyl)oxy]undecanamide (**asc-C11-EA**) (1.87 µmol, 62% yield over two steps) as a colorless oil.

^{1}H NMR (400 MHz, CD_3OD) 1.12 (3H, d, *J* = 6.1 Hz), 1.21 (3H, d, *J* = 6.2 Hz), 1.33 (8H, m), 1.45 (1H, m), 1.54 (1H, m), 1.61 (2H, m), 1.76 (1H, ddd, *J* = 13.0 Hz, *J* = 11.4 Hz, *J* = 3.2 Hz), 1.95 (1H, dt, *J* = 13.0 Hz, *J* = 3.8 Hz), 2.20 (2H, t, *J* = 7.8 Hz), 3.28 (2H, t, *J* = 5.9 Hz), 3.52 (1H, ddd, *J* = 11.2 Hz, *J* = 9.7 Hz, *J* = 4.6 Hz), 3.58 (2H, t, *J* = 5.8 Hz), 3.63 (1H, dq, *J* = 9.2 Hz, *J* = 6.1 Hz), 3.71 (1H, s.br), 3.78 (1H, m), 4.64 (1H, s.br) - (Fig. S43-44)
^{13}C NMR (100 MHz, CD_3OD) 18.1 (6'-C), 19.4 (11-C), 26.9, 27.0 (3-C, 8-C), 30.3, 30.4, 30.6, 30.7 (4,5,6,7-C), 36.0 (3'-C), 37.1 (2-C), 38.4 (9-C), 42.9 ($NHCH_2$-), 61.7 (-CH_2OH), 68.3 (4'-C), 70.0 (2'-C), 71.2 (5'-C), 72.6 (10-C), 97.6 (1'-C), 176.7 (1-C) - (Fig. S45-46)

ESI-(-)-MS/MS	obs. *m/z* [M – H]	calc. *m/z* [M – H]	Molecular formula	Δ [ppm]
$[M-H]^-$	374.2559	374.2548	$C_{19}H_{36}NO_6$	-3.0
$[M+AcO]^-$	434.2759	434.2759	$C_{21}H_{40}NO_8$	-4.0
MS/MS $[M-H]^-$	244.1923	244.1918	$C_{13}H_{26}NO_3$	-2.2

Fig S17: ^{1}H NMR (400 MHz, CD_3OD) of methyl (2*R*)-[(2,4-di-*O*-benzoyl-3,6-dideoxy-α-L-*arabino*-hexopyranosyl)oxy]propanoate (**2**)

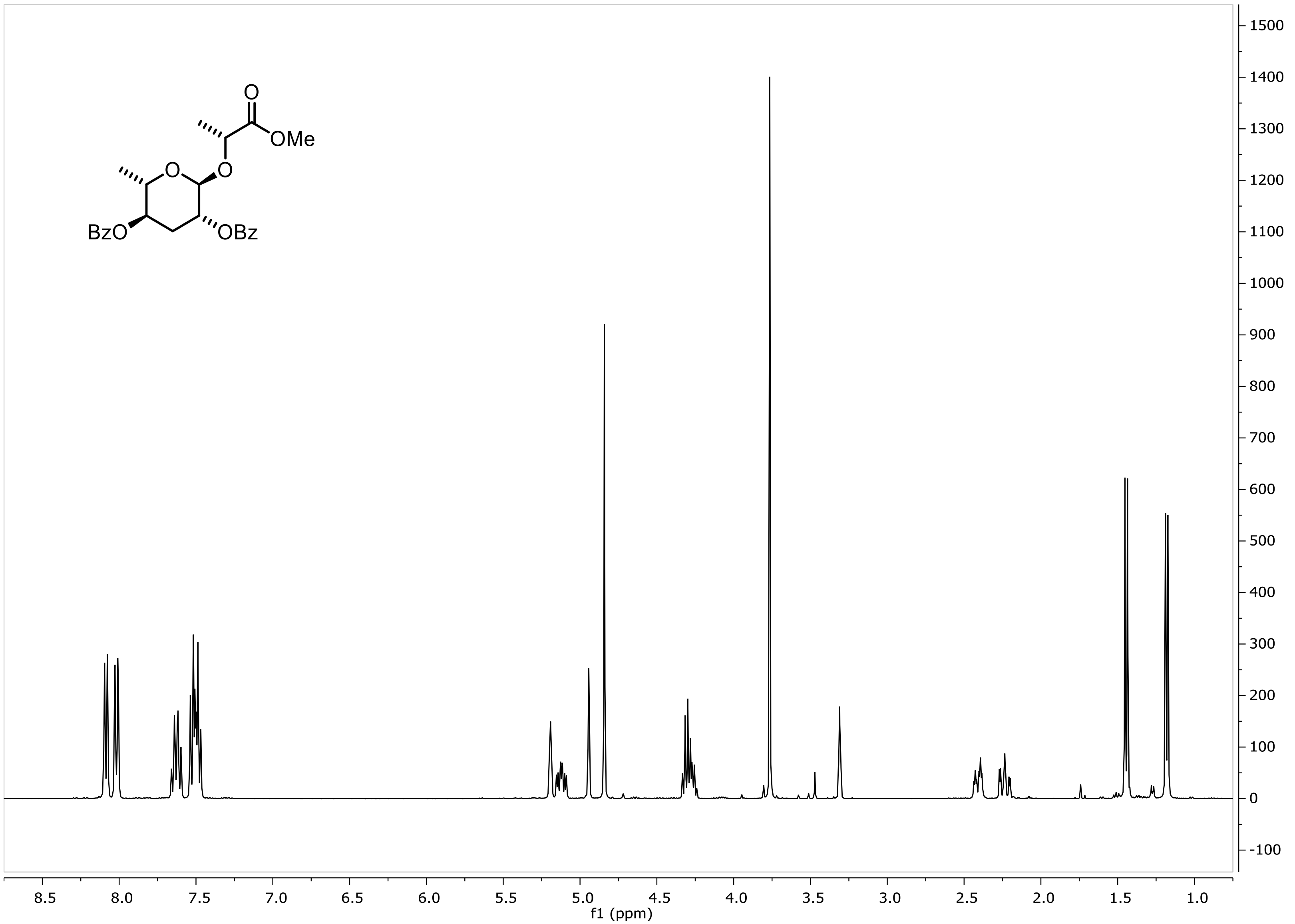

Fig S18: ^{13}C NMR (100 MHz, CD_3OD) of methyl (2*R*)-[(2,4-di-*O*-benzoyl-3,6-dideoxy-α-L-*arabino*-hexopyranosyl)oxy]propanoate (**2**)

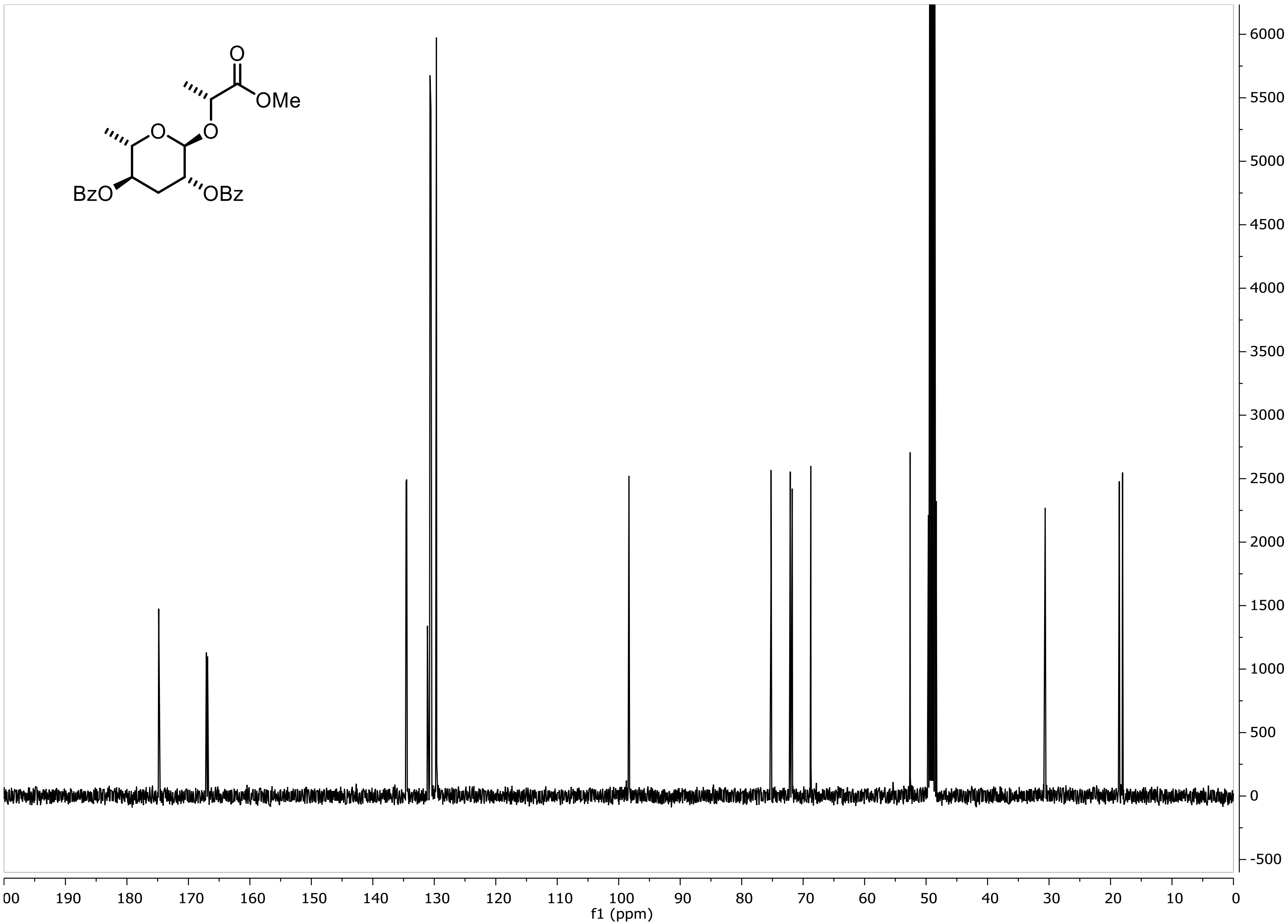

Fig S19: ^{1}H NMR (400 MHz, CD_3OD) of (2*R*)-[(3,6-dideoxy-α-L-*arabino*-hexopyranosyl)oxy]propanoic acid (**asc-C3**)

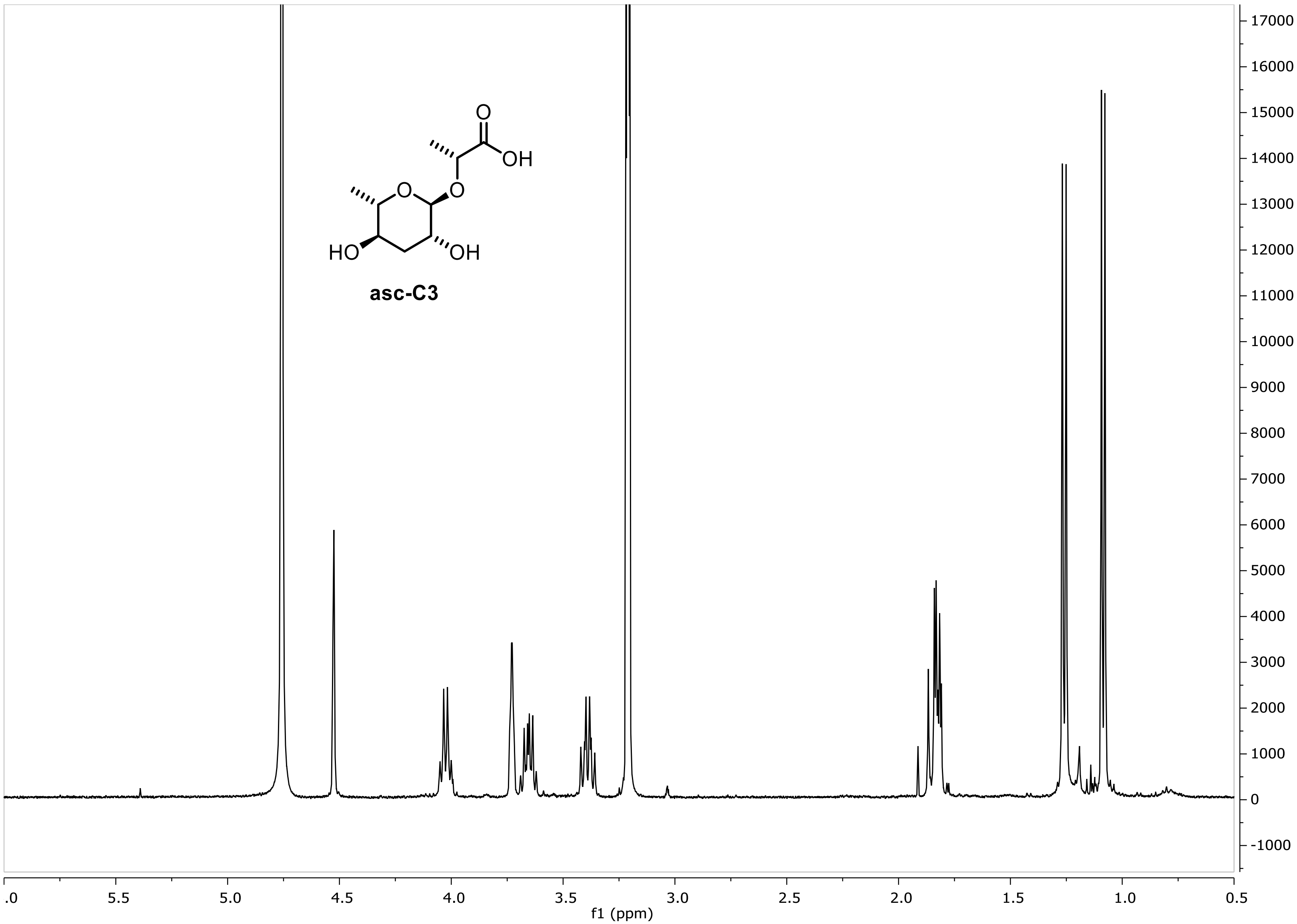

Fig S20: ^{13}C NMR (100 MHz, CD_3OD) of (2*R*)-[(3,6-dideoxy-α-L-*arabino*-hexopyranosyl)oxy]propanoic acid (**asc-C3**)

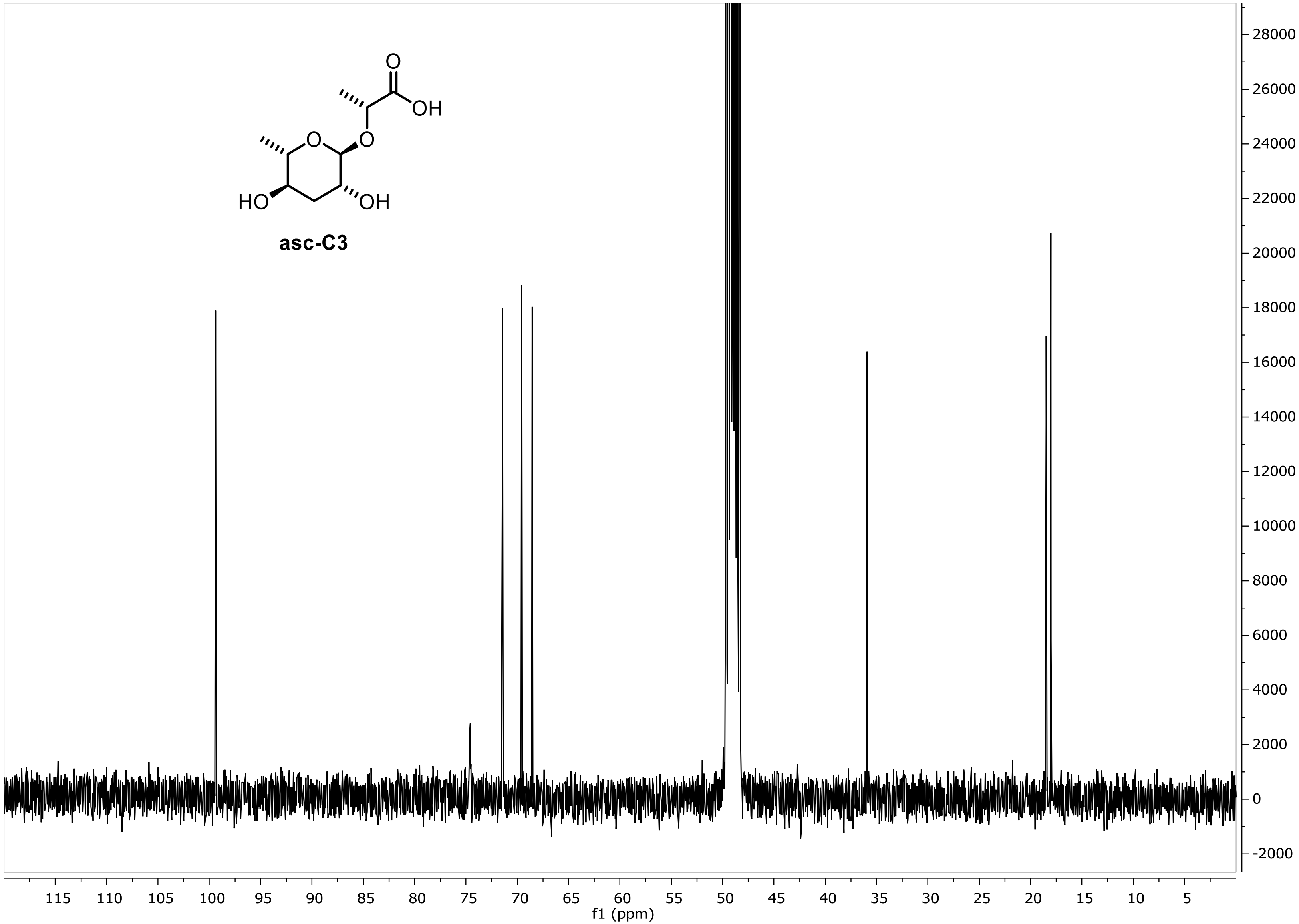

Fig S21: ^{1}H NMR (100 MHz, CD_3OD) of ethyl (3*R*)-[(2,4-di-*O*-benzoyl-3,6-dideoxy-α-L-*arabino*-hexopyranosyl)oxy]butanoate (**3**)

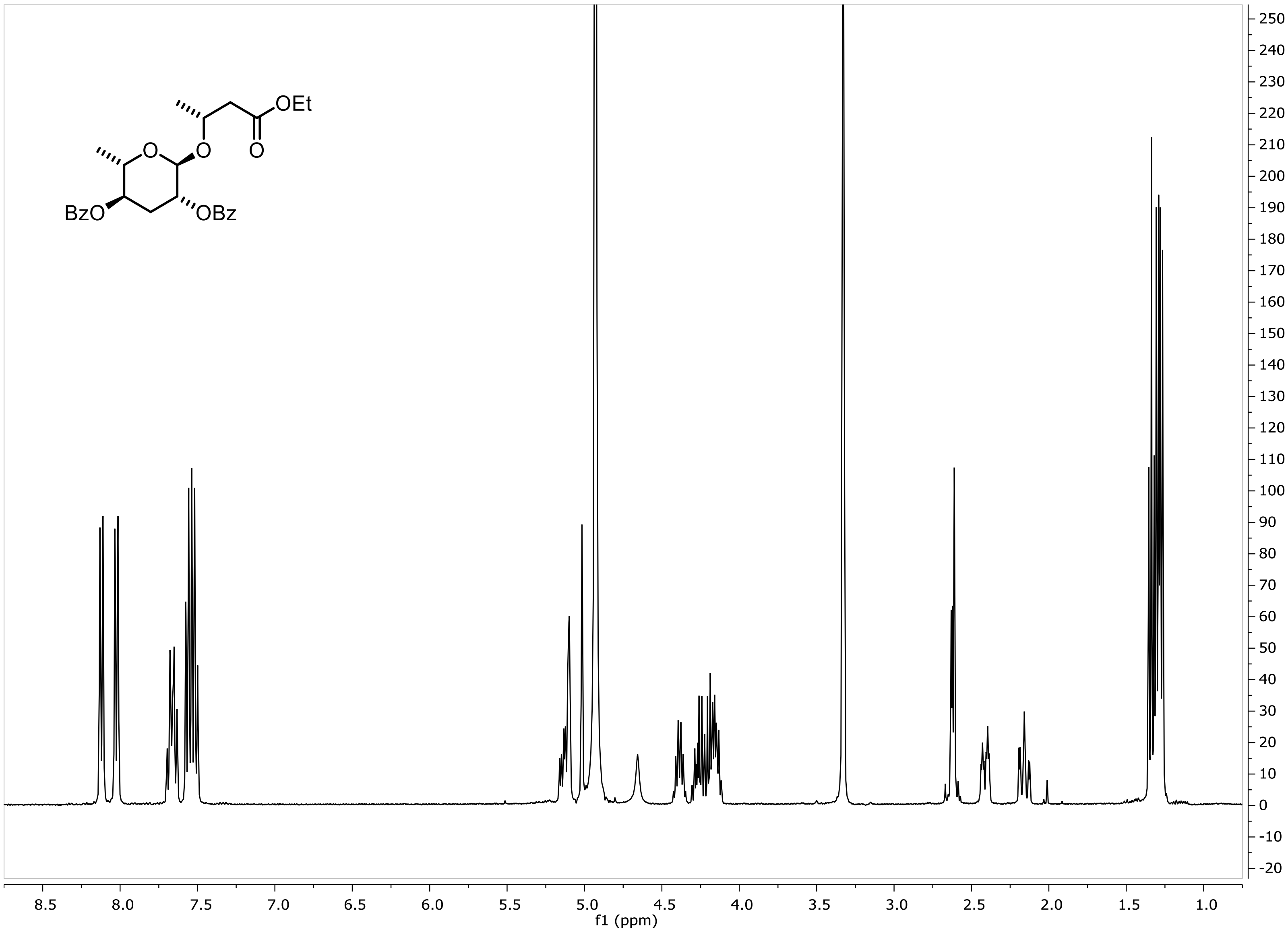

Fig S22: ^{13}C NMR (100 MHz, $CDCl_3$) of ethyl (3*R*)-[(2,4-di-*O*-benzoyl-3,6-dideoxy-α-L-*arabino*-hexopyranosyl)oxy]butanoate (**3**)

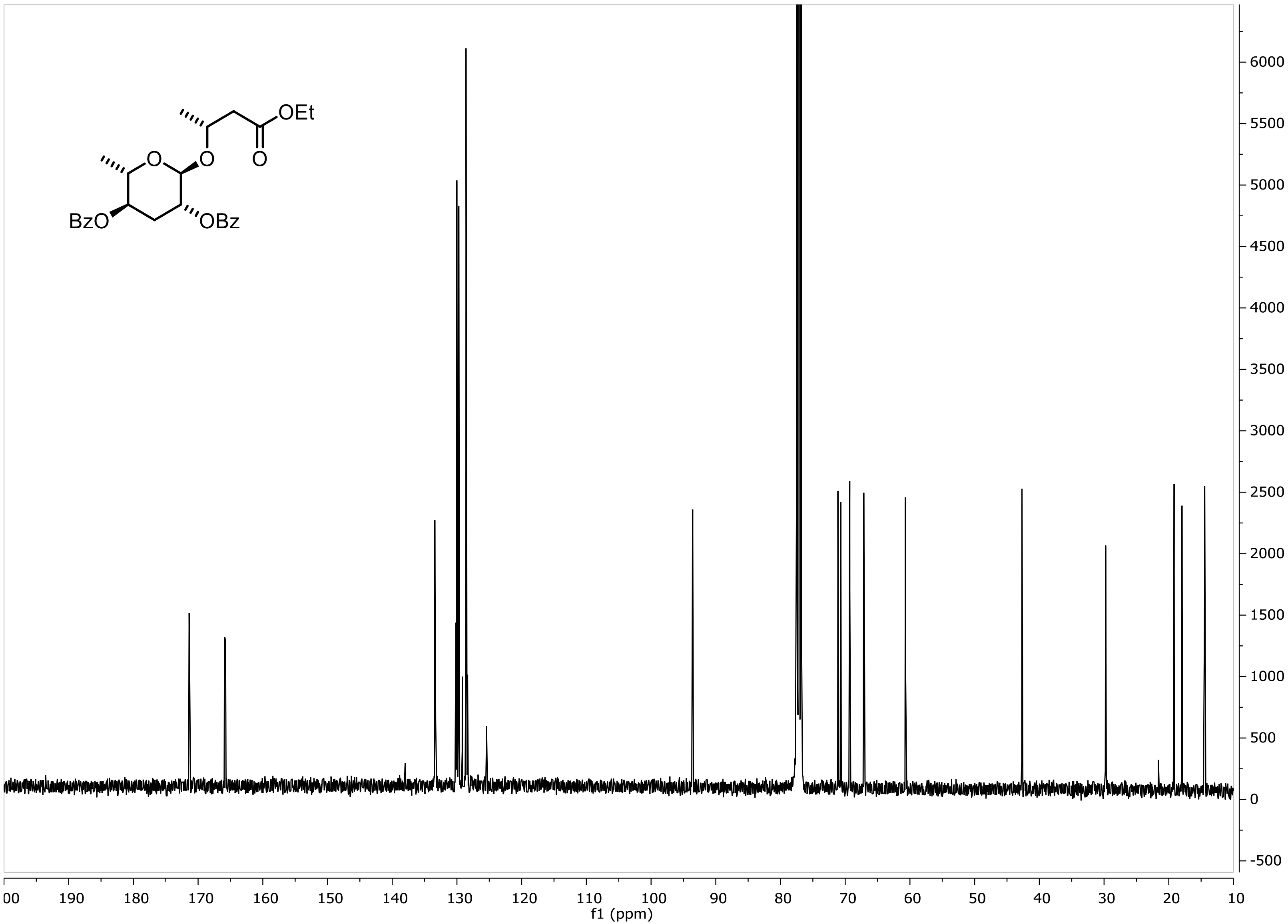

Fig S23: ^{1}H NMR (400 MHz, CD_3OD) of (3*R*)-[(3,6-dideoxy-α-L-*arabino*-hexopyranosyl)oxy]butanoic acid (**asc-C4**)

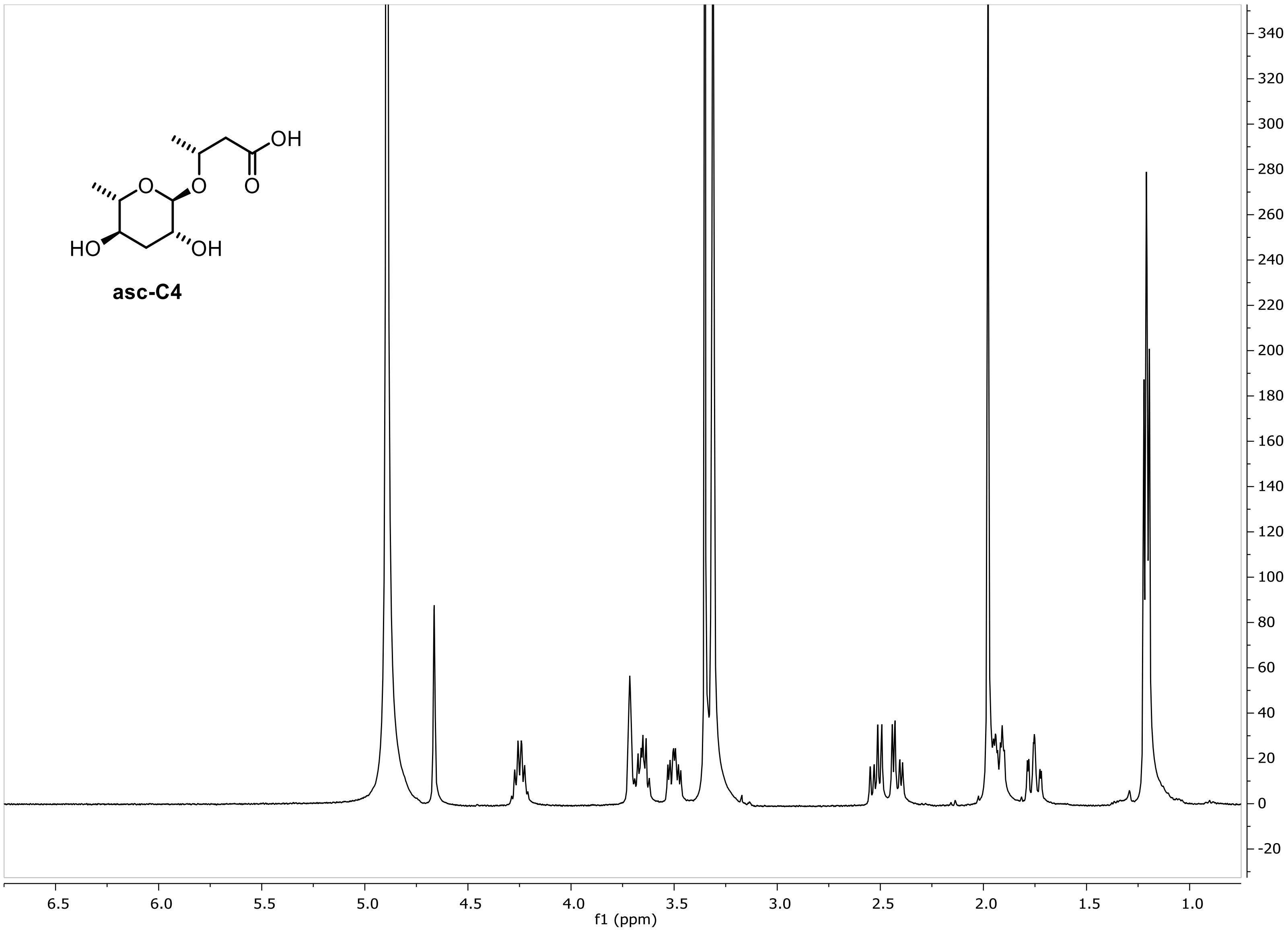

Fig S24: ^{13}C NMR (100 MHz, CD_3OD) of (3*R*)-[(3,6-dideoxy-α-L-*arabino*-hexopyranosyl)oxy]butanoic acid (**asc-C4**)

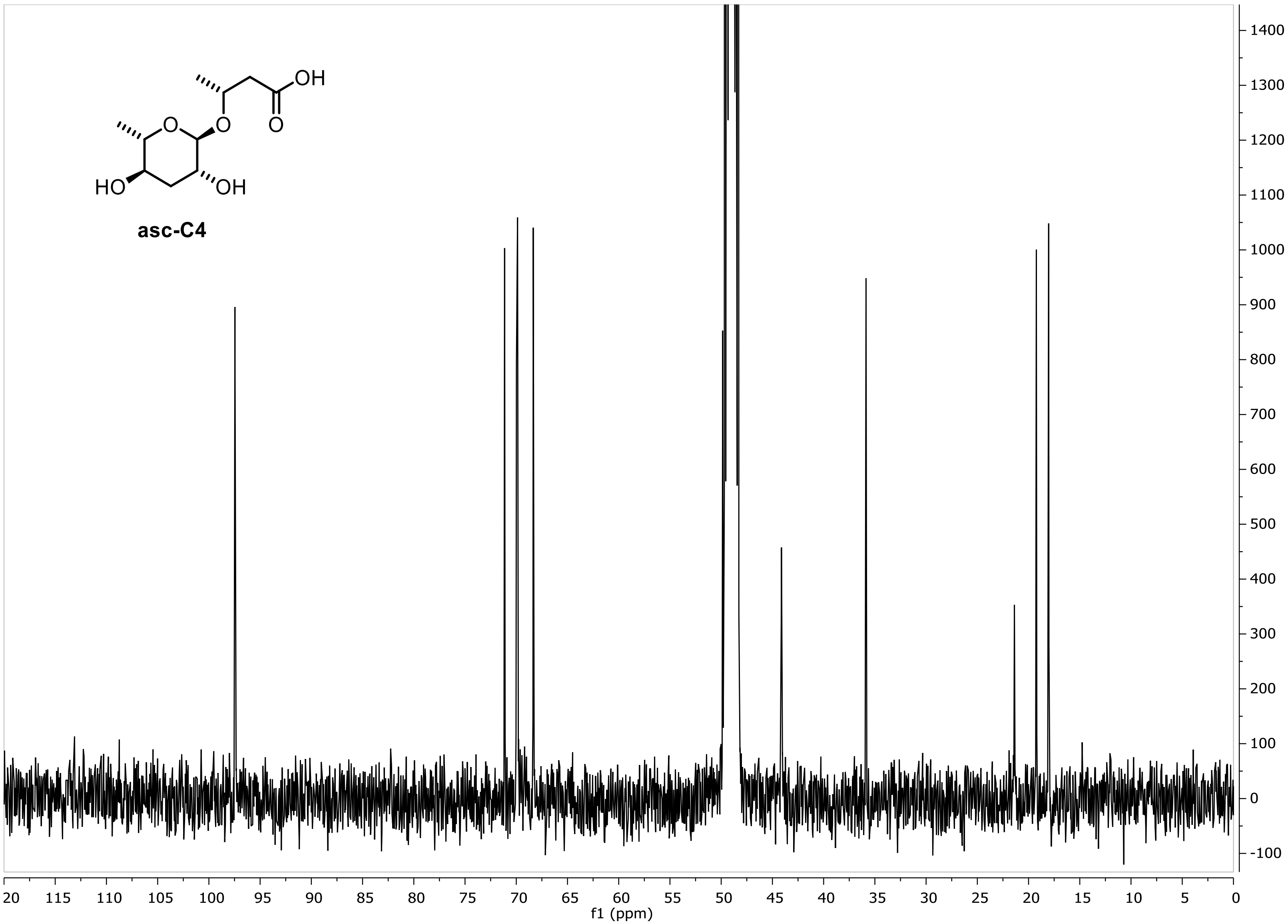

Fig S25: ^{1}H NMR (400 MHz, CD_3OD) of methyl (17*R*)-[(2,4-di-*O*-benzoyl-3,6-dideoxy-α-L-*arabino*-hexopyranosyl)oxy]-(10*E*)-octadecenoate (**5**)

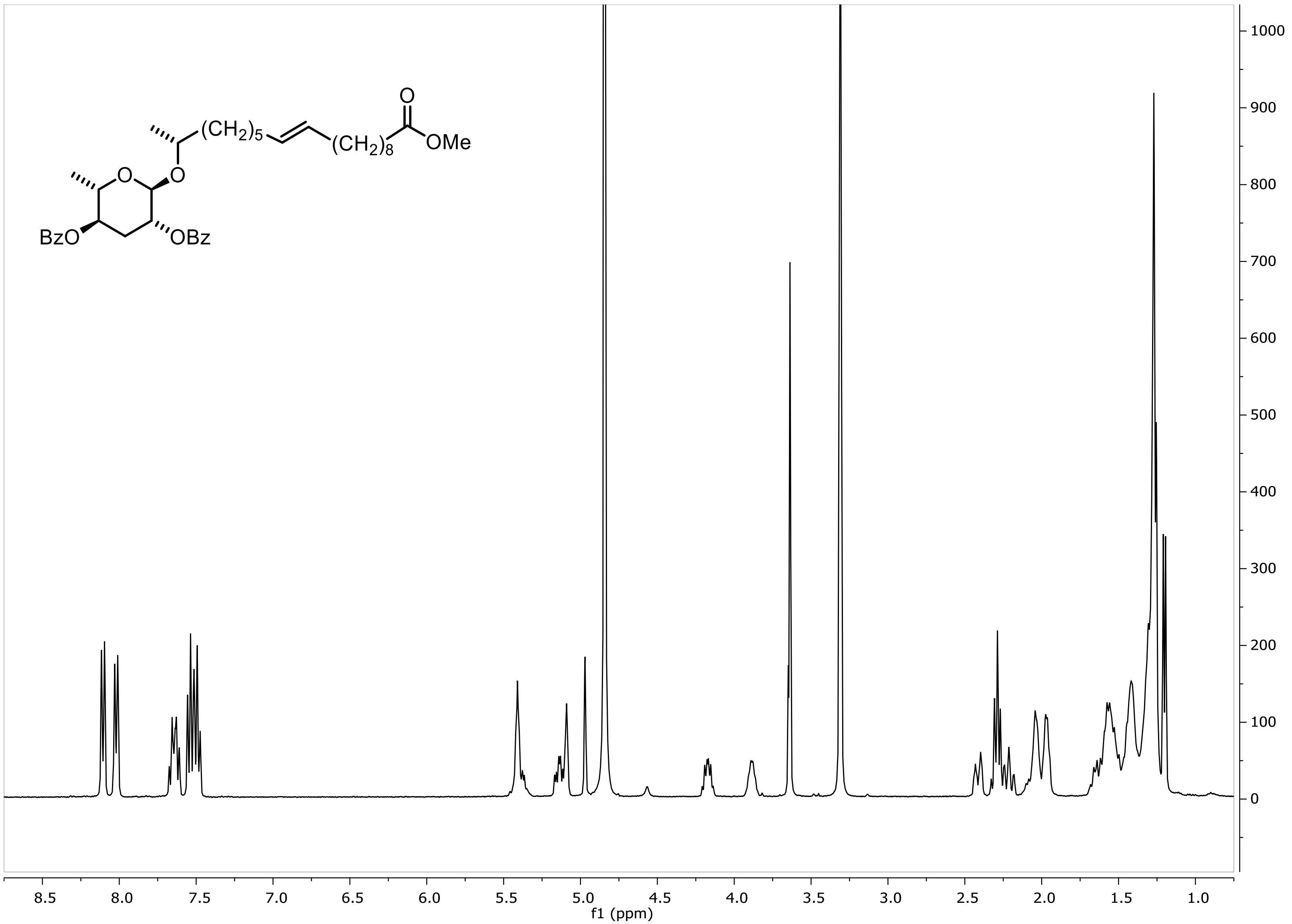

Fig S26: *dqf*-COSY (400 MHz, CD_3OD) of methyl (17*R*)-[(2,4-di-*O*-benzoyl-3,6-dideoxy-α-L-*arabino*-hexopyranosyl)oxy]-(10*E*)-octadecenoate

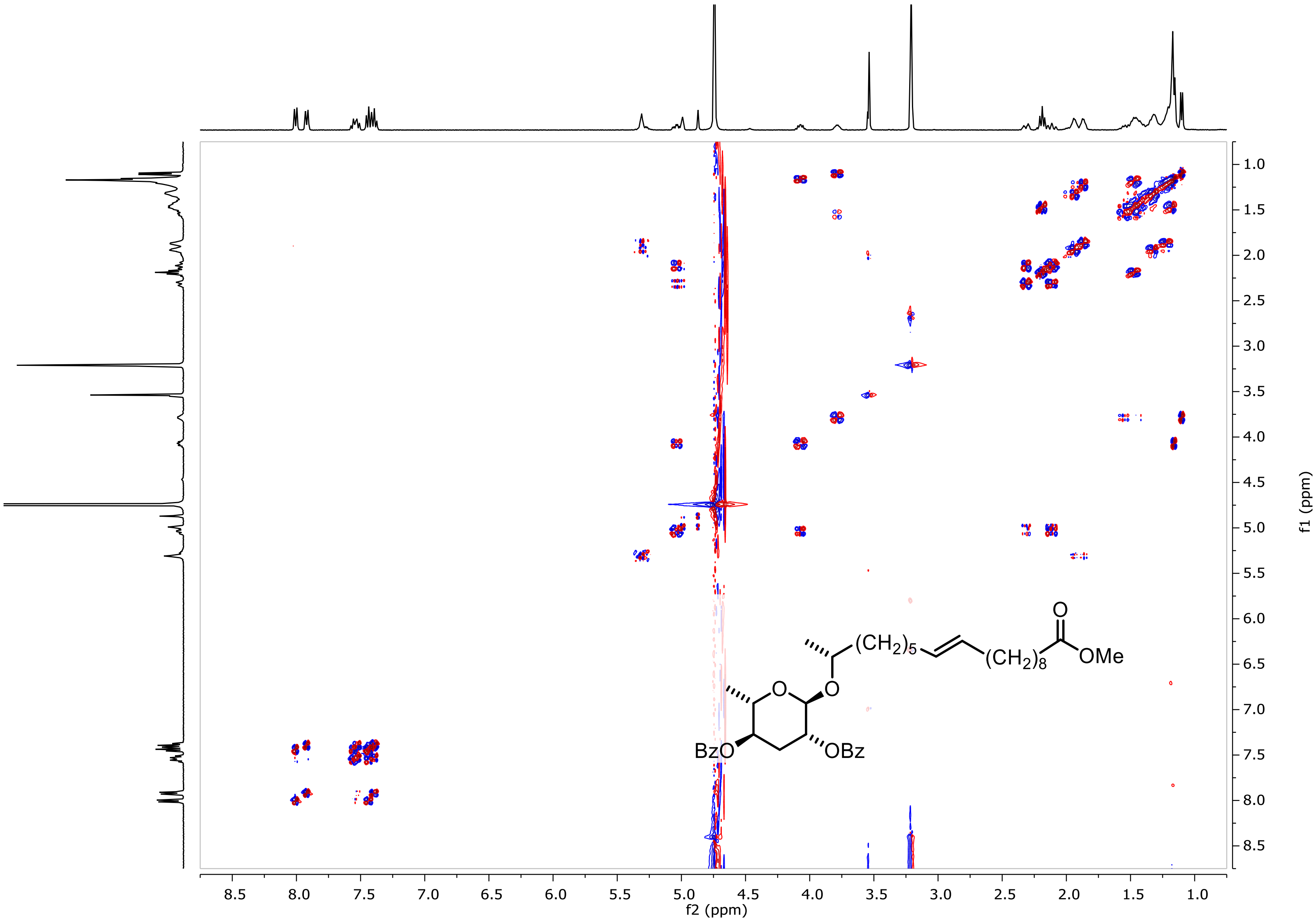

Fig S27: [13]C NMR (100 MHz, CD_3OD) of methyl (17*R*)-[(2,4-di-*O*-benzoyl-3,6-dideoxy-α-L-*arabino*-hexopyranosyl)oxy]-(10*E*)-octadecenoate (**5**)

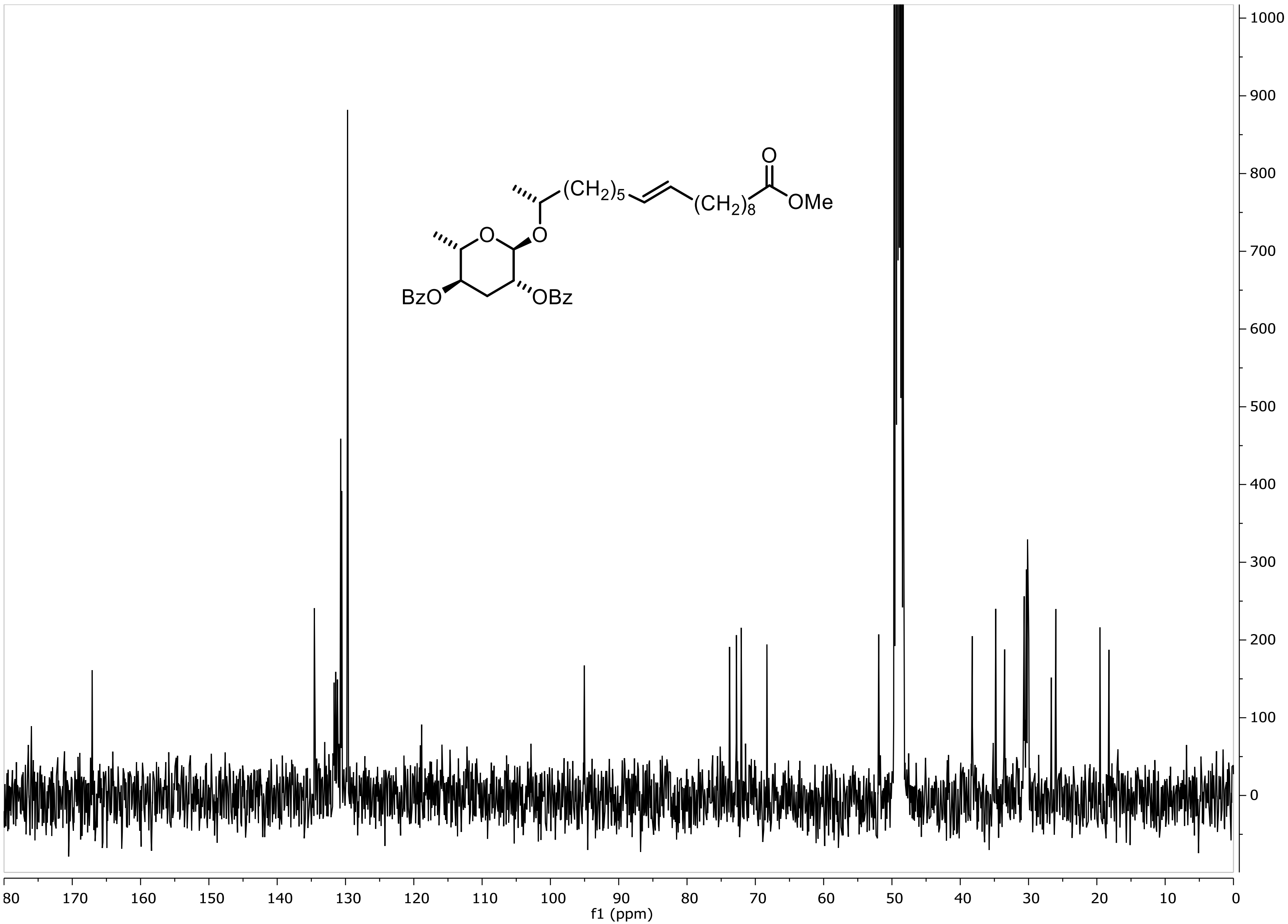

Fig S28: HSQC (CD_3OD) of methyl (17*R*)-[(2,4-di-*O*-benzoyl-3,6-dideoxy-α-L-*arabino*-hexopyranosyl)oxy]-(10*E*)-octadecenoate (**5**)

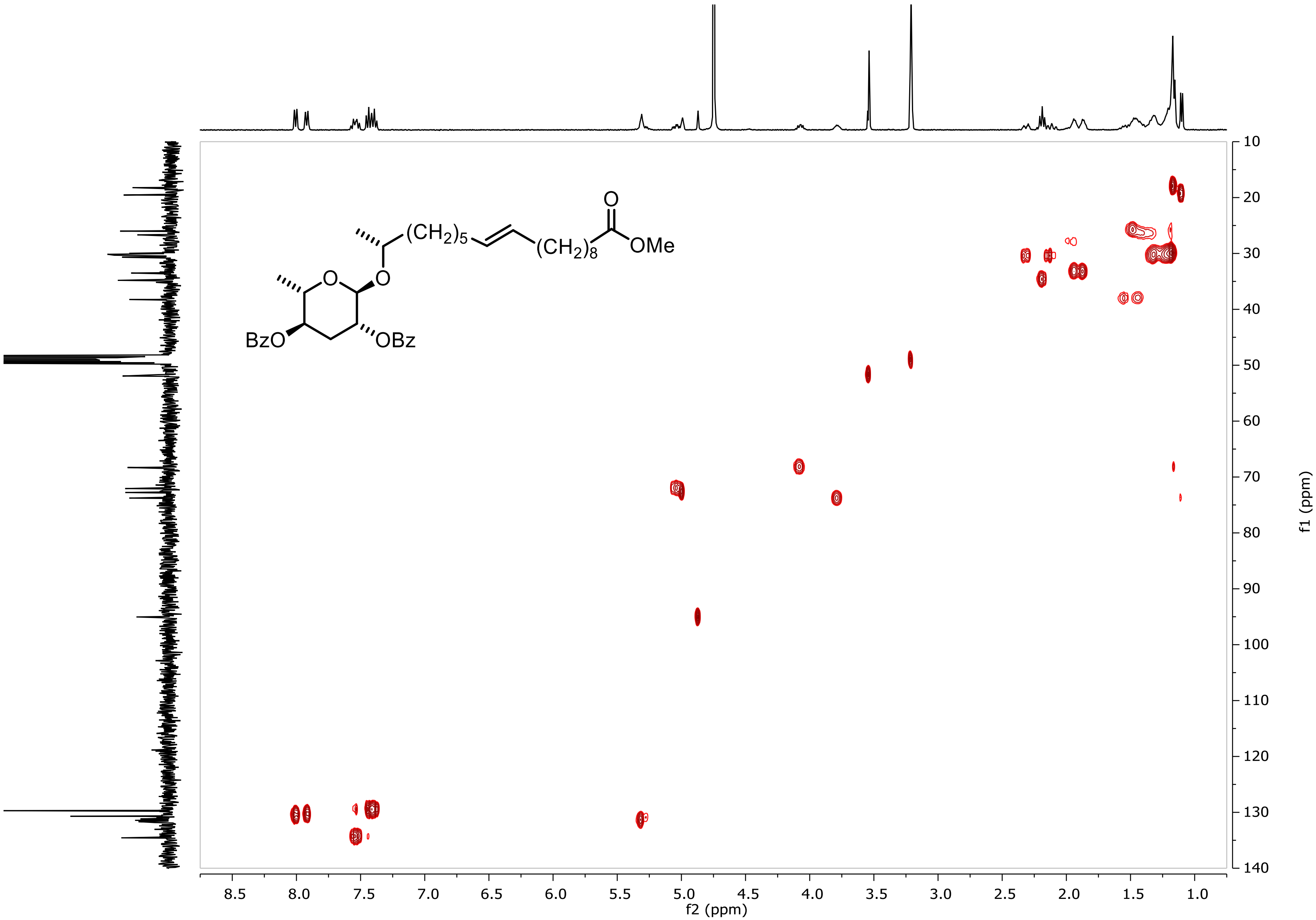

Fig S29: ^{1}H NMR (400 MHz, CD_3OD) of methyl (17*R*)-[(2,4-di-*O*-benzoyl-3,6-dideoxy-α-L-*arabino*-hexopyranosyl)oxy]octadecanoate (**6**)

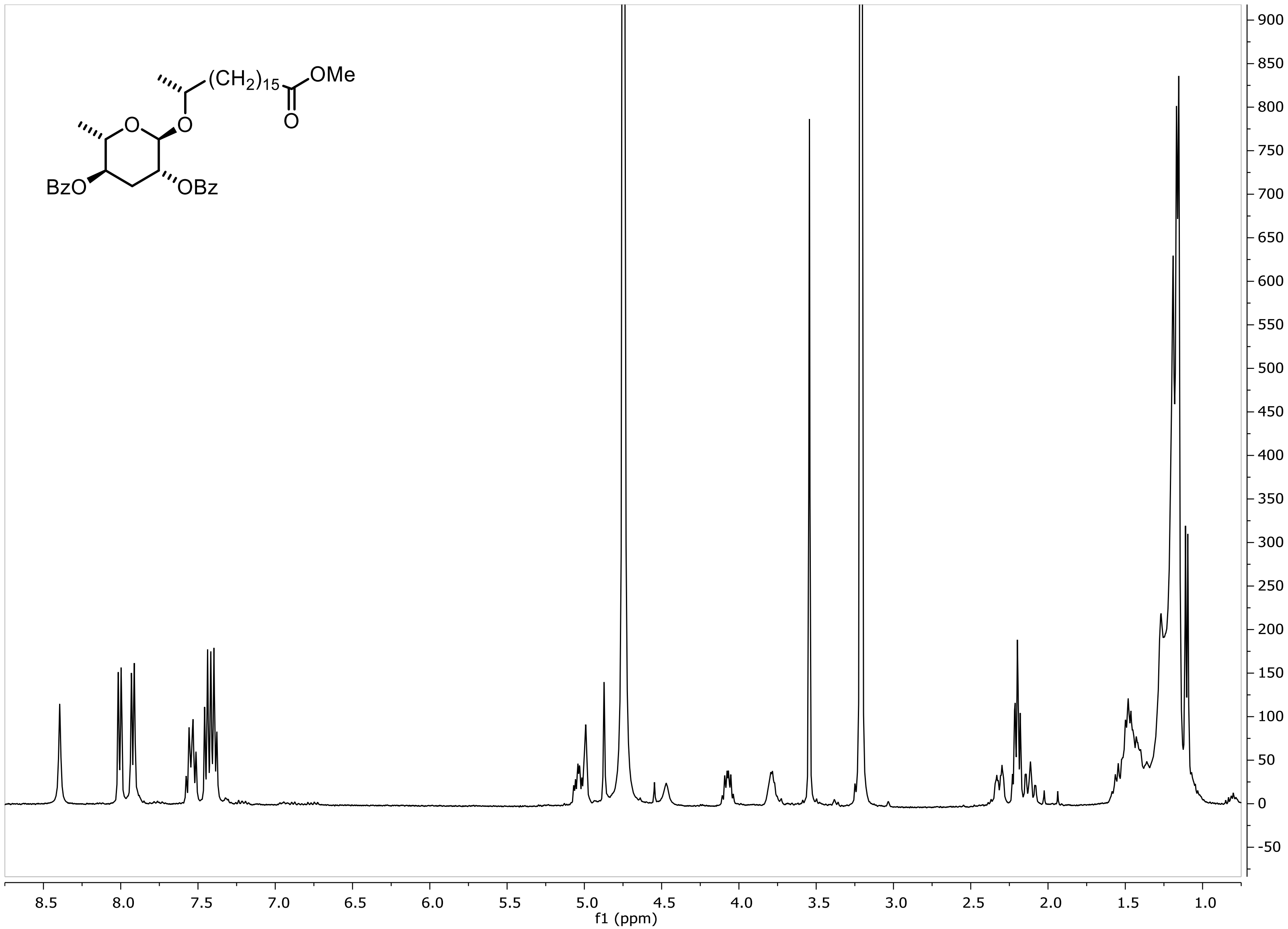

Fig S30: *dqf*-COSY (400 MHz, CD_3OD) of methyl (17*R*)-[(2,4-di-*O*-benzoyl-3,6-dideoxy-α-L-*arabino*-hexopyranosyl)oxy]octadecanoate (**6**)

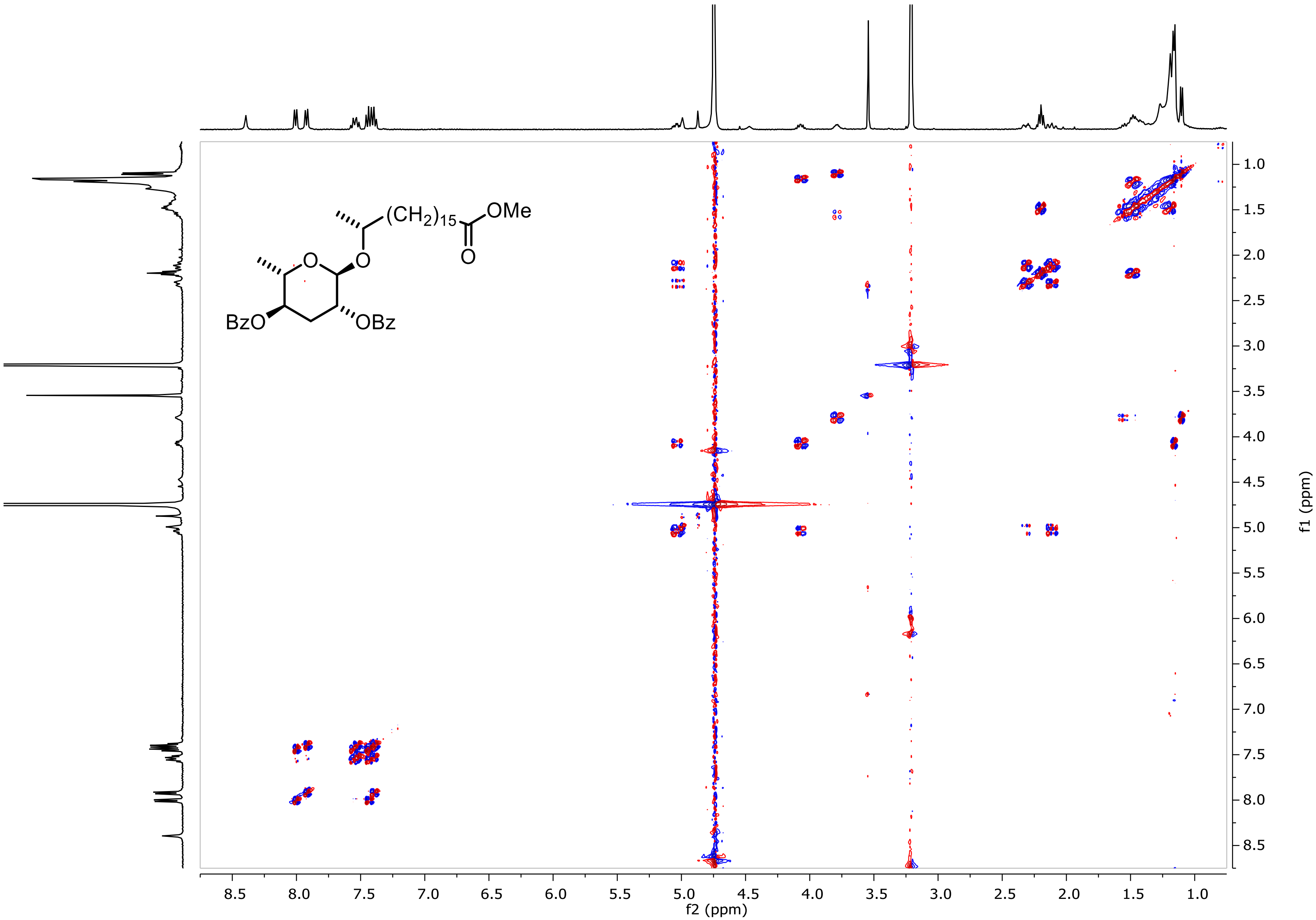

Fig S31: HSQC(CD_3OD) of methyl (17*R*)-[(2,4-di-*O*-benzoyl-3,6-dideoxy-α-L-*arabino*-hexopyranosyl)oxy]octadecanoate (**6**)

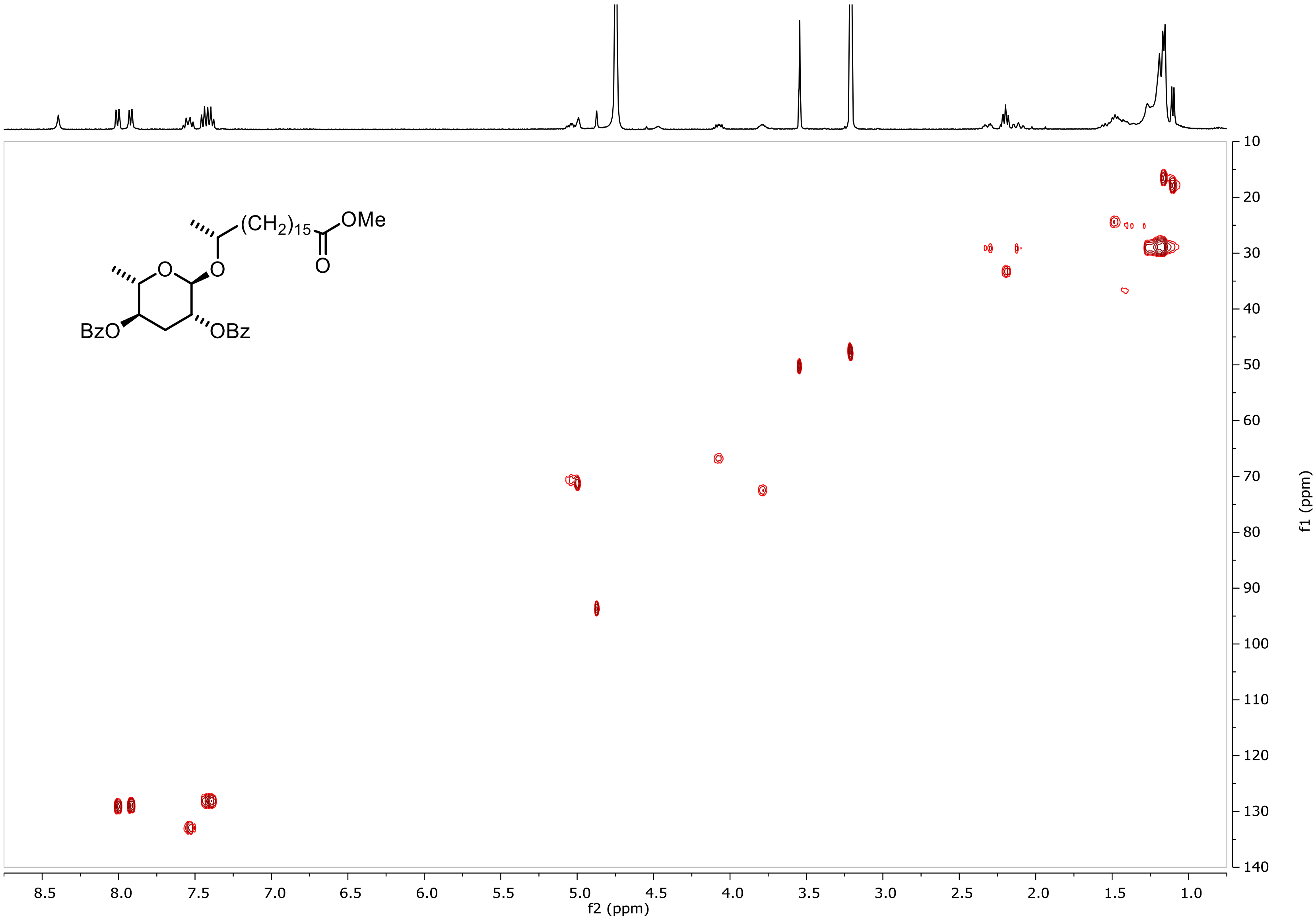

Fig S32: ^{1}H NMR (400 MHz, CD_3OD) of (17*R*)-[(3,6-dideoxy-α-L-*arabino*-hexopyranosyl)oxy]octadecanoic acid (**asc-C18**)

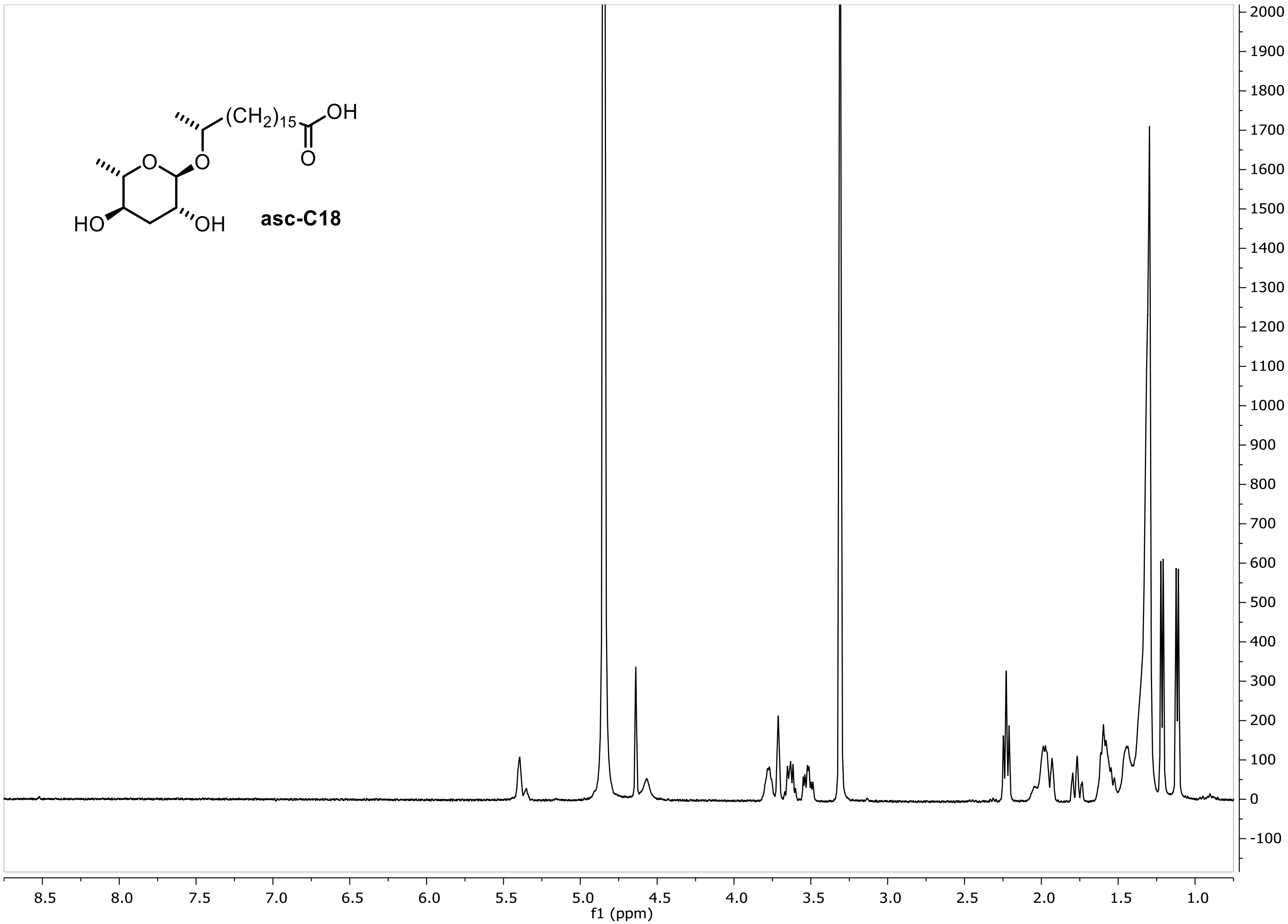

Fig S33: ^{13}C NMR (100 MHz, CD_3OD) of (17*R*)-[(3,6-dideoxy-α-L-*arabino*-hexopyranosyl)oxy]octadecanoic acid (**asc-C18**)

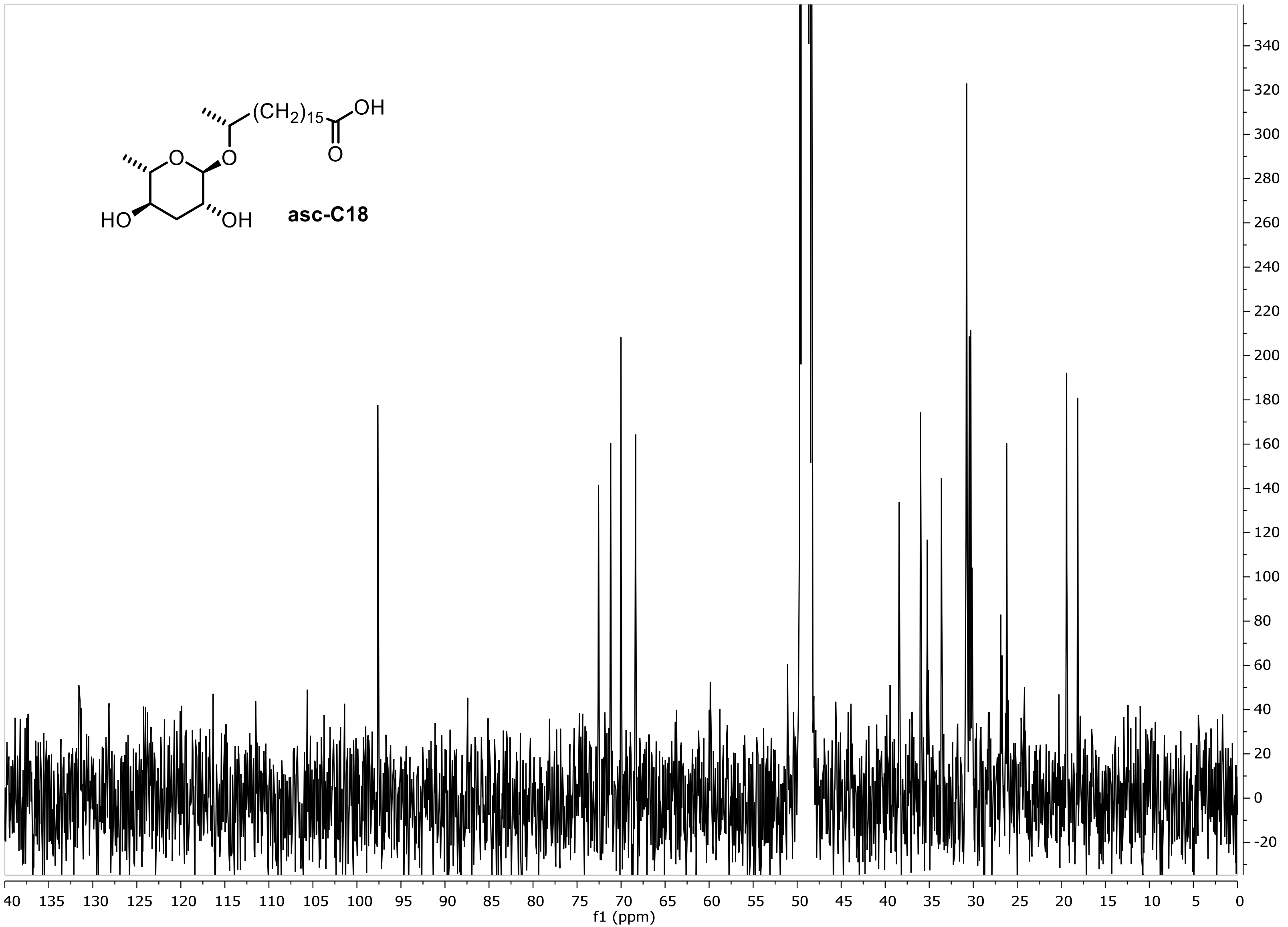

Fig S34: ^{1}H NMR (400 MHz, CD_3OD) of methyl 20-[(2,4-di-*O*-benzoyl-3,6-dideoxy-α-L-*arabino*-hexopyranosyl)oxy]-(10*E*)-eicosenoate (**8**)

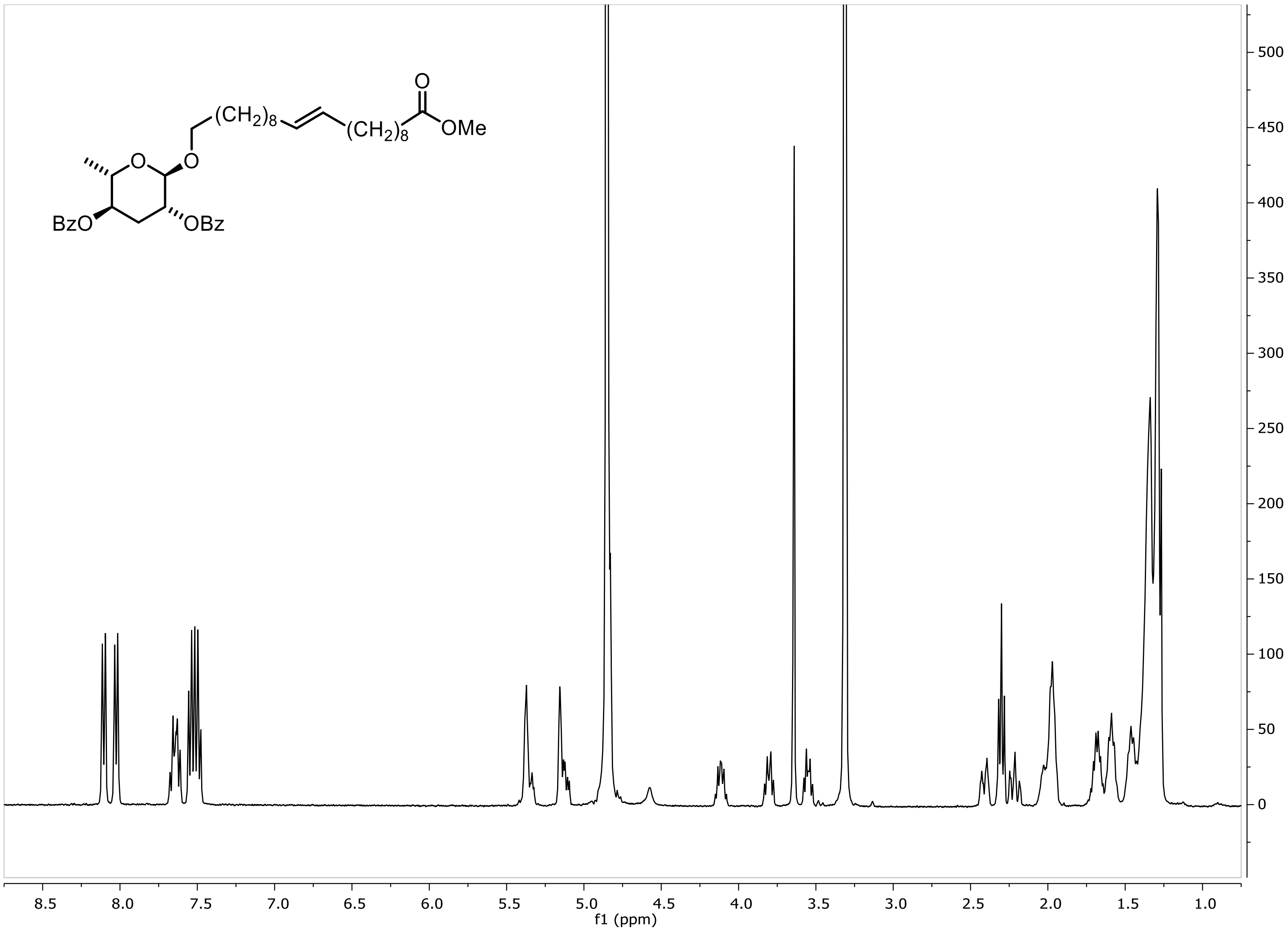

Fig S35: *dqf*-COSY (400 MHz, CD_3OD) of methyl 20-[(2,4-di-*O*-benzoyl-3,6-dideoxy-α-L-*arabino*-hexopyranosyl)oxy]-(10*E*)-eicosenoate (**8**)

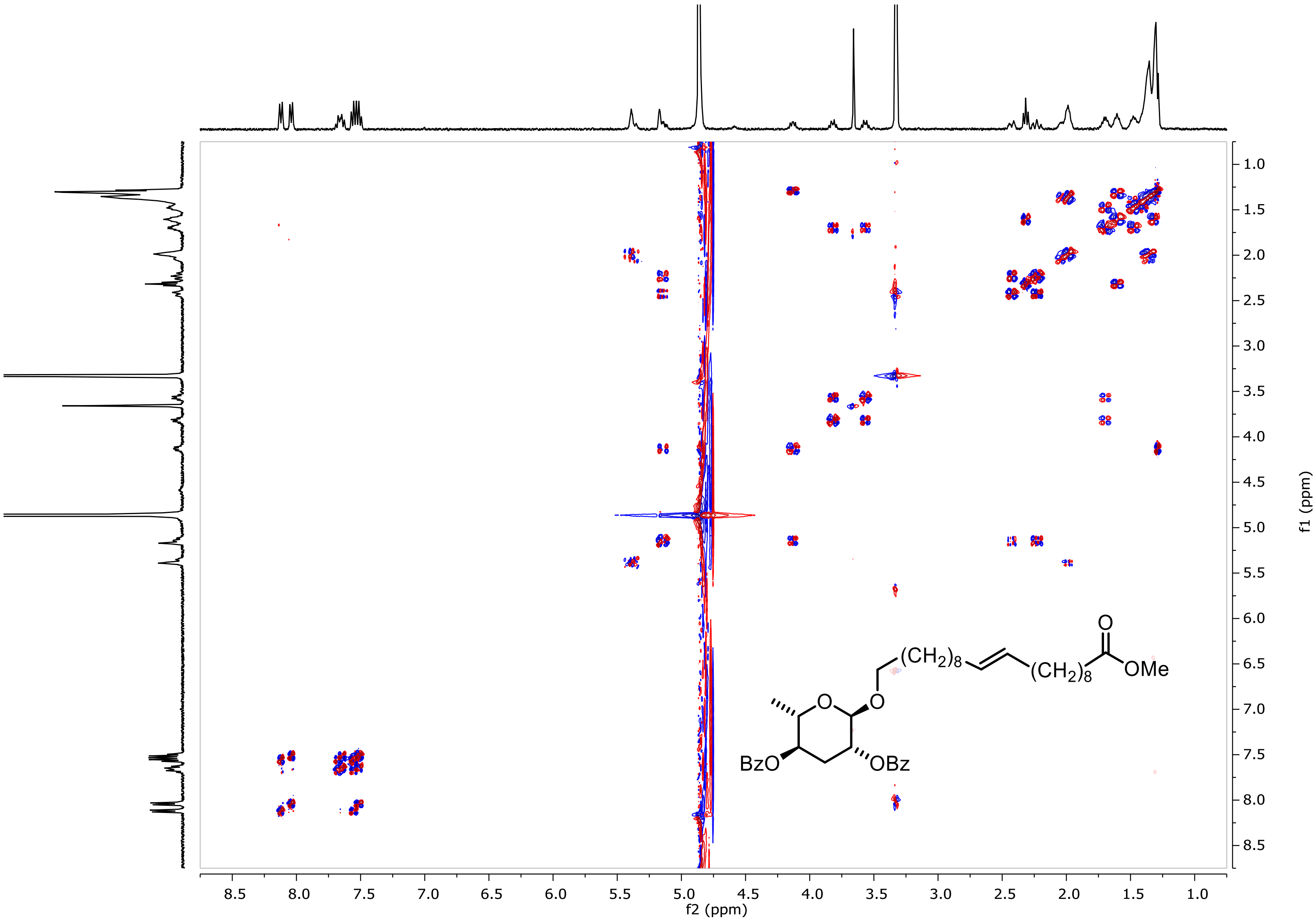

Fig S36: HSQC (CD_3OD) of methyl 20-[(2,4-di-*O*-benzoyl-3,6-dideoxy-α-L-*arabino*-hexopyranosyl)oxy]-(10*E*)-eicosenoate (**8**)

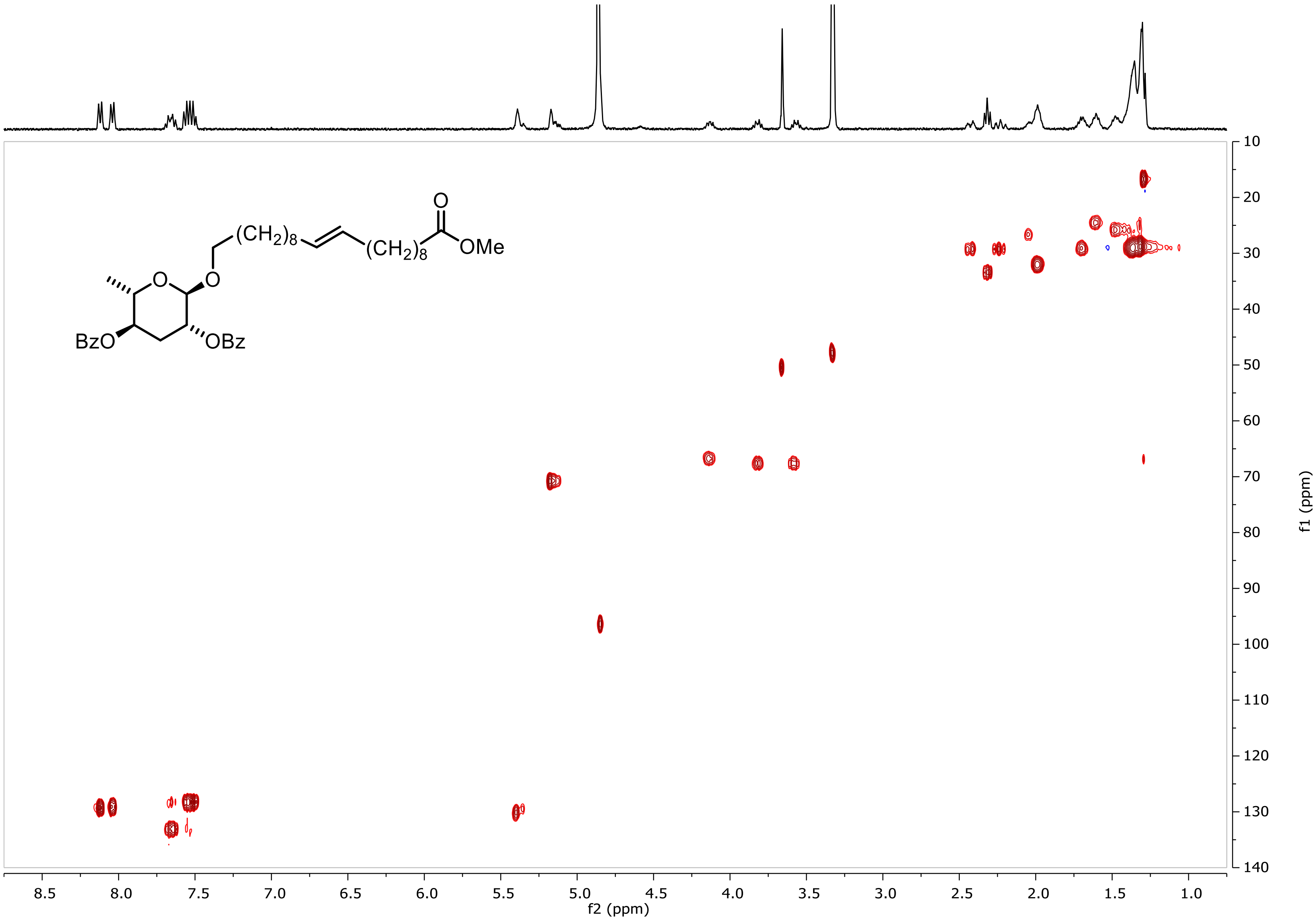

Fig S37: ^{1}H NMR (400 MHz, CD_3OD) of methyl 20-[(2,4-di-*O*-benzoyl-3,6-dideoxy-α-L-*arabino*-hexopyranosyl)oxy]eicosanoate (**9**)

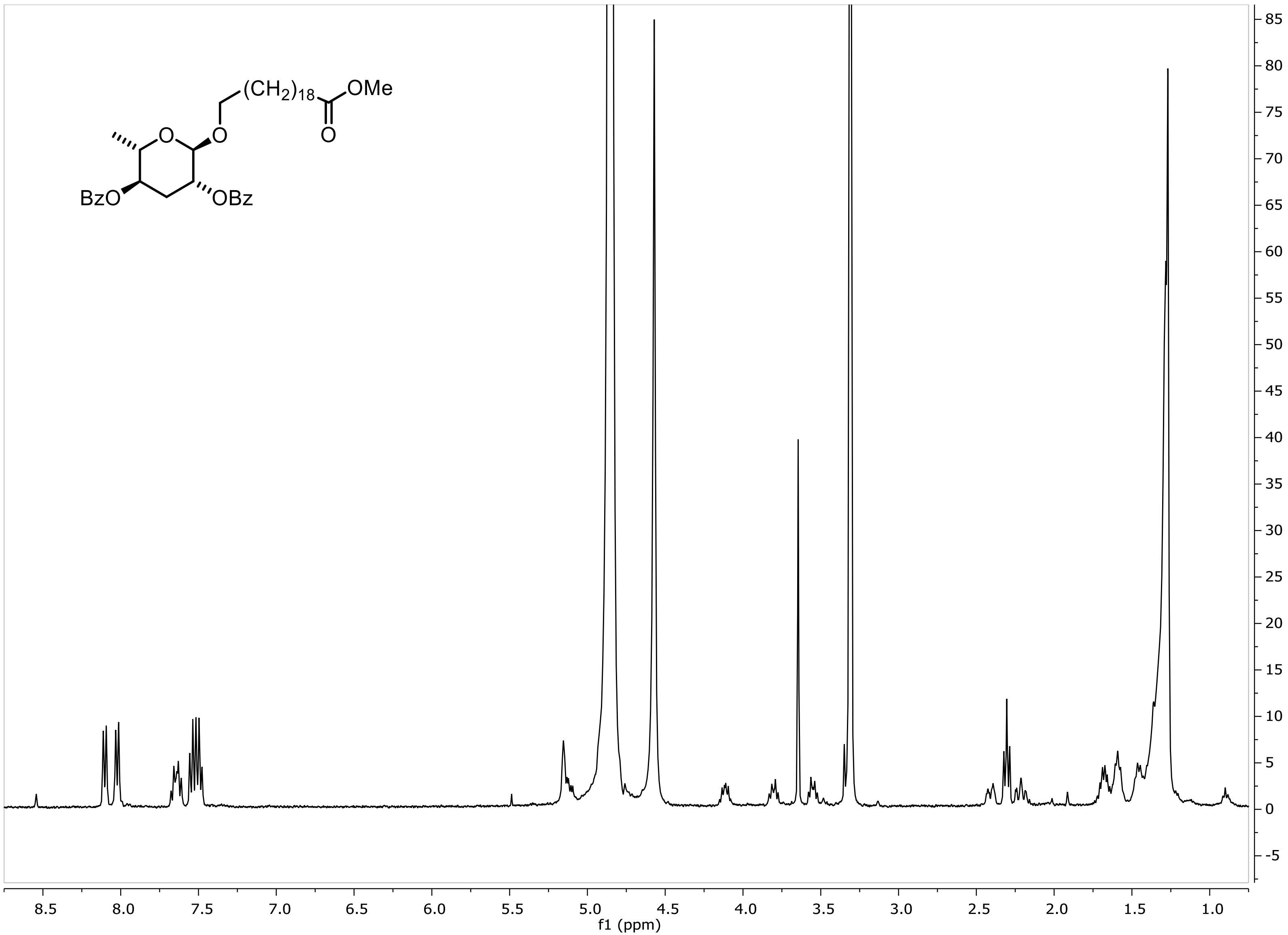

Fig S38: *dqf*-COSY (400 MHz, CD_3OD) of methyl 20-[(2,4-di-*O*-benzoyl-3,6-dideoxy-α-L-*arabino*-hexopyranosyl)oxy]eicosanoate (**9**)

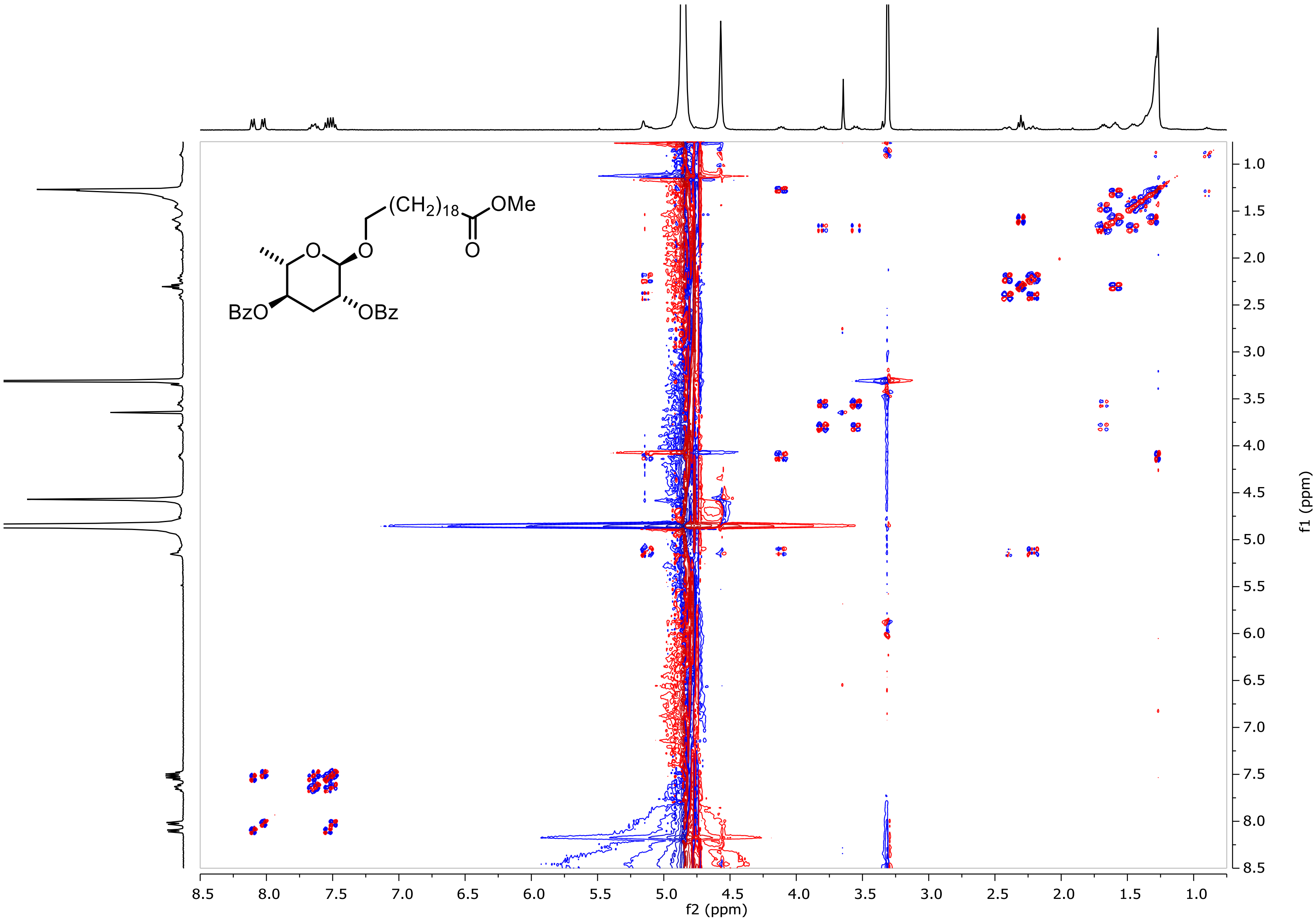

Fig S39: HSQC (CD_3OD) of methyl 20-[(2,4-di-*O*-benzoyl-3,6-dideoxy-α-L-*arabino*-hexopyranosyl)oxy]eicosanoate (**9**)

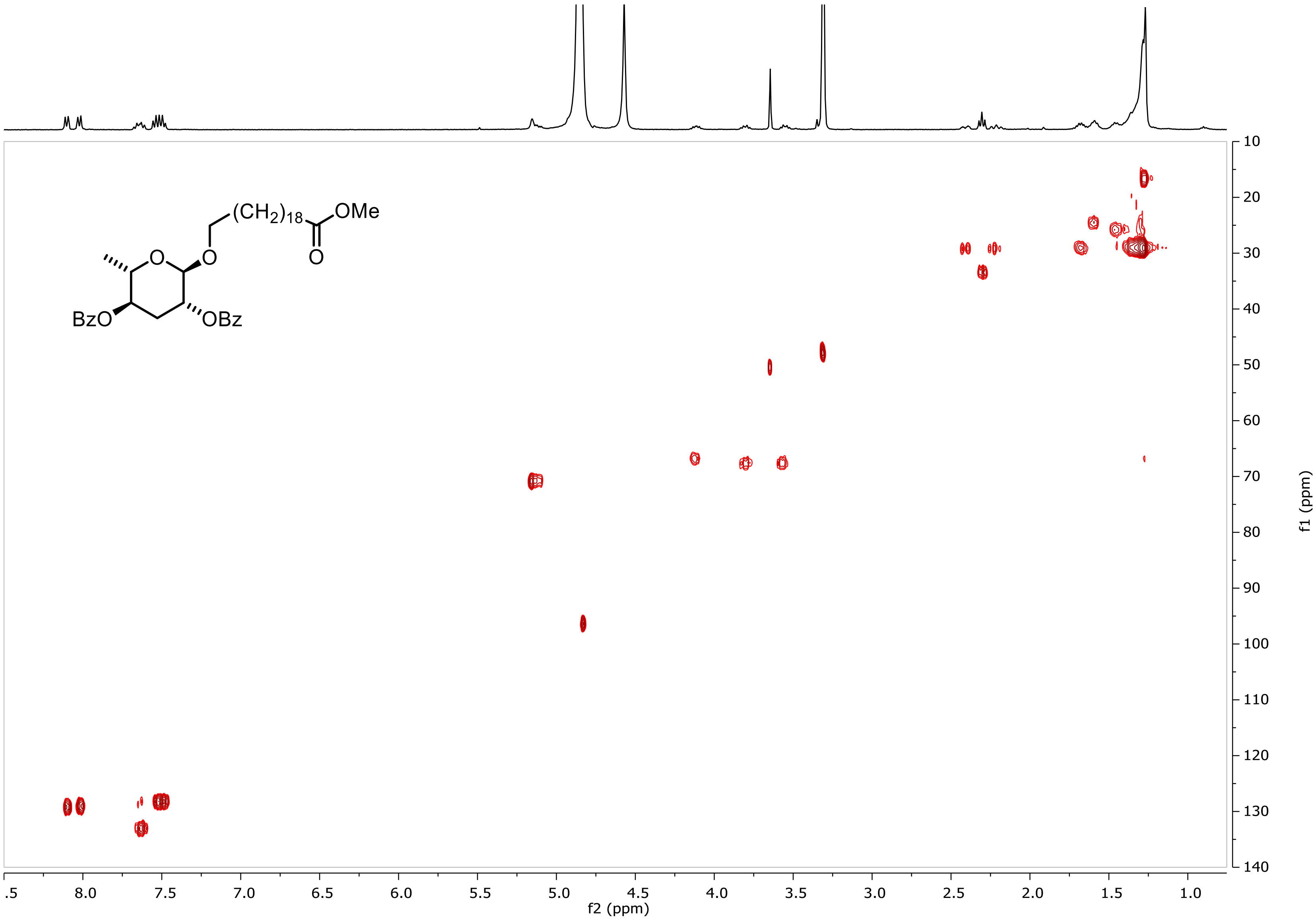

Fig S40: ^{1}H NMR (400 MHz, CD_3OD) of 20-[(3,6-dideoxy-α-L-*arabino*-hexopyranosyl)oxy]eicosanoic acid (**asc-ωC20**)

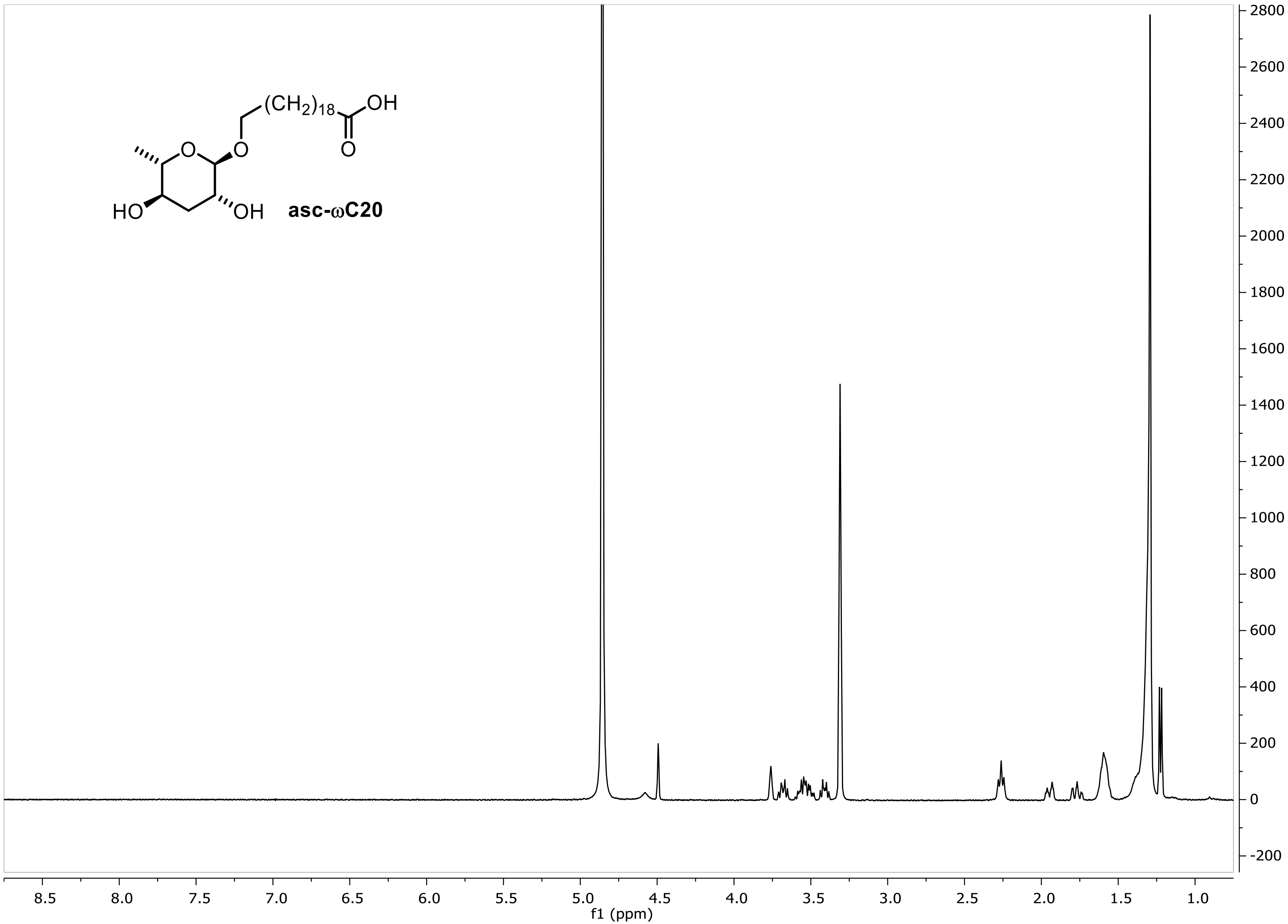

Fig S41: ^{13}C NMR (100 MHz, CD_3OD) of 20-[(3,6-dideoxy-α-L-*arabino*-hexopyranosyl)oxy]eicosanoic acid (**asc-ωC20**)

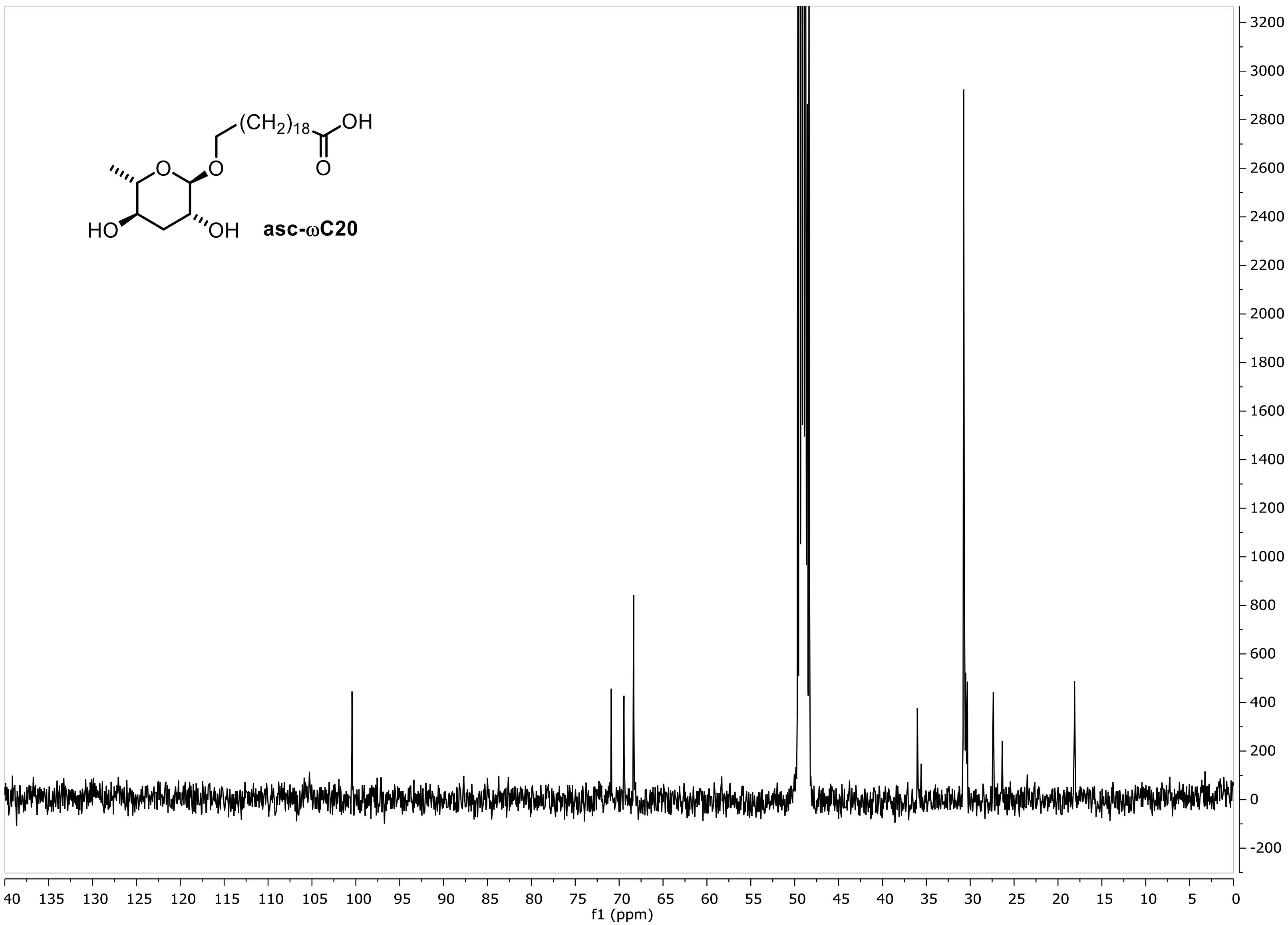

Fig S42: ^{1}H NMR (400 MHz, CD_3OD) of methyl (10*R*)-[(3,6-dideoxy-α-L-*arabino*-hexopyranosyl)oxy]undecanoate (**asc-C11-OMe**)

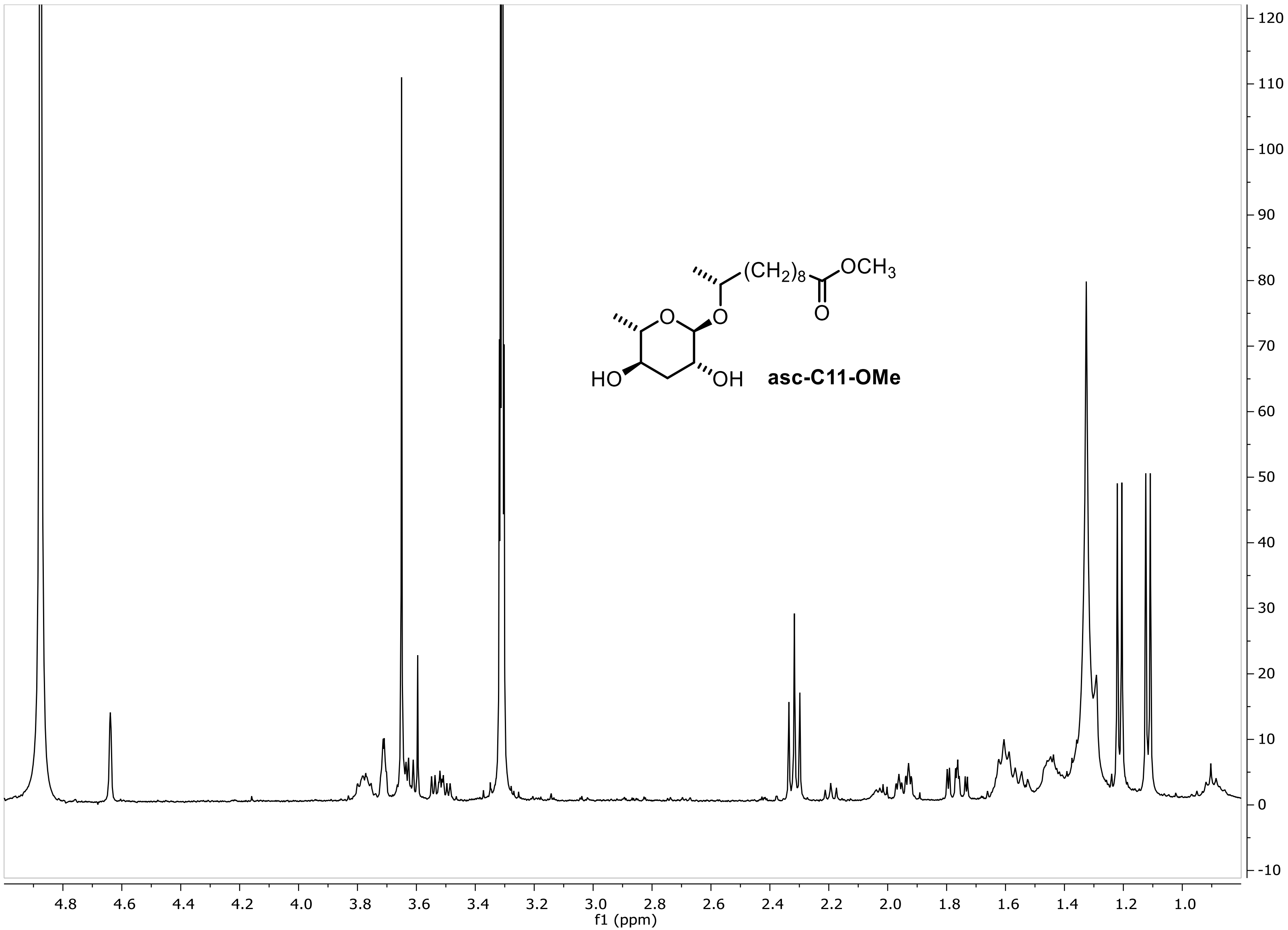

Fig S43: ^{1}H NMR (400 MHz, CD_3OD) of *N*-(2-hydroxyethyl) (10*R*)-[(3,6-dideoxy-α-L-*arabino*-hexopyranosyl)oxy]undecanamide (**asc-C11-EA**)

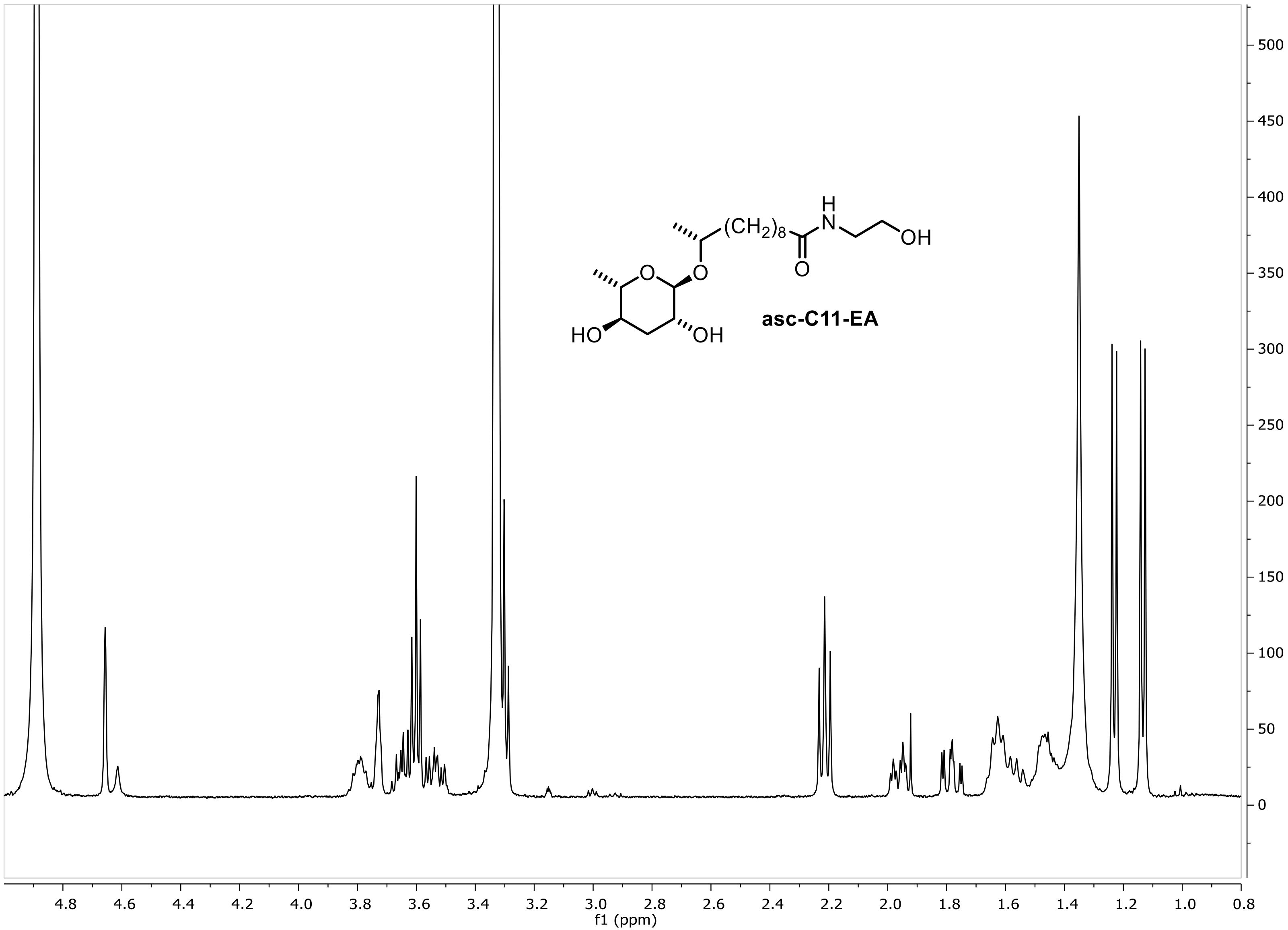

Fig S44: *dqf*-COSY (400 MHz, CD_3OD) of *N*-(2-hydroxyethyl) (10*R*)-[(3,6-dideoxy-α-L-*arabino*-hexopyranosyl)oxy]undecanamide (**asc-C11-EA**)

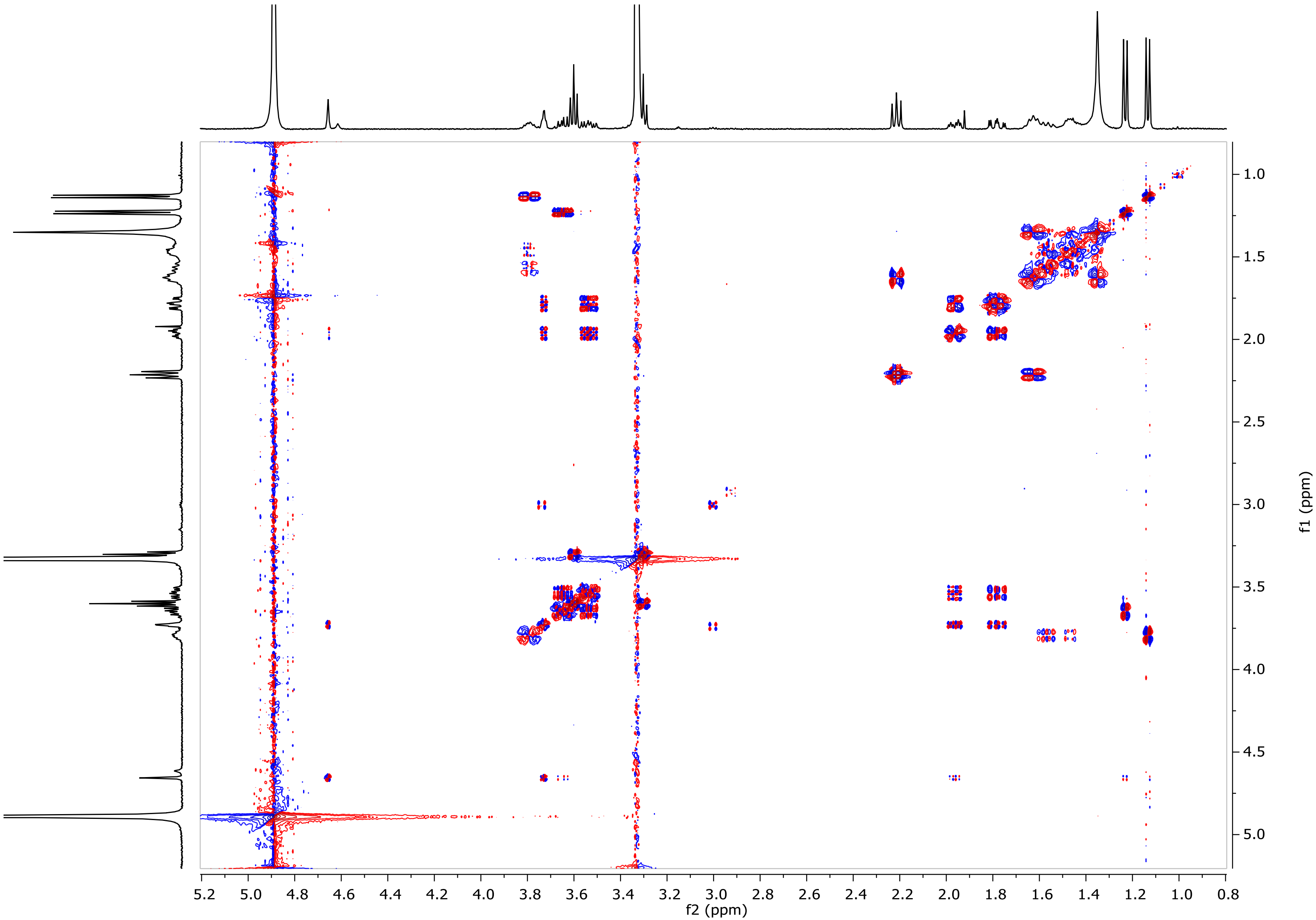

Fig S45: HSQC (CD_3OD) of *N*-(2-hydroxyethyl) (10*R*)-[(3,6-dideoxy-α-L-*arabino*-hexopyranosyl)oxy]undecanamide (**asc-C11-EA**)

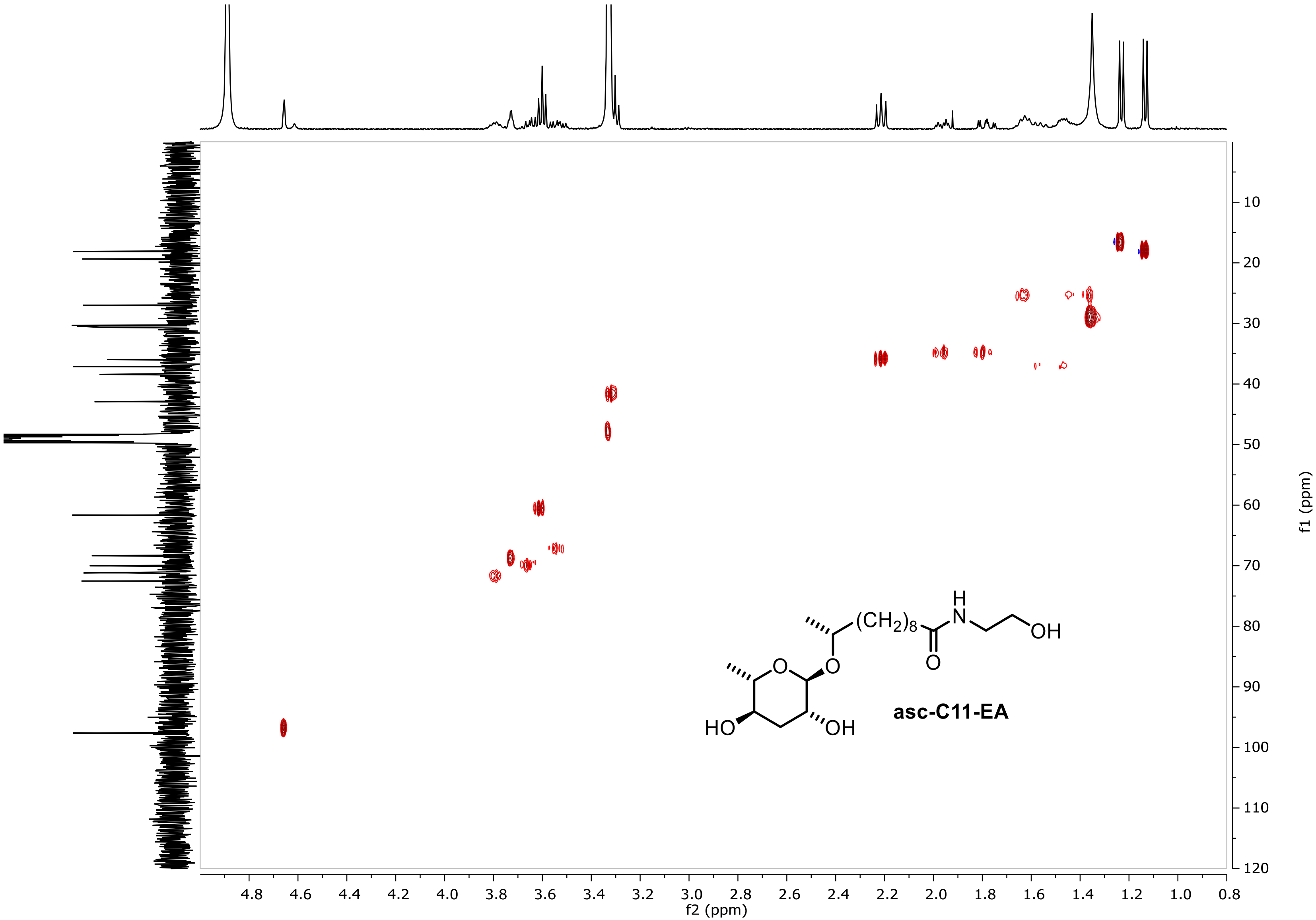

Fig S46: ^{13}C NMR (100 MHz, CD_3OD) of *N*-(2-hydroxyethyl) (10*R*)-[(3,6-dideoxy-α-L-*arabino*-hexopyranosyl)oxy]undecanamide (**asc-C11-EA**)

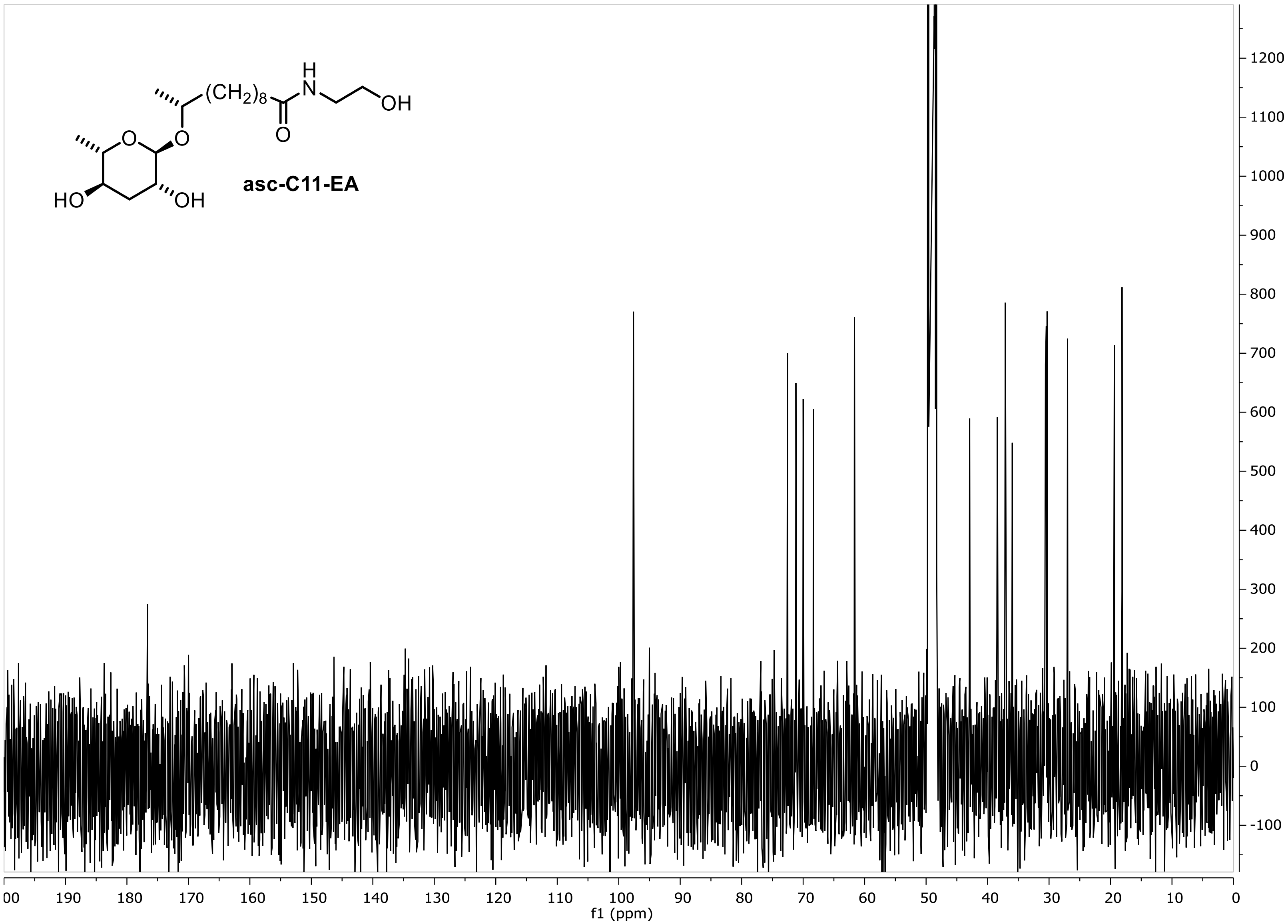

References

[1] Choe, A.; Chuman, T.; von Reuss, S. H.; Dossey, A. T.; Yim, J.; Ajredini, R.; Kolawa, A. A.; Kaplan, F.; Alborn, H. T.; Teal, P. E.; Schroeder, F. C.; Sternberg, P. W.; Edison A. S. *Proc. Natl. Acad. Sci. U. S. A.* **2012**, *109*, 20949−20954.

[2] Noguez, J. H.; Conner, E. S.; Zhou, Y.; Ciche, T. A.; Ragains, J. R.; Butcher, R. A. *ACS Chem. Biol.* **2012**, *7*, 961-966.

[3] Butcher, R. A.; Ragains, J. R.; Kim, E.; Clardy, J. *Proc. Natl. Acad. Sci. U. S. A.* **2008**, *105*, 14288−14292.

[4] Srinivasan, J., von Reuss, S. H., Bose, N., Zaslaver, A., Mahanti, P., Ho, M., O'Doherty, O., Edison, A.S., Sternberg, P. W., Schroeder, F. C. *PLoS Biol.* **2012**, *10*, e1001237.

[5] von Reuss, S. H.; Bose, N.; Srinivasan, J.; Yim, J. J.; Judkins, J. C.; Sternberg, P. W.; Schroeder, F. C. *J. Am. Chem. Soc.* **2012**, *134*, 1817−1824.

[6] Pungaliya, C.; Srinivasan, J.; Fox, B. W.; Malik, R. U.; Ludewig, A. H.; Sternberg, P. W.; Schroeder, F. C. *Proc. Natl. Acad. Sci. U. S. A.* **2009**, *106*, 7708−7713.

[7] Dong, C. F.; Dolke, F.; von Reuss, S. H. *Org. Biomol. Chem.* **2016**, *14*, 7217−7225.

[8] Hollister, K. A.; Conner, E. S.; Zhang, X.; Spell, M.; Bernard, G. M.; Patel, P.; de Carvalho, C. G. V.; Butcher, R. A.; Ragains, J. R. *Bioorg. Med. Chem.* **2013**, *21*, 5754–5769.

[9] Butcher, R. A.; Fujita M.; Schroeder, F. C.; Clardy, J. *Nat. Chem. Biol.* **2007**, *3*, 420-422.

[10] Manosalva, P.; Manohar, M.; von Reuss, S. H.; Chen, S.; Koch, A.; Kaplan, F.; Choe, A.; Micikas, R. J.; Wang, X.; Kogel, K.-H.; Sternberg, P. W.; Williamson, V. M.; Schroeder, F. C.; Klessig, D. F. *Nat. Commun.* **2015**, *6*, 7795.

[11] Jeong, P.-Y.; Jung, M.; Yim, Y.-H.; Paik, Y.-K. *Nature* **2005**, *433*, 541-545.